POLITECNICO DI TORINO

SCHOOL OF PLANNING AND DESIGN

DEPARTMENT OF REGIONAL AND URBAN STUDIES AND PLANNING (DIST)

Master's degree in
Territorial, Urban, Environmental and Landscape Planning

Master Thesis

Fractal and Network-based analysis of historic and modern street patterns across European cities

Supervisor:
Prof. Luca S. D'Acci

Co-supervisor:
Prof. Giancarlo Cotella

Candidate:
Anara Kulzhanova

Academic Year 2024/2025

Abstract

In urban studies, historic districts are often portrayed as inherently walkable because their street networks emerged through organic development rather than planned design. These areas typically feature frequent intersections, richer route choice, and more engaging streetscapes than the larger blocks and regular alignments characteristic of many modern planned districts. Such interpretations often rely on the idea that historic areas possess a form of geometric complexity described as "fractal-like", yet this characteristic has rarely been evaluated systematically or directly linked to measurable street-network indicators.

This thesis addresses this gap by examining whether differences in geometric complexity and street network structure correspond to the walkability-related properties commonly attributed to fractal-like street form. The analysis, therefore, focuses on whether fractal dimension, as a quantitative measure of this complexity, captures variations in street morphology and how it correlates with key topological indicators of street-network configuration.

The study covers 100 European cities, each represented by a pair of contrasting districts: an organically evolved historic core and a typical planned modern extension. Geometric complexity is measured using fractal dimension and two indicators of street grain: intersection density (nodes per km^2) and average segment length. Network structure is assessed using graph-based indicators, including meshedness (redundancy of alternative paths), reachability index (number of intersections accessible within 600m), route straightness (deviation from a straight line), and harmonic mean shortest path length (average minimum travel distance).

The results show that historic areas generally exhibit a higher fractal dimension ($\widetilde{D} \approx 1.5$, SD = 0.07) than modern districts ($\widetilde{D} \approx 1.4$, SD = 0.07), reflecting their more irregular and compact street structure. This difference is accompanied by denser intersections (103 vs 87 per km^2), shorter average street lengths (78 vs 88 m), and roughly 20% higher local reachability. However, both morphologies display similar route straightness and shortest-path metrics, indicating that global-scale connectivity is less sensitive to underlying geometric variation.

These findings demonstrate that fractal dimension captures consistent variations in both geometric and topological properties of street networks across contrasting urban morphologies. By linking fractal geometry with network-based measures, the research provides an empirically grounded framework for examining street-network structure and clarifying the morphological foundations of walkability in different urban contexts.

Keywords: street-network morphology, fractal dimension, topological indicators, walkability, urban form.

Table of Contents

List of Figures

List of Tables

Chapter 1: Introduction

1.1. Background

Understanding the city inevitably involves recognizing the multiple layers through which it operates (Boeing, 2018; Merlo & Lavoratti, 2024). This intricate nature – commonly referred to as *urban complexity* – manifests not only in the visible arrangement of streets, buildings, and public spaces, but also in the less tangible systems of social, economic, and infrastructural flows that continuously shape the city's evolution (Lynch, 1960; Jacobs, 1961; Batty, 2005; Salingaros & Pagliardini, 2016). While these dimensions are deeply interconnected, the physical form of the city provides a concrete and observable foundation for study. By focusing on measurable spatial arrangements, researchers can translate the abstract concepts of urban complexity into empirical comparisons across diverse urban settings (Strano et al., 2014).

Among all urban elements, the street network plays a uniquely foundational role in shaping city form and experience (Marshall, 2004; Yoo & Lee, 2017). It serves as the primary "skeleton" of urban space, enabling movement, and connecting diverse land uses (Jacobs, 1961; Marshall, 2004; Porta et al., 2006; Yoo & Lee, 2017). Its geometry and topology not only structure circulation and accessibility but also register the city's historical trajectories of growth (Hillier & Hanson, 1984; Shen, 2002). Whether organically evolved or systematically designed, the configuration of street patterns directly shapes travel distance, navigability, and the overall structure of urban environments. Thus, focusing on their geometry and connectivity offers a practical and measurable basis for comparing the capacity of different street patterns to support or limit potential pedestrian mobility and access (Louf & Barthélemy, 2014; Boeing, 2017; Reza et al., 2024).

Figure 1.1. Urban layout of Kotor, Montenegro (Tiefenbacher, 2022)

Historic city centers often display organically evolved street networks characterized by narrow, winding streets, and irregular intersections developed incrementally over time. These patterns evolve in response to local topography, socio-economic demands, and historical events (Jacobs, 1961; Salingaros, 2000). Such adaptive growth produces highly intricate configurations, often accompanied by irregular building footprints, mixed land uses, and non-uniform spatial patterns (Salingaros, 1998;

Frankhauser, 2004). Cities like Rome and Kotor (Figure 1.1) exemplify how centuries of layered development generate street systems deeply tied to cultural identity. These unplanned fabrics often reveal fractal traits – structural patterns repeating across multiple spatial scales – forming nested layers, with major routes branching into progressively smaller lanes (Salingaros & Pagliardini, 2016; Mehaffy et al., 2010; Sreelekha et al., 2020).

In contrast, modern urban expansions frequently employ grid street patterns that exemplify a more systematic and planned approach to city form. Rooted in rational design principles, grid layouts are characterized by regular, orthogonal streets and uniform block sizes, which aim to maximize clarity, order, and navigability (Southworth & Ben-Joseph, 2003; Sevtsuk et al., 2016). Such patterns emerged prominently during periods of rapid urban expansion and modernization, often reflecting Enlightenment ideals of efficiency and control over the urban environment (Scott, 1998; Alexander, 2001; Batty, 2005). Iconic examples include the rectilinear streets of Barcelona's Eixample and the extensive street grids of Chicago and New York (Figure 1.2). While grids promote legibility and facilitate movement, they can also impose a certain rigidity, often disregarding local topography or pre-existing circulation patterns (Monclús, 2003). Nonetheless, their simplicity and scalability have made grids a recurrent model in urban planning, representing a contrasting yet equally significant approach to structuring street networks (Boeing, 2020).

Figure 1.2. Urban layout of New York, USA (Moreira, 2020)

These two types of urban patterns are sometimes seen as opposing forces, yet modern cities increasingly blend both organic and grid elements. For instance, Barcelona (Figure 1.3) and Portland exemplify hybrid urban structures, where a dense historical core is surrounded by gridded expansions (Marshall, 2004; Mehaffy et al., 2010). This combination creates urban environments where multiple spatial logics – understood as distinct principles shaping street layout and connectivity – coexist and interact within a single

city (Louf & Barthélemy, 2014; Yoo & Lee, 2017). Hybrid forms can be both historically rich and spatially adaptable, but they also present unique challenges for urban design (Talen, 2003; Ewing & Handy; 2009).

Figure 1.3. Urban layout of Barcelona, Spain (Moreira, 2020)

This contrast between historic, organically developed districts and more systematically planned modern grids within the same city offers a valuable lens for examining morphological variation. Comparing these distinct zones side by side makes it possible to assess how differences in street-network structure impact spatial properties such as connectivity, redundancy, and access – within a controlled urban context (Masucci et al., 2009). Focusing on intra-city variation helps reduce the influence of external factors such as climate, governance, or demographics, which often complicate cross-city comparisons.

One practical lens for interpreting these spatial patterns is urban grain – the typical size and arrangement of blocks and parcels, determined by the underlying street layout (Sevtsuk et al., 2016; Zhao et al., 2023). It captures the characteristic rhythm and scale of the built fabric: finer grain is frequently linked to adaptability, permeability, and access, while coarser grain may support larger land uses or clearer management boundaries (Pafka & Dovey, 2016; Zhao et al., 2023). This variation often follows a spatial gradient, with block structures becoming coarser and less intricate toward the urban periphery (Sreelekha et al., 2020). Though finer grain is generally associated with pedestrian accessibility, studies have shown that the relationship between urban grain and walkability is not always linear, depending on context and street-network structure (Sevtsuk et al., 2016). Accordingly, comparative analysis across diverse morphologies requires a metric capable of capturing both fine-grained detail and broader structural order across scales.

While urban grain captures the local texture of the built fabric, it lacks a mechanism to describe structural complexity across spatial scales – a gap fractal geometry helps to fill. Introduced by Mandelbrot (1983), it

describes how spatial patterns extend and repeat across different scales. This property is quantified by the fractal dimension (D) – a single value that expresses the degree to which a form fills space across multiple levels of observation (Fankhauser, 1998; Chen, 2013; Jahanmiri & Parker, 2022). In urban studies, D has been used to characterize irregular spatial structures and to complement conventional metrics such as density or block size (Goodchild & Mark, 1987; Sreelekha et al., 2017). Recent work has also formalized fractality in discrete street networks (networks composed of intersections and street segments), adapting classical concepts to graph-theoretic framework that connect geometric form to network topology (Babič et al., 2022; Bunimovich & Skums, 2024).

Beyond its value as a static descriptor, D has been linked to processes of urban transformation. According to Chen and Huang (2019), changes in fractal dimension can indicate urban growth trajectories, including patterns of expansion, densification, and infill development. These dynamics are often embedded in the physical form of the city and become evident when comparing areas shaped in different historical periods. In this context, fractal dimension provides a means to read morphological change within cities, offering a more dynamic perspective than static morphological metrics alone.

Fractal dimension thus serves as a concise summary of the geometric side of urban complexity, capturing both the density and spatial irregularity of the street network across scales (Hyseni et al., 2021). Street patterns, however, are more than fixed geometries; their configuration defines the network's structural frame, shaping connectivity, route options, and resilience (Louf & Barthélemy, 2014; Masucci et al., 2009; Boeing, 2018, 2021). This internal arrangement underpins accessibility and influences broader functional outcomes, such as travel times, congestion patterns, and traffic demand (Marshall, 2004; Masucci et al., 2009; Babič et al., 2022). At neighborhood scales, the literature calls for quantitative approaches that integrate the analysis of design and configuration of urban street networks, linking geometry and topology to assess their combined influence on connectivity and accessibility (Louf & Barthélemy, 2014; Boeing, 2017; Sharifi, 2019).

Taken together, these arguments suggest a dual perspective on street networks: one concerned with geometric form, the other with topological configuration. The geometric or morphological dimension – encompassing urban grain, density, and spatial irregularity – is measured by the fractal dimension (D), as well as metric proxies such as intersection density and average edge length (Louf & Barthélemy, 2014; Boeing, 2018). The topological dimension is described by connectivity indicators, including the meshedness coefficient (route redundancy), reachability index (local access), mean straightness (route directness), and harmonic mean shortest path length (average minimum trip length). Framed this way, the analysis establishes a shared basis for assessing diverse European morphologies and directly informs the problem statement that follows.

1.2. Problem statement

Despite frequent references to the fractal characteristics of urban street networks (Lu & Tang, 2004; Mehaffy et al., 2010; Daniel et al., 2021), the empirical relationship between fractal dimension (D) and core network properties – particularly connectivity and accessibility – remains unclear. While existing studies suggest that higher D values may correspond to more continuous and integrated street structures (Salingaros, 1998; Lu et al., 2016), most analyses have focused on comparisons between different cities, where social, economic, demographic, and spatial contexts vary (Chen & Luo; 1998; Fankhauser, 2004; Strano, 2014; Boeing, 2018; Lagarias & Prastacos, 2021).

This cross-city approach, however, lacks sensitivity to the intra-city variation of street-network structure, where differing historical trajectories, urban policies, and design logics frequently produce sharp contrasts within the same metropolitan area. For example, districts such as Ciutat Vella and Eixample in Barcelona are shaped by entirely different planning logics and exhibit distinct spatial structures, despite existing within a single administrative context (Monclús, 2003). A focused, intra-city analysis thus offers a controlled framework to better isolate the relationship between D and street network indicators while minimizing external variability.

As a result, the core problem emerges: does fractal dimension serve only as a geometric descriptor, or can it also reflect deeper structural differences in street-network configuration? Building on this, the study explores whether D can function as a conceptual bridge between morphological indicators and topological network measures. To do so, it adopts a comparative, intra-city framework, focusing on pronounced contrasts between organically evolved and planned grid districts within the same metropolitan context. By testing the relationship between fractal dimension and street-network indicators at the neighborhood scale, this thesis contributes both to theoretical work on urban morphology and to the development of empirical tools for evaluating street-network configuration across diverse urban forms.

1.3. Research Scope and Objectives

This study focuses on European cities that contain clearly differentiated historic (organic) districts and planned grid expansions. By analyzing such contrasts within a single urban context, this research minimizes confounding influences such as climate, governance, or regional economics. Establishing relationships in these sharply contrasting cases also lays a methodological foundation for future work on hybrid and transitional urban areas.

All measurements are taken from the present-day network at the neighborhood scale, where planning decisions are typically implemented. The analysis is framed by two complementary perspectives:

1. A cross-sectional comparison looks across several cities to ask how historic and modern districts differ on average.

2. Within-city pairings examine how divergent planning logics manifest side-by-side in a shared geographic context.

The research links morphological indicators (fractal dimension and urban grain measures) to topological indicators that capture connectivity, route directness, and travel efficiency. These metrics, specified in the Methods chapter, allow a unified assessment of street form and structure. Accordingly, the overarching ***aim*** is to examine whether fractal dimension offers a consistent numerical basis for distinguishing street-network types, based on its relationship with key topological indicators within contrasting urban contexts.

The *objectives* of the study are:

O1 – To quantify and compare the geometric complexity of historic-core and modern districts within each city using fractal dimension (D), intersection density, and average edge length.

O2 – To assess and compare topological structure through selected connectivity indicators, including meshedness coefficient, reachability index, mean straightness, & harmonic mean shortest path length.

O3 – To examine intra-city correlations between fractal dimension (D) and selected topological indicator, evaluating whether fractality corresponds with variations in street network connectivity as widely claimed in the literature.

Research questions:

RQ1: How do historic and modern districts differ in street-network morphology and structure across European cities?

RQ2: To what extent does fractal dimension (D) capture the geometric differences observed between these contrasting urban forms?

RQ3: How does fractal dimension relate to key topological indicators of street-network configuration commonly associated with walkability?

Hypotheses:

H1 – Historic street networks will exhibit significantly higher geometric complexity, as expressed through fractal dimension, than modern planned networks.

H2 – Historic districts will demonstrate higher pedestrian-scale reachability and redundancy due to their finer urban grain, supporting the claim that fractal-like morphologies enhance local accessibility.

H3 – Fractal dimension will show a positive association with local-scale connectivity indicators (meshedness and reachability index), but a weaker or inconsistent association with global network measures (route straightness and harmonic mean shortest path length).

1.4. Thesis Structure

The thesis is structured into a series of interrelated chapters that collectively address the central research questions and support a systematic analysis of geometric and topological properties of street networks in European cities.

Chapter One introduces the research context, outlines the motivation for the study, and defines the scope and analytical focus. It presents the main aim, objectives, and research questions, and sets out the hypotheses.

Chapter Two provides a review of relevant literature, establishing the theoretical basis for reading urban form through street networks. It explores key concepts and debates on the physical dimension of urban complexity, the historical evolution of street patterns, urban grain, fractal geometry, and indicators of street-network structure. The chapter concludes by identifying gaps that motivate the empirical analysis.

Chapter Three outlines the methodological framework. It describes the selection of study areas and data sources, explains how physical complexity is assessed, including the computation of fractal dimension and derivation of graph-theory metrics. It further details the analytical approach at both the cross-sectional and intra-city levels, including procedures to assess associations and interpret typological variations.

Chapter Four presents the results derived from the applied methodology. It includes a comparative analysis of street-network patterns, reports the distribution of fractal dimension (D) values in historical and modern urban areas, examines variations in topological indicators, and analyzes relationships between D and street network indicators.

Chapter Five interprets the findings in relation to the research questions and existing literature. It discusses the results, reflects on their implications for understanding urban morphology and street-network analysis, and acknowledges study limitations.

Chapter Six concludes the thesis by synthesizing the key findings in relation to the research aim and questions. It highlights the contribution of the study, discuss broader implications for urban design and morphological analysis, and outlines directions for future research.

Chapter 2: Literature review

This chapter reviews key literature on urban complexity with a specific focus on its spatial and structural dimensions as they relate to street networks. It begins by outlining the theoretical foundations that frame cities as complex systems, emphasizing the shift from descriptive interpretations of urban form to quantitative approaches that measure geometric and structural variation. The chapter then traces the historical evolution of urban patterns, contrasting organically developed historic fabrics with systematically planned modern layouts, and examining the assumptions commonly associated with each.

Particular attention is given to methods for quantifying spatial complexity, with a focus on fractal geometry and the use of street networks as proxies for urban form. The chapter critically evaluates the conceptual basis and empirical application of fractal dimension in urban studies, highlighting both its analytical value and methodological limitations. Subsequent sections explore the relationship between street morphology and network structure through graph-theoretic approaches, addressing how different configurations shape structural connectivity and accessibility potential.

Rather than conflating spatial form with observed behavior or subjective perception, this review centers on the structural conditions that enable or constrain movement within the urban fabric. By synthesizing debates across urban morphology, network science, and fractal analysis, this chapter establishes the theoretical foundation for examining whether fractal dimension captures structural variation in street-network form across contrasting urban contexts.

2.1. Urban complexity: conceptual foundations

Cities develop through many small adjustments rather than a single design moment (Alexander, 1965; Batty, 2005; Boeing, 2018). Their street layouts, block structures, and built fabric accumulate through repeated actions such as plot subdivision, route extension, infill construction, and incremental densification. These processes are shaped by everyday practices, regulatory decisions, and physical constraints, which together leave a long-term imprint on spatial form (Salingaros, 2000; Batty, 2005).

Over time, these numerous minor interventions produce spatial patterns that are far more irregular and differentiated than those arising from a single coordinated plan (Batty, 2005; Boeing, 2018; Merlo & Lavoratti, 2024). *Complexity theory* describes this cumulative evolution by viewing cities as systems in which spatial configuration results from the interplay of many heterogeneous actors and conditions, each

influencing the built environment in partial and often indirect ways (Batty, 2005; Strano et al., 2014; Boeing, 2018).

The concept of *urban complexity* is commonly discussed through four ideas: self-organization, emergence, nonlinearity, and multi-scale structure. These ideas help explain why urban morphology often shows irregular geometry, layered subdivision, and substantial variation across scales.

2.1.1. Self-organization and emergence

A defining mechanism of such systems is *self-organization*, which refers to the formation of spatial patterns through local adjustments rather than coordinated design. For instance, Alexander's (1965) essay *"A City is Not a Tree"* illustrates this concept by comparing traditional urban neighborhoods to semi-lattice structures: places where streets, buildings, and public spaces overlap and interconnect organically, rather than following a rigid, hierarchical "tree-like" plan. This demonstrates how urban form can be the product of local adaptation and collective negotiation, which are often regarded as signatures of self-organized development.

Closely related to self-organization is the concept of *emergence*, defined by Goldstein (1999) as the appearance of new spatial patterns that cannot be attributed to any single local intervention. In urban contexts, this may include hierarchical street arrangements (i.e. primary, secondary, tertiary streets), recurrent block proportions, or distinctive neighborhood structures that result from long sequences of the bottom-up interactions (Batty, 2005). Boeing (2018) shows that such emergent forms arise from decentralized negotiations rather than formal planning.

2.1.2. Nonlinearity in urban processes

Urban systems often exhibit *nonlinear* behavior: small local changes often trigger large systemic effects (Batty, 2005; Boeing, 2018). For instance, adding a single connecting street can reduce travel distances across a neighborhood, while closing a short link may reroute movement across a wide area. Similarly, a minor shift in intersection placement can alter block size, street continuity, or local connectivity (Crucitti et al., 2006; Porta et al., 2006).

These effects are not always intuitive or proportional, and they challenge the assumptions behind traditional *linear planning models*, which tend to expect predictable, incremental outcomes. A classic example of where such models fall short is the phenomenon of *induced demand*, where increasing road capacity unintentionally intensify traffic volumes rather than relieve them. Figure 2.1 illustrates how lane additions may fail to resolve congestion.

If this **is** a problem…

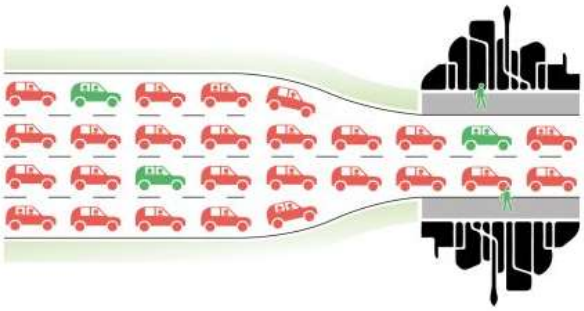

then this **is not** a solution…

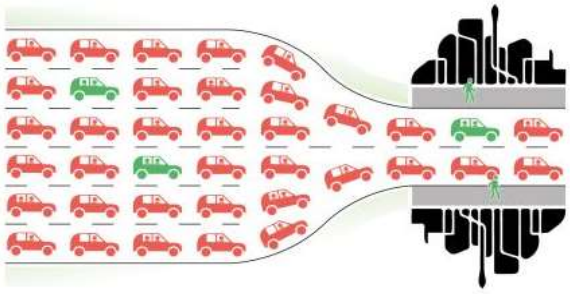

Figure 2.1. Example of Induced demand: more lanes, same problem (Verkade, 2020)

2.1.3. From nonlinearity to self-similarity

The recognition of nonlinear change introduces the concept of *self-similarity*, referring to the recurrence of related spatial patterns across different scales. Fankhauser (1998) observes that small elements of the built fabric – such as local branching or subdivision – often mirror larger structural arrangements, producing a multi-scale coherence associated with *fractal geometry*. This suggests that cities, much like natural systems, tend to develop through repeated subdivision processes that generate irregular but internally consistent spatial arrangements (Batty & Longley, 1994; Salingaros, 1998; Jiang, 2007).

Rather than implying visual repetition, self-similarity in urban structures reflects a consistent mode of spatial subdivision in parcels, blocks, and street segments vary systematically with scale (Batty, 2008). These variations cannot be captured by Euclidean measures alone, which focus on single dimensions of size or distance. Self-similar structure therefore provides the conceptual basis for describing urban morphology through measures such as the fractal dimension, which evaluates how intensively the built environment occupies space across multiple scales.

2.1.4. Complexity as a basis for analyzing urban form

The ideas discussed above provide a general foundation for interpreting cities as products of cumulative, multi-scale spatial processes. They highlight how incremental adjustments – such as parcel reshaping, path extension, or gradual densification – can generate built environments marked by irregular geometry, nested subdivisions, and considerable variation in grain and orientation. These characteristics appear not only in historic districts but also in peripheral settlements, informal expansions, and certain planned extensions where the built fabric has been modified repeatedly over long periods (Thomas et al., 2007; Sreelekha et al., 2020).

Understanding urban complexity therefore requires attention to how different morphological settings express these processes. Some urban areas show dense layers of incremental change, producing fine-grained blocks, irregular alignments, and mixed-use structures. Others reflect more consolidated or coordinated interventions, which may generate regular street grids, larger parcels, and predictable block

patterns (Boeing, 2021). Even within a single city, these contrasting conditions can coexist, illustrating how varied historical trajectories, governance structures, and developmental pressures shape the spatial outcome.

Complexity perspectives also underline that no single geometric or structural property captures the full range of variation found in urban form (Batty, 2005). Instead, built environments combine multiple layers of subdivision, circulation, and land use that have accumulated at different moments and rates (Hillier, 1996; Fankhauser, 1998). This accumulation produces urban fabrics that differ not only in their visible structure but also in their *depth of adaptation*, meaning the extent to which their present-day layout reflects long sequences of change (Salingaros, 1998; Mehaffy et al., 2010).

These distinctions provide the conceptual bridge to the next section. If cities evolve through heterogeneous and path-dependent processes, then different urban typologies – such as organically developed districts and planned extensions – will exhibit distinct forms of complexity. Section 2.2 therefore examines these typological differences and outlines how contrasting generative processes shape the spatial characteristics observed in contemporary urban environments.

2.2. Typological transitions in urban form

Urban form is not static; it evolves through an ongoing interplay of technological change, economic forces, cultural practices, and geographic context (Hillier, 1996; Wang et al., 2024; Merlo & Lavoratti, 2024). Over time, this interaction has produced a wide spectrum of spatial arrangements, ranging from irregular, organically developed fabrics to highly regular grid-based schemes. Each configuration reflects the planning norms, construction methods, and social expectations dominant at the time of its formation (Jacobs, 1961; Kostof, 1991; Marshall, 2009; Strano et al., 2014).

2.2.1. Organic patterns: Bottom-up spatial intelligence

Settlements that developed before the industrial age typically display irregular parcels, sinuous streets, and nested public spaces. Their geometry emerged incrementally through day-to-day decisions rather than a single blueprint, resulting in compact, pedestrian-scaled quarters where social exchange and local commerce were woven into the street fabric (Salingaros, 2000; Knowles, 2006).

Pagliardini et al. (2010) observe that such morphologies follow implicit, context-specific rules grounded in climate, topography, and building practice. In Mediterranean towns, for example, narrow streets and shaded passages correspond to climatic moderation strategies, while in hill settlements, terraced routes frequently conform to slope terrain (Hakim, 1986; Marshall, 2009). Alexander (1965) describes these morphologies

as example of *organized complexity*, characterized by the diversity of elements held together by recurrent spatial relationships that emerge through local negotiation.

Although such environments often originated in pre-industrial contexts, their spatial configurations continued to evolve through continuous modification in response to shifting needs (Batty, 2005). Even in formally planned settlements, such as Roman military camps, the initial geometric order was frequently reconfigured through subsequent subdivision and iterative development. This results in hybrid morphologies that combine imposed structure with incremental adaptation, where small plots repurposed and streets realigned without large-scale disruption (Bertuglia & Staricco, 2000; Salingaros, 2000).

2.2.2. Transition to grid-based and modernist planning

The rapid urbanization of the 19th and 20th centuries marked a decisive shift in planning paradigms. As the global urban population expanded dramatically – growing thirtyfold between 1800 and 1960 – the informal growth patterns of earlier settlements were replaced by more standardized layouts designed to accommodate large-scale development and infrastructural coordination (Kostof, 1991).

Grid plans became central tools of modernization. Their regular geometry supported coordinated infrastructure, administrative control, and predictable land subdivision (Le Corbusier, 1935; Scott, 1998; Marshall, 2004). These schemes also aligned with emerging transport technologies, especially tram and rail systems that required clear axial routes (Duany et al., 2000). In many contexts, the grid reflected broader political objectives: colonial governance, state-building, or rationalized land management (Kostof, 1991; King, 2004).

2.2.3. Grid patterns: Top-down spatial intelligence

Grid-based environments are characterized by repeated block modules, linear corridors, and uniform intersection spacing (Kostof, 1991; Scott, 1998; Boeing, 2021). Their appeal lies in their administrative clarity and scalability, making them suitable for large-scale development and real estate markets (Southworth & Ben-Joseph, 2003; Sennett, 2018). By establishing predictable parcels and circulation routes, grid layouts enable coordinated infrastructure delivery, clear land valuation, and standardized building procedures (Kostof, 1991; Boeing, 2020; Sreelekha et al., 2020).

The simplicity of the grid pattern also supports extension: its geometry can be expanded in any direction without altering the internal logic of blocks or streets. This quality made it attractive in colonial, industrial, and frontier contexts, where rapid land allocation and governance required easily reproducible spatial templates (Scott, 1998; Kostof, 1991; King, 2004). The regular spacing of intersections further facilitates the introduction of modern utilities, including tramlines, sewerage systems, and electricity networks, all of which benefit from linear and predictable routing.

In modernist planning discourse, the grid was reimagined as a tool for utopian design, with models like the Ville Radieuse envisioning zoned, geometrically clear cities optimized for the efficient use of transport and sunlight (Le Corbusier, 1935; Holston, 1989; Mumford, 1961). Although rarely implemented in full, this model deeply influenced urban renewal strategies and reinforced the association between rationalized spatial order and modernization efforts across Europe, North America, and parts of the Global South (see Figure 2.2).

New Orleans, USA | Avola, Italy | Buenos Aires, Argentina

Figure 2.2. Grid street networks in different regional contexts

For example, Barcelona's Eixample demonstrates how a rational grid can undergo significant adaptation. Originally designed by Ildefons Cerdà, the district exhibits a regular orthogonal structure combined with chamfered intersections and internally subdivided blocks. While the underlying geometry is strictly ordered, later phases of development introduced variations in block occupation, intersection treatment, and building intensities. These changes produced a hybrid condition in which planned structure persists alongside local divergences generated by piecemeal development.

2.2.4. Hybrid and alternative structuring principles

Beyond the binary distinction between organic and grid-based patterns, many cities exhibit hybrid configurations shaped by overlapping phases of development. Medieval settlements with Roman origins often combine a core grid overlaid by later organic growth. Radial-concentric systems (e.g., Moscow), curvilinear garden-city plans (e.g., Letchworth), and star-shaped fortifications (e.g Palmanova) represent alternative structuring principles aimed at fusing order with symbolic meaning or natural forms (Howard, 1902; Holston, 1989; King, 2004; Batty & Longley, 1994; Sennett, 2018).

These patterns illustrate that urban form is frequently the product of layered transformation, where successive interventions introduce new ordering systems without erasing prior structures (Batty, 2005; King, 2004; Marshall, 2004). Although such morphologies are significant within broader urban morphological discourse, their detailed analysis lies outside the specific comparative focus of this study and is therefore not discussed further.

2.2.5. Contemporary relevance of typological differences

The distinction between organic and grid-based patterns continues to inform debates about urban development. These patterns differ not only in appearance, but also in the type of complexity they exhibit. Traditional urban forms display "organized complexity" – a coherent yet diverse structure of interdependent elements – though may pose challenges in infrastructure provision and formal governance (Alexander, 1965). In contrast, grid plans often tend toward mechanical order or "organized simplicity" when their design does not sufficiently accommodate the unpredictable needs of everyday social life (Jacobs, 1961; Salingaros, 2000; Pagliardini et al., 2010; Portugali, 2011).

Both logics continue to inform contemporary planning discourse. Movements such as New Urbanism, Smart Growth, and sustainable urbanism draw on lessons from both organic and grid-based traditions (Duany et al., 2000; Alexander, 2001). A clear example is the Vauban district in Freiburg, where an initially regular street framework has been altered by car-free internal routes and small courtyards that subdivide larger blocks within a planned layout (Coates, 2013; Pafka & Dovey, 2016). From a structural perspective, this ongoing dialogue reinforces the relevance of examining how different morphological principles encode distinct development processes.

Typological differences also matter because they shape the underlying spatial framework inherited by later interventions. As the next section discusses, street networks form the primary structural layer through which these typological conditions become spatially legible. Section 2.3 therefore examines how different development processes influence the arrangement of circulation routes and the structural backbone of the built environment.

2.3. Street network configuration as the structural backbone

Street networks constitute the most persistent and analytically tractable component of urban form. As continuous arrangements of routes and intersections, they structure how blocks, parcels, and public spaces are organized and connected (Jiang & Claramunt, 2004; Porta et al., 2006; Marshall, 2009; Boeing, 2018). Their visible geometry records accumulated decisions made through historical development, infrastructural intervention, and incremental modification, thereby encoding the spatial structure of the city in a legible and quantifiable form (Zhao et al., 2023).

Because development processes differ across urban typologies, their street networks express contrasting spatial conditions. Incrementally formed districts tend to produce fine-grained, irregular alignments and varied junction spacing, while planned extensions often introduce more regular block modules, straighter routes, and consistent intersection patterns (Marshall, 2004; Salingaros, 2000). These differences make street networks the primary layer through which the generative processes discussed in Section 2.2 become spatially legible.

Despite their apparent diversity, street systems often display recognizable structural tendencies. Local adjustments and historical layering can produce coherent arrangements even within networks that appear irregular (Pagliardini et al., 2010; Boeing, 2021). These patterns reflect core elements of spatial organization – junction density, block subdivision, and segment orientation – that together shape urban geometry (Hillier, 1996; Salingaros, 2000; Southworth & Ben-Joseph, 2003). Because these features arise from long-term processes, street networks offer a consistent entry point for analyzing how different morphological settings encode their development histories.

The analytical value of street networks extends beyond their visible geometry. Network-science approaches conceptualize streets as interconnected systems, allowing examination of how spatial relations – not only distances – structure access across the urban fabric (Porta et al., 2006; Barthelemy, 2011; Strano et al., 2014). Variations in block size, intersection density, and segment orientation influence the number of available paths, the ease of movement between locations, and the distribution of connectivity within a given area (Hillier, 1996; Crucitti et al., 2006). Fine-grained networks with shorter segments and frequent junctions often support multiple route options and short pedestrian paths, whereas coarser arrangements with larger blocks tend to reduce local permeability (Pafka & Dovey, 2016). Yet empirical evidence shows that these relationships vary across contexts and scales, highlighting the need for comparative, context-sensitive analysis (Hillier, 1996; Porta et al., 2006; Boeing, 2018).

These structural characteristics also follow scale-dependent organization, aligning with broader theories of urban complexity. Studies show that local street patterns often relate to larger spatial arrangements, producing forms of multi-scalar coherence even where visual regularity is absent (Jiang, 2007; Wang et al., 2024). This makes street networks particularly suited for quantitative analysis, since their geometric and topological properties can be examined consistently across multiple spatial extents.

Because street networks are persistent, legible, and structurally explicit, they serve as a robust proxy for examining geometric complexity in this study. Their configuration can be analyzed using established techniques from fractal geometry and graph theory, providing a systematic basis for comparing paired districts shaped by different developmental trajectories. The following sections introduce the analytical tools used to measure these properties: Section 2.4 introduces the concepts of urban grain and permeability as a means to describe fine-scale morphological variation; Section 2.5 reviews fractal approaches to urban morphology; and Section 2.6 introduces the indicators used to characterize street-network structure. The final subsection then synthesizes these strands to define the research gap addressed in this thesis.

2.4. Urban grain, permeability, and street-network patterns

As discussed in Section 2.3, the configuration of street networks shapes not only geometric form but also the structural conditions that enable or constrain spatial access, route diversity, and navigational choices

within the built environment. A critical aspect of this structural variation lies in the concepts of *urban grain* and *permeability*, which together offer insight into how different street-network patterns affect accessibility, connectivity, and spatial legibility – particularly at the pedestrian scale (Pafka & Dovey, 2016).

Urban grain refers to the size, regularity, and arrangement of the physical units that compose the built fabric – most commonly parcels and blocks (Bentley et al., 2003). Grain is typically conceptualized as a spectrum ranging from *fine* to *coarse*, depending on block size, street spacing, and subdivision patterns. Fine-grained networks are characterized by small blocks, short street segments, and high intersection density (Figure 2.3a). Conversely, coarse-grained structure (Figure 2.3b) tend to result from car-oriented or large-scale planned development, exhibiting longer street segments, larger parcels, and wider intersection spacing (Southworth & Ben-Joseph, 2003; Sennett, 2018).

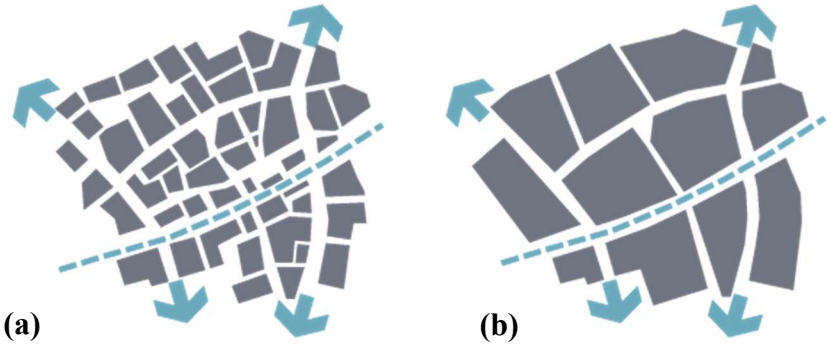

Figure 2.3. Representative block configurations illustrating a continuum from fine (a) to coarse (b) grain (EPOA, 2018)

Closely related – but conceptually distinct – is the concept permeability, which refers to the degree of movement potential within a street network. It captures how connected the street layout is, how many alternative paths exist between locations, and how direct those routes are (Hillier, 1996; Pafka & Dovey, 2016). A highly permeable street network supports multiple route choices and shorter detours, whereas low permeability restricts access to a few major routes, often increasing walking distances, even when origins and destinations are physically close.

While fine grain often contributes to high permeability, the relationship is not absolute. Some coarse-grain grids (e.g., Manhattan) maintain high permeability due to consistent spacing and through-connections, while some fine-grain historical areas may include cul-de-sacs or fragmented segments that reduce local connectivity. These distinctions underscore the importance of disaggregating geometric layout from topological aspect: grain and permeability are correlated but capture different aspects of network structure.

2.5. Fractal geometry and urban street form

Quantifying the physical dimension of urban complexity requires moving beyond descriptive or purely conceptual interpretations of urban form. This section outlines why quantitative approaches are necessary

for studying irregular, layered spatial structures, and introduces fractal dimension as a tool for characterizing geometric complexity in urban street networks.

2.5.1. Why and How we quantify urban form

Urban form has traditionally been examined through qualitative interpretation and typological analysis. While these approaches provide valuable insight, they are limited in their capacity to capture the irregularity, variation, and layered organization characteristic of urban systems (Batty & Longley, 1994; Talen, 2003; Boeing, 2018). In response to this limitation, researchers have increasingly emphasized the need for quantitative approaches capable of translating complex urban patterns into analyzable and comparable metrics.

As Talen (2003, p. 203) asserts, meaningful urban analysis must move beyond visual description to measurable structure:

> *"…without the tools to effectively measure and represent these [i.e., spatial and structural aspects of urban form] ideas – essential for implementation – the concepts prove intangible…"*

This opinion echoes Batty and Longley's (1994) call for moving from description to quantification when studying cities as evolving systems. Similarly, Boeing (2018, p. 285) similarly emphasizes the need to measure urban complexity formally, asking how complexity in urban form might be "assessed" rather than only described. These arguments reflect a broader disciplinary shift toward metrics that can compare urban structures consistently across space and time.

Formal quantitative approaches enable researchers to characterize spatial patterns – such as dispersion, fragmentation, continuity, and grain – in a systematic and replicable manner. Such measures help distinguish configurations that may appear similar visually but differ in their underlying organization (Clifton et al., 2008; Yuan et al., 2018). The growth of spatial datasets and computational methods has further strengthened the feasibility of applying such metrics in comparative studies spanning large geographical areas (Boeing, 2018).

Within this broader shift, fractal analysis offers a particularly relevant framework for studying urban form. Developed in mathematics to describe scale-dependent and irregular shapes, fractal geometry provides concepts and techniques for examining patterns that recur across multiple spatial extents (Batty & Longley, 1994; Batty, 2005). Its relevance to urban morphology stems from repeated observations that cities tend to exhibit hierarchical subdivision, nested structures, and scale-rich variation – properties that conventional Euclidean measures cannot adequately capture.

Applications of fractal geometry in urban studies have examined the branching structure of street networks, the subdivision of blocks, and the dispersal of built form, demonstrating how these elements often display

characteristic degrees of irregularity and scaling (Chen & Luo, 1998; Shen, 2002; Lu & Tang, 2004). This aligns with broader theories of urban complexity, in which built fabric emerges through incremental processes that generate both diversity and coherence across scales.

While various quantitative approaches exist – such as simulation models or cellular automata that replicate urban growth dynamics (Batty, 1997, 2005; van Vliet et al., 2012) – fractal analysis provides a static yet structurally expressive means of examining existing spatial patterns. Rather than modelling temporal change, it focuses on the geometric properties of form itself, offering a way to describe how spatial detail accumulates and how urban form fills space at different levels of measurement (Batty & Longley, 1994).

In summary, quantifying urban form allows researchers to move from descriptive characterization to systematic comparison. Fractal analysis, in particular, offers tools for interpreting the scale-rich, irregular, and multi-layered geometry that typifies urban street networks. The next section introduces fractal dimension as a specific metric derived from this framework, used to quantify geometric complexity in a consistent and comparable way.

2.5.2. Fractal geometry in urban studies

The application of fractal theory in urban studies has significantly advanced the understanding of spatial organization and urban form. The concept of a fractal, first introduced by Benoît B. Mandelbrot, describe a geometric object formed through an iterative process, producing complex shapes composed of repeated elements at progressively finer resolutions (Mandelbrot, 1983; Terzidis 2006). This property – known as *scale invariance* – implies that patterns remain consistent regardless of the level of magnification (Salingaros, 2003; Jevric et al., 2016; Jahanmiri & Parker, 2022).

A classic example of this principle is the coastline paradox (Figure 2.4), which illustrates how measurements of length vary with scale, reflecting the increasing detail observed at finer resolutions (Mandelbrot, 1983). Initially, geographers recorded a certain length for the British coastline, but as measurement methods became more precise, the recorded length changed (Salingaros, 2003, p.5). Each time the coastline was measured with greater accuracy – the length appeared to increase. This puzzling phenomenon

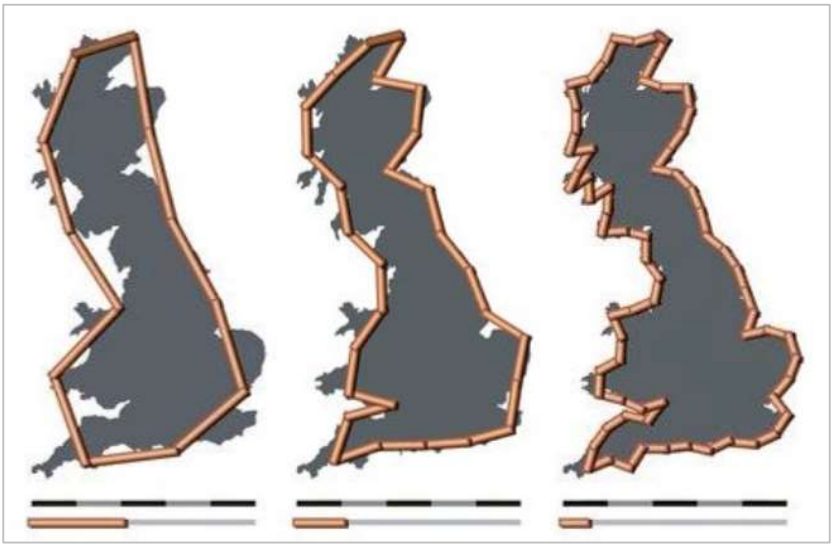

Figure 2.4. Coastline paradox (Jahanmiri & Parker, 2022)

was later explained by fractal geometry: the 'length' of a coastline is not fixed, but scale-dependent (Salingaros, 2003).

This paradox demonstrates that some forms cannot be adequately described by conventional Euclidean measures and instead follow fractal characteristics in which complexity increases with resolution. As one zooms in, finer details often mirror the larger structure – a characteristic seen in natural forms like trees and rivers, as well as in urban systems where neighborhoods or street layouts reflect broader city patterns (Salingaros, 2000; Lorenz, 2003; Kartal & Inceoglu, 2023).

While these features are broadly observed in natural and technological systems, they are particularly useful for interpreting the built environment. Cities frequently display fractal characteristics in their street networks, block arrangements, and built densities, depending on the scale of observation (Batty & Longley, 1994; Lu et al., 2016; Kartal & Inceoglu, 2023). By applying fractal geometry to urban morphology, researchers can reveal the generative processes shaping spatial organization and describe how complex forms emerge from repeated local transformations (Jevric et al., 2014; Zhang & Li, 2012; Jin et al., 2017).

Fractal geometry and Urban form

Urban growth is a dynamic process that results from the collective activities of individuals and communities over time, leading to the development of complex, layered structures (Ben-Hamouche, 2009; Kartal & Inceoglu, 2023). These processes generate forms that are difficult to describe using Euclidean geometry, which relies on rigid shapes and fixed dimensions (e.g., 1 for lines, 2 for areas, 3 for volumes). Instead, many urban layouts often require the use of rational numbers to express their inherent complexity.

Fractal geometry, unlike Euclidean geometry, provides a means to quantify and analyze the irregularity and self-organizing nature of urban environments. Figure 2.5 presents three distinct fractal patterns: a leaf vein, the Sierpinski Carpet, and an urban pattern. While these forms differ in their context and scale, they share a common recursive logic in which smaller components reproduce aspects of the larger structure (Lorenz, 2003; Jiang, 2007, 2021).

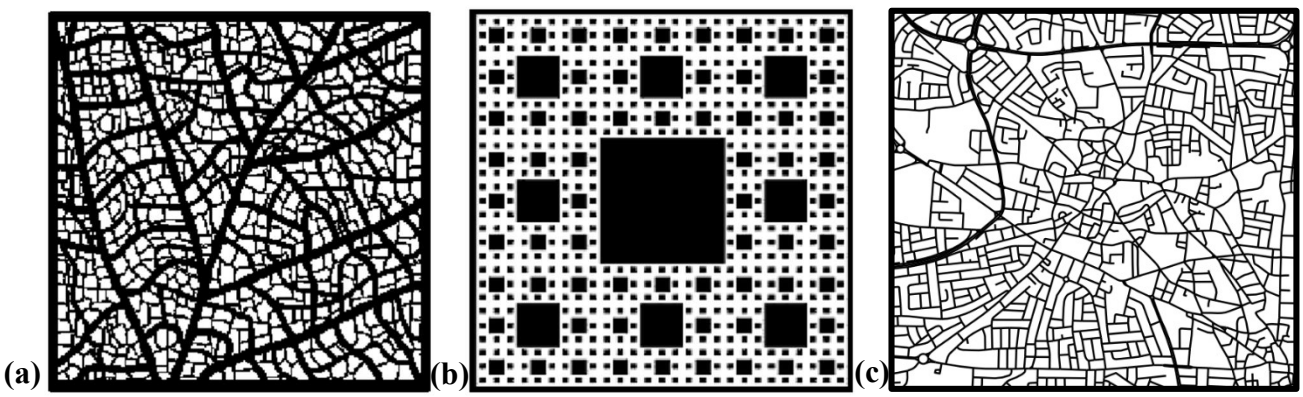

Figure 2.5. Examples of fractal pattern.

a) a leaf vein (Jiang, 2021) b) the Sierpinski Carpet (Jiang, 2021) c) street network of Larnaca (Cyprus)

The leaf vein demonstrates recursive branching patterns that distribute nutrients efficiently across the leaf's surface (Figure 2.5a). This structure resembles flow distribution in urban street networks (Figure 2.5c) (Wang et al, 2017). Regarding the Sierpinski Carpet (Figure 2.5b), it is often referenced since mirrors the scaling and void patterns seen in cities (Jiang, 2021). This fractal is formed by recursively subdividing a square and removing certain sections, creating a pattern that appears similar regardless of the scale at which it is examined. Therefore, the concept of fractals, initially studied in mathematical contexts, has become increasingly relevant in understanding the geometry of urban landscapes.

The presence of fractal patterns in urban structures is not limited to visual similarities; it also reflects underlying spatial dynamics shaping cities (Batty, 1997; Encarnacao et al, 2012). For instance, building and street-network densities typically decline progressively outward from the center to the periphery, forming a self-replicating spatial gradient (Lu & Tang, 2004; Kalapala et al., 2006; Zhang & Li, 2012; Lu et al, 2016). These findings highlight the self-organizing nature of urban form, reinforcing the idea that fractal principles not only describe physical structures but also capture the underlying dynamics of urban development and spatial organization.

Fractal Dimension as a measurement tool

A central metric in fractal analysis is the fractal dimension (D), which quantifies how space is filled or occupied as one zoom into finer scales (Mandelbrot, 1983; Batty, 2012; Wang et al., 2017; Jahanmiri & Parker, 2022). It typically ranges between 1 and 2 (Figure 2.6), reflecting the intermediate complexity of urban forms - more intricate than a simple line (D = 1) but not fully occupying a plane (D = 2) (Batty & Xie, 1996; Jevric et al., 2016).

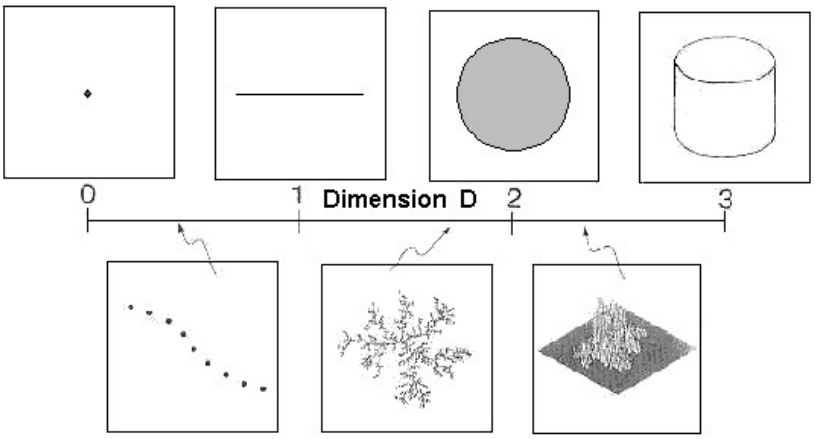

Figure 2.6. Comparison between the dimensions of traditional and fractal geometries (Batty&Longley, 1994)

This metric helps differentiate between compact and dispersed urban patterns and has been widely applied in the analysis of road networks, building distributions, land-use configurations, and urban sprawl (Lu et al., 2016). Beyond static structure, changes in fractal dimension over time have been used to indicate urban growth dynamics (Chen & Huang, 2019).

An intuitive way to understand this concept is through the example of a fractal tree, where each branch splits into smaller ones, following a consistent ratio (Figure 2.7). At each iteration, the number of branches increases, but their lengths decrease proportionally.

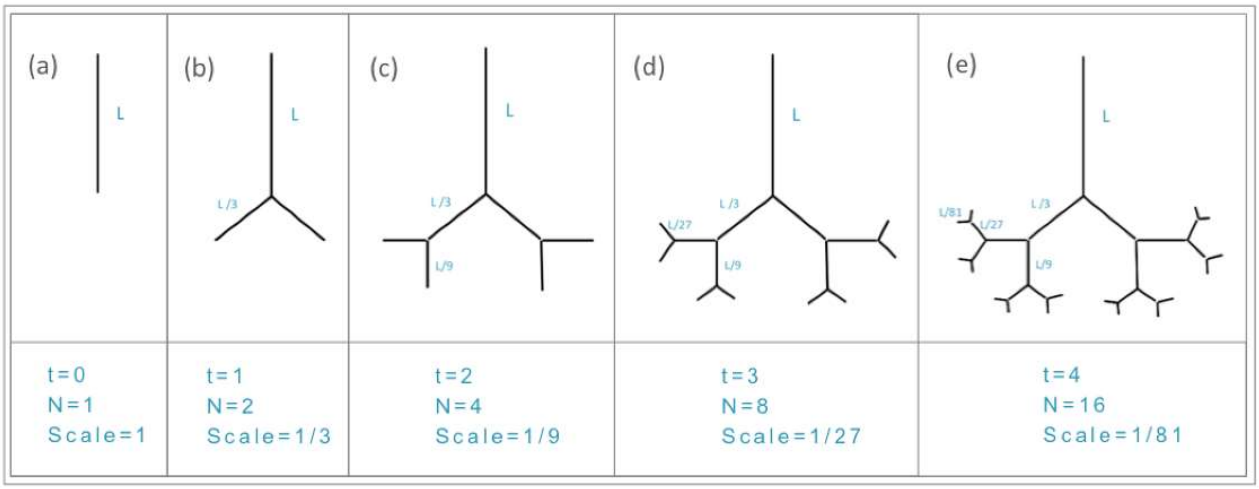

Figure 2.7. Example of a simplified formation process of a fractal tree (Jahanmiri & Parker, 2022)

The fractal dimension can be estimated using the relation:

$$D = \frac{\log N}{\log S}$$

where t refers to iteration stage, N is the number of branching at each iteration, and S is the scaling factor by which the branches shrink. For example, if each branch splits into two smaller branches, each half the length of the previous, then $N = 2$ and $S = 2$, yielding $D = \log 2 / \log 2 = 1$, which corresponds to a one-dimensional line. However, if the branching pattern is more intricate, filling more space, D approaches value toward 2, indicating a structure more complex than a line but less than a fully filled plane.

Scientific debates and Methodological challenges

While fractal analysis offers a quantitative perspective, its interpretation has been the subject of sustained debate. One recurring critique concerns the reduction of complex urban environments to a single numerical value. Skeptics such as Mulligan (1997) argue that aggregated fractal measures may oversimplify the richness of urban systems and provide limited new insight into their formation. This critique is especially relevant when cities are divided into discrete zones or parcels to calculate a single fractal dimension, as such aggregation may overlook the integrated and holistic nature of urban structure.

Related concerns focus on the explanatory limits of fractal metrics. Although fractal dimension can describe how spatial detail accumulates across scales, it does not inherently account for the socio-institutional processes that shape urban form or explain *why* cities exhibit fractal-like patterns in the first place (Batty, 2008; Tannier & Pumain, 2005). In this sense, fractal measures quantify *outcomes* of urban development rather than the mechanisms that generate them.

A second set of challenges arises from the variability of fractal properties across different components of the built environment. Fractal characteristics are well documented in street networks, urban boundaries, and land-use distributions, yet each component may display distinct scaling behaviors (Frankhauser, 1998). As Chen (2013) notes, a single fractal dimension may therefore be insufficient to represent the entire urban fabric. This observation has prompted discussions about the need to complement fractal dimension with additional morphological indicators to improve the accuracy and interpretability of urban analysis (Batty & Longley, 1994; Batty, 2012; Jahanmiri & Parker, 2022).

A key theoretical link between fractal dimension and urban structure concerns density, since fractal dimension formally expresses how a form fills available space (Batty, 1991; Longley & Mesev, 2002). Higher fractal dimensions indicate more heterogeneous arrangements, with greater diversity in the size and distribution of elements. Yet fractal dimension is not a proxy for density: urban areas with similar density values may exhibit markedly different fractal characteristics (Thomas et al., 2007; Jahanmiri & Parker, 2022). Instead, it complements traditional density-based analysis by distinguishing between compactness arising from uniform structure and compactness emerging from heterogeneous subdivision (Lu et al., 2016; Jahanmiri & Parker, 2022).

Beyond general morphology, fractal analysis has also been applied to land-use configurations and zoning (Batty et al., 2008; Yu & Zhao, 2021; Jahanmiri & Parker, 2022). Studies show that different urban systems often display distinct fractal signatures (Thomas et al., 2007; Batty et al., 2008). For example, research on London's built environment indicates that commercial and industrial areas tend to exhibit higher fractal dimensions due to their irregular layouts, whereas residential districts – typically shaped by more uniform planning – tend to display lower values (Batty et al., 2008). These findings demonstrate how fractal analysis can illuminate spatial inconsistencies or reveal how different zoning practices contribute to variations in urban complexity.

Taken together, these debates underscore that while fractal analysis enriches the study of urban form, its interpretation requires contextual understanding. Cities are shaped by multiple factors, including planning regulations, transportation networks, and historical development trajectories, all of which influence their fractal properties (Batty, 2005; Lu et al., 2016; Jahanmiri & Parker, 2022). A high fractal dimension does not necessarily indicate desirable spatial qualities, nor does a low value imply inadequacy. As Batty and Longley (1994, p. 333) emphasize, the central challenge is to "explore the relationship between city size, fractal dimension, changing densities and changing form", while ensuring that fractal measures complement – not oversimplify – the dynamic and interconnected nature of urban environments.

The role of fractal analysis in contemporary urban studies

Fractal principles underpin computational models designed to simulate urban growth and land-use changes. Since the early 1990s, models like Cellular Automata (CA) and Agent-Based Models (ABM) have employed fractal-based algorithms to replicate urban spatial patterns (Jahanmiri & Parker, 2022). These models apply fractal rules to recreate complex urban structures emerging from simple local interactions (White & Engelen, 1993; van Vliet et al., 2012). For example, White and Engelen's CA model of Berlin's urban growth demonstrated that the fractal dimension of their simulated city closely mirrored real-world measurements (White & Engelen, 1993). These models provide valuable predictive insights for urban planners, allowing them to test various "what-if" scenarios and forecast potential urban developments based on historical trends. However, while effective at simulating iterative urban processes, these models are best suited for exploring hypothetical urban outcomes rather than predicting actual urban dynamics (Batty, 2012; Batty & Milton, 2021).

In recent years, fractal analysis has become more integrated with GIS and remote sensing technologies, expanding its applications in contemporary urban research. This integration has been crucial for predicting urban expansion and evaluating resilience to disruptions like climate change and infrastructure failures. Additionally, machine learning algorithms have started to incorporate fractal analysis to better understand urban dynamics. For instance, convolutional neural networks (CNNs) are used to detect fractal patterns in satellite imagery or street network data. These tools help researchers model urban growth trajectories, identify areas at risk of sprawl, and assess how cities might respond to changes in population or environmental conditions.

Despite these advancements, the core value of fractal analysis within urban morphology remains underexplored in terms accessible to both academics and practitioners. Understanding its limitations, particularly in relation to planning policies and socio-economic dynamics, is crucial for making meaningful contributions to urban studies. Future research should integrate fractal measures with other urban metrics to develop a more comprehensive framework for urban analysis and planning. Combining fractal analysis with measures of connectivity and accessibility, could offer deeper insights into urban systems, bridging the gap between mathematical abstraction and practical planning needs. As cities evolve, refining these methodologies will be crucial for designing more resilient and adaptable urban spaces.

2.5.3. Relevance for this study

In this research, the adoption of fractal analysis is grounded in the recognition that urban street networks often exhibit fractal characteristics (Batty & Longley, 1994; Badhrudeen et al., 2022). Instead of relying on qualitative descriptions of irregularity, fractal dimension provides a formal metric to quantify how densely and unevenly urban space is filled (Jahanmiri & Parker, 2022). This makes it particularly well suited for

the comparative purposes of this research, which examines whether differences in street-network configuration correspond to systematic variations in their underlying spatial structure.

2.6. Network-based measures of street structure

Urban form cannot be fully understood through geometric or morphometric attributes alone. While block size, parcel subdivision, and spatial layout express the physical grain of the built environment, the relational structure of streets emerges from the connections among individual segments and junctions. These interdependencies create structural properties that are not visible from geometry alone and often reveal deeper organizational logics embedded in the network (Hillier & Hanson, 1984; Jiang & Claramunt, 2004; Boeing, 2018; Merlo & Lavoratti, 2024). Street networks therefore provide a critical lens through which the configurational dimension of urban form becomes legible.

Street configuration reflects the cumulative actions that shape how places connect, separate, or integrate across scales. Even networks that appear visually similar may differ substantially in their underlying relational structure – whether through variations in junction arrangement, degree distribution, or path redundancy (Porta et al., 2006; Cardillo et al., 2006). For this reason, network-based indicators have become central to contemporary urban morphological research, complementing geometric measures by revealing how spatial elements relate to one another within the broader system.

This section reviews key literature on the use of graph-theoretical and spatial-network indicators in understanding street-structure complexity. It situates these measures within urban morphology rather than treating them as proxies for mobility or performance, aligning with the analytic goals of this study.

2.6.1. From morphological form to structure capacity

Urban form is often described and analyzed through its morphological typologies – whether organic, grid-based, or hybrid – captured through metrics such as block size, street spacing, and fractal dimension. These measures describe *what* the physical structure looks like. However, they do not describe *how* the elements relate or how the network is organized as a system (Marshall, 2004; Boeing, 2018).

Network analysis addresses this gap by conceptualizing street systems as graphs composed of nodes and edges. This allows the structure to be examined in terms of:

- **Connectivity** – how many links exist and where;
- **Reach** – how far one can walk within a certain number of steps;
- **Redundancy** – how many alternative paths are available;
- **Continuity** – how street alignments extend across space;
- **Granularity** – how evenly connections are distributed;

These properties reveal systemic structure independent of geometric appearance. A street network may appear dense but its internal connections are fragmented, or it may appear coarse yet maintain strong coherence through efficient connections (Crucitti et al., 2006; Porta et al., 2006; Hillier, 1996). The shift from morphological form to structural capacity therefore extends the analysis of urban complexity from shape to relations. As Jiang & Claramunt (2004) note, street networks are *"both geometric entities and relational structures",* and their dual nature requires analytical tools capable of capturing both dimensions.

2.6.2. Topological indicators of street networks

To provide a structural reading of street networks, a wide range of indicators has been developed (Wu et al., 2021). These measures vary in scope - some are topological, describing how elements are connected regardless of geometry, while others are spatial, capturing the physical distribution and density of street components (Xie & Levinson, 2006). Together, they provide complementary insights into how well a network supports movement, access, and internal flow.

This study draws upon both graph-theoretical concepts and spatial network analysis to select relevant metrics. While indicators such as average path length describe the topological structure of connectivity, others like intersection density reflect the spatial intensity of the network. The most relevant measures within the context of street-network analysis are presented in Table 2.1.

Table 2.1. Core indicators for accessibility and connectivity

Level	Type	Measure	What it describes	Key reference(s)
Node-level	Topological	Degree centrality	Number of edges (streets) connected to a node – indicates local connectivity.	Porta et al. (2006); Barthelemy, 2011;
	Topological	Betweenness Centrality	How often a node/edges lies on shortest paths – control over flows.	Porta et al. (2006); Wasserman & Faust (1994)
	Topological	Closeness Centrality	Mean distance from a node to all other ones – indicates accessibility.	Porta et al. (2006); Barthelemy, 2011;
	Spatial	**Reachability index**	Nodes reachable within a set network radius (e.g., 600m) – walk-scale access.	Sevtsuk & Mekonnen (2012);
Edge-level	Spatial	**Average shortest path length (ASPL)**	Mean shortest-path distance between all node pairs in the network.	Cardillo et al. (2006);
	Spatial	**Average edge length**	The mean physical length of all edges (street segments) in the network.	Marshall (2004); Boeing (2018);
	Spatial	**Intersection density**	Number of junctions per km² – proxy for permeability and spatial intensity.	Marshall (2004); Boeing (2018);
Network-level	Spatial	Road density	Total street length per km² – indicates overall network provision/availability.	Marshall (2004); Boeing (2018);
	Topological	**Meshedness coefficient**	Normalized loop richness – captures redundancy and alternative routes.	Strano et al. (2012); Fleischmann et al. (2025);
	Topological	**Mean straightness**	The inverse of the detour ratio, i.e. measure of how direct a route is.	Vragović et al. (2005); Labatut (2018);

In what follows, this study adopts a focused set of indicators. Two core metrics – Average shortest path length (spatial) and Reachability index (spatial) – are used to assess relational compactness and accessibility, without requiring large territorial coverage. Conversely, indicators such as betweenness

centrality and global closeness – commonly used to assess through-movement or flow concentration – are excluded due to the limited spatial coverage of the sample areas. In compact study zones, global centrality values tend to be skewed or uninformative, as most nodes lie within proximity and the network lacks larger-scale structure for meaningful path differentiation (Barthélemy, 2011). Instead, the focus is placed on metrics that are sensitive to local variation and urban granularity**,** aligning with the goals of evaluating spatial heterogeneity and adaptability within compact urban settings.

Recent work has emphasized the value of combining geometric and topological indicators when assessing urban complexity (Boeing, 2018; Zhao et al., 2023). While fractal dimension captures the degree of geometric subdivision and irregularity, network measures reveal how those subdivisions translate into relational structure. Together, they provide a more complete understanding of how street networks differ in form, particularly in cases where visual or historical distinctions alone do not fully explain underlying structural variation.

In this thesis, graph-based metrics are used to compare paired districts shaped by contrasting typological trajectories. These measures are not treated as proxies for movement, functioning, or livability but as structural descriptors that allow differences in network configuration to be identified and assessed. When considered alongside fractal dimension, they form a consistent analytical framework for evaluating geometric complexity within the built environment.

2.7. Synthesis & Research Gap

Across the diverse strands of urban morphology research, several gaps remain unresolved. First, studies of geometric complexity and network structure tend to evolve along parallel but weakly connected trajectories. Work on fractal geometry emphasizes spatial subdivision, scale-dependency, and irregularity (Batty & Longley, 1994; Lu et al., 2016), while graph-theoretical research focuses on connectivity, hierarchy, and topological performance (Porta et al., 2006; Barthélemy, 2011). Only limited research examines how geometric complexity and relational structure interact, particularly within street networks shaped by different development processes. As a result, the relationship between fractal richness and structural accessibility remains empirically underexplored.

A second gap concerns the scale of analysis. Many network-based studies rely on global centrality indicators optimized for metropolitan or citywide networks. However, these measures often lose discriminatory power in compact districts, where nodes lie in proximity and the network lacks larger-scale differentiation (Barthélemy, 2011). This creates a methodological blind spot for understanding variation within historic centers, fine-grained morphologies, or small-area comparative studies. There is a clear need for local-scale, structure-sensitive indicators that reveal internal heterogeneity in dense urban networks.

A third gap is the lack of controlled comparative research. Existing literature often examines single cases or cross-city comparisons where contextual variables differ substantially. Few studies adopt paired-district designs that hold socio-spatial context constant while isolating morphological differences. Consequently, it remains unclear whether contrasts between incremental and planned morphologies produce measurable differences in geometric complexity or topological structure.

Finally, there is limited work that explicitly links fractal measures with graph-based indicators in a unified analytical framework. While fractal dimension captures the geometric richness of urban form, it does not explain how that form structures movement or accessibility. Conversely, network metrics reveal relational properties but do not quantify how the underlying geometry varies. Integrating these two perspectives offers a more comprehensive basis for identifying structural differences that are not evident through visual or historical analysis alone.

Taken together, these gaps justify the dual-method approach adopted in this thesis. By combining fractal dimension with selected local-scale network indicators, and applying them to paired districts shaped by contrasting developmental trajectories, the study provides new empirical evidence on how geometric and topological complexity correspond within the built environment.

Chapter 3: Methodology

This chapter presents the methodological framework developed to investigate how contrasting street network patterns – particularly those observed in historical (organically evolved) and modern (planned grid) urban zones – relate to the spatial configuration of street form across selected European cities. The analysis is grounded in the recognition that street networks display varying degrees of internal complexity, which is captured not only through their visual geometry but also through their organizational connectivity. The chapter is organized as follows:

- Section 3.1 outlines the analytical framework and rationale guiding the methodological choices;
- Section 3.2 explains the criteria used for selecting study areas and compiling spatial datasets;
- Section 3.3 details computations of fractal dimension as a geometric measure;
- Section 3.4 specifies graph-based indicators used to characterize street-network structure.

3.1. Overview of Methodological Approach

The analytical strategy adopted in this study centers on examining the geometric and structural properties of urban street networks through two primary dimensions:

- **Geometric texture**, referring to the degree of spatial irregularity and multi-scale variation observed in a street pattern. This aspect is evaluated through fractal dimension analysis, which expresses how fragmented or continuous street geometry is across spatial scales.
- **Street network structure** is characterized by a set of graph-theoretic indicators, including intersection density, average edge length, meshedness coefficient, reachability index, mean straightness, and harmonic mean shortest path length. These metrics describe how street networks are connected, how direct paths are, and the extent of route redundancy.

Rather than classifying urban forms into rigid typologies (e.g., “organic” vs. “grid”), the study uses a paired, intra-city comparative design: for each city, one organically evolved historic core and one planned modern district are analyzed within a common spatial extent. This design controls for local context (e.g., culture, topography, policy) and allows a direct structural comparison between distinct spatial configurations.

The methodological approach integrates:

- GIS-based preprocessing of spatial vector data,
- Fractal analysis using box-counting methods,
- Computation of morphological and topological indicators using Python-based tools.

Throughout, the study is careful to distinguish between structural properties (i.e., the geometric and topological features of the street network) and actual urban "function" or use (i.e. walkability). All indicators measure physical or structural potential for pedestrian accessibility and connectivity, not observed movement, traffic flow, or behavioral outcomes. Any reference to accessibility or connectivity in the following chapters refers to the network's *structural capacity* – the extent to which its configuration could support pedestrian movement.

This integrated methodological approach enables a systematic comparison of how historic and modern street networks differ in their geometric complexity and structural arrangement, laying the groundwork for subsequent analysis and interpretation.

3.2. Study Area and Data Sources

3.2.1. Study Area Selection

This study encompasses 100 European cities, selected to capture a broad spectrum of urban contexts across the continent. To ensure balanced geographical coverage, Europe was divided into four macro-regions – North, West, South, and East - within each, a balanced set of countries was chosen (Figure 3.1). From each country, five cities were included, giving equal weight to each macro-region. The full list of countries and cities is presented in Appendix A-1.

Figure 3.1. Map of countries included in the analysis

Within each city, two distinct zones were identified (Figure 3.2):

- **Historic district:** Characterized by organically evolved, irregular, and fine-grained street patterns.
- **Modern district:** Defined by systematically planned, regular, and grid-like layouts.

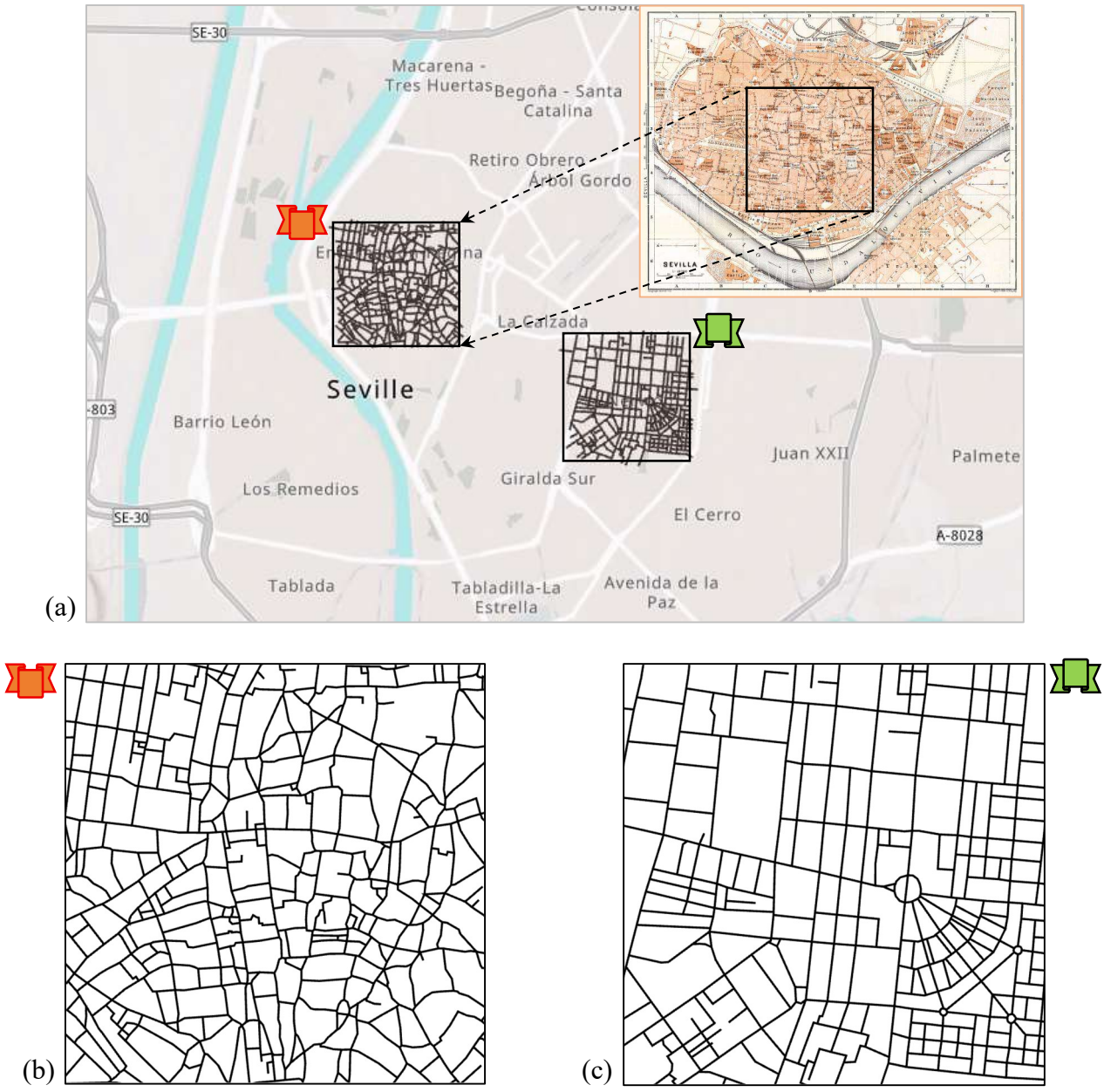

Figure 3.2. a) Road network boundaries in Seville; (b) Zoomed-in view of the historical area; (c) Zoomed-in view of the modern area

The primary selection criterion was the presence of a *visually and structurally distinct* contrast between these two district types. Cities were included only if they exhibited this clear dichotomy (Figure 3.3); cases lacking a meaningful organic-planned distinction (such as Turin, with a predominantly grid-based fabric) were excluded to maintain analytical rigor (Figure 3.4). The focus was further narrowed to residential or mixed-use neighborhoods representing everyday urban life, with industrial areas and zones fragmented by major infrastructure (e.g., highways, railways, rivers) excluded to avoid spatial discontinuities.

Figure 3.3. Thessaloniki (Greece) – mixed grid and organic layout

Figure 3.4. Turin (Italy) – Predominantly grid-based layout

To standardize comparisons, each zone was delineated as a 1.2 km × 1.2 km area, reflecting a typical walkable neighborhood scale (about 10–15 minutes on foot). This fixed spatial extent controls for differences in city size and ensures that all metrics are comparable across cases. Zones were selected and mapped at a consistent working scale (1:10,000) to capture relevant detail while minimizing edge effects.

The overall selection approach prioritized morphological clarity – distinct patterns that could be consistently analyzed using fractal methods. In this context, while hybrid and alternative morphologies - such as radial-concentric forms or curvilinear garden city layouts – represent important aspects of urban morphology, they were excluded from this study. This is due to the methodological constraints of fractal dimension techniques, which are more effective when applied to patterns that exhibit geometric regularity or scale-invariance – characteristics that hybrid forms often lack.

3.2.2. Dataset Compilation

Spatial data for the street networks were primarily sourced from OpenStreetMap (OSM) and ArcGIS Online, supplemented by national or regional geoportals where available geoportals (e.g., *Geoportale Regione Siciliana* for Southern Italy). The OSMnx Python library (Boeing, 2017) was used to automate the extraction, formatting, and initial cleaning of street network data. Graph topology was simplified to merge contiguous sub-segments into single edges between “true” nodes (i.e., intersections and dead-ends) while preserving edge geometry and lengths attributes (Figure 3.5). This ensured a consistent structural basis for subsequent network indicators.

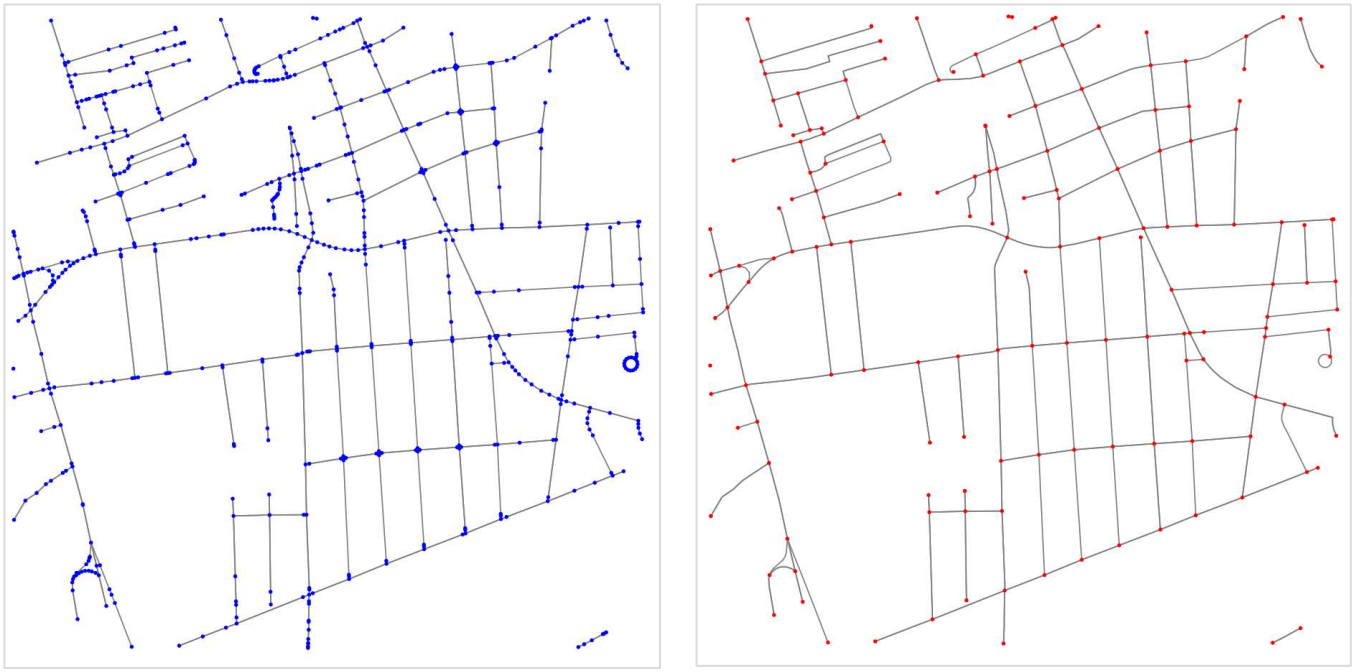

Figure 3.5. Topological correction via graph simplification.
***Left*: Original OSM graph. *Right*: Simplified graph, producing the true topological skeleton.**

While this process produced topologically consistent networks, it did not address limitations in the underlying OSM data, such as incomplete coverage or generalization. In cities where OSM coverage was incomplete – particularly within historic cores – georeferenced historical cartographic maps were used to validate street layouts and ensure accurate reconstruction of legacy street structures (Figure 3.6)

As a result, historic cores required special treatment to ensure spatial authenticity. Scanned cartographic maps dated from the 17th to 19th centuries (Figure 3.6) were collected and georeferenced using known control points to align with modern spatial coordinates. These georeferenced maps were overlaid with OSM-derived road data to validate the presence and configuration of legacy street patterns, ensuring accurate identification and extraction of historic network structures.

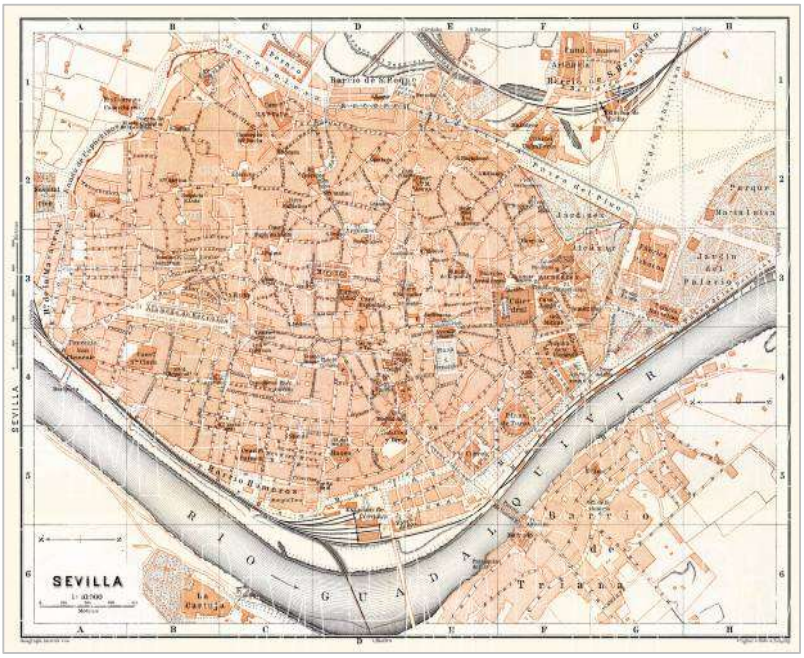

Figure 3.6. Seville (Spain) city map (Wagner & Debes, 1899)

To further validate both historic and modern zones, high-resolution imagery from Google Earth Pro was employed. This visual cross-referencing confirmed phases of urban growth, differentiated pre-industrial organic development from planned post-industrial expansions, and flagged any inconsistencies in the raw

data. Google Earth's historical imagery feature proved especially valuable in verifying the temporal accuracy of the selected zones.

Next, with validated datasets in place, preprocessing was undertaken to prepare the data for fractal geometry analysis using Fractalyse 3.0 software. This included dissolving multipart lines, correcting disconnected segments, removing duplicates, and consolidating parallel features such as sidewalks and carriageways into single lines (Figure 3.7). These steps prevented inflated density values and ensured robust measures of geometric texture**.**

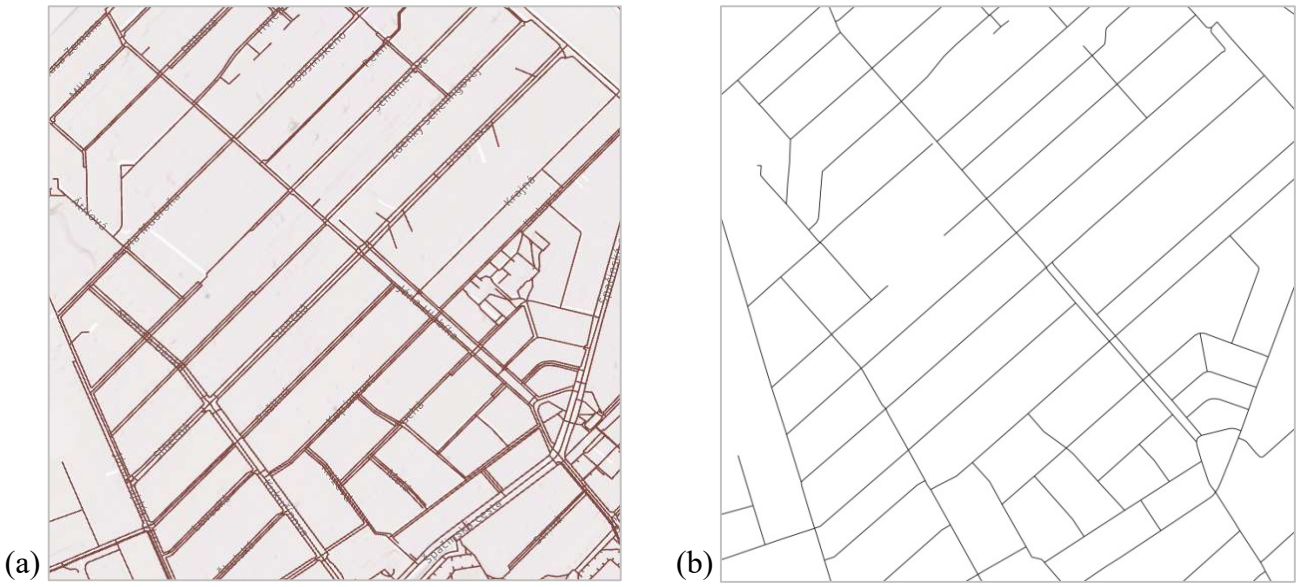

Figure 3.7. Example of network preprocessing in Trnava (Slovakia): (a) original OSM road data; (b) cleaned and unified street network

Finally, all cleaned and validated datasets were exported in shapefile format for use in both fractal dimension analysis (Section 3.3) and graph-theoretic assessment (Section 3.4).

3.2.3. Workflow and Limitations

The entire geoprocessing workflow is summarized in Figure 3.8, illustrating each stage from data extraction to street network cleaning and export as shapefiles for analysis.

Despite these measures, minor uncertainties remain – particularly in cities with limited open-source data coverage or variable-quality historical maps. However, these are mitigated by cross-validation and visual inspection, making relative comparisons robust and minimizing the likelihood of systematic bias. These limitations and their implications are discussed in the Research Limitations section.

Full Python scripts are included in Appendix A-2 to support methodological transparency and enable future replication of the approach.

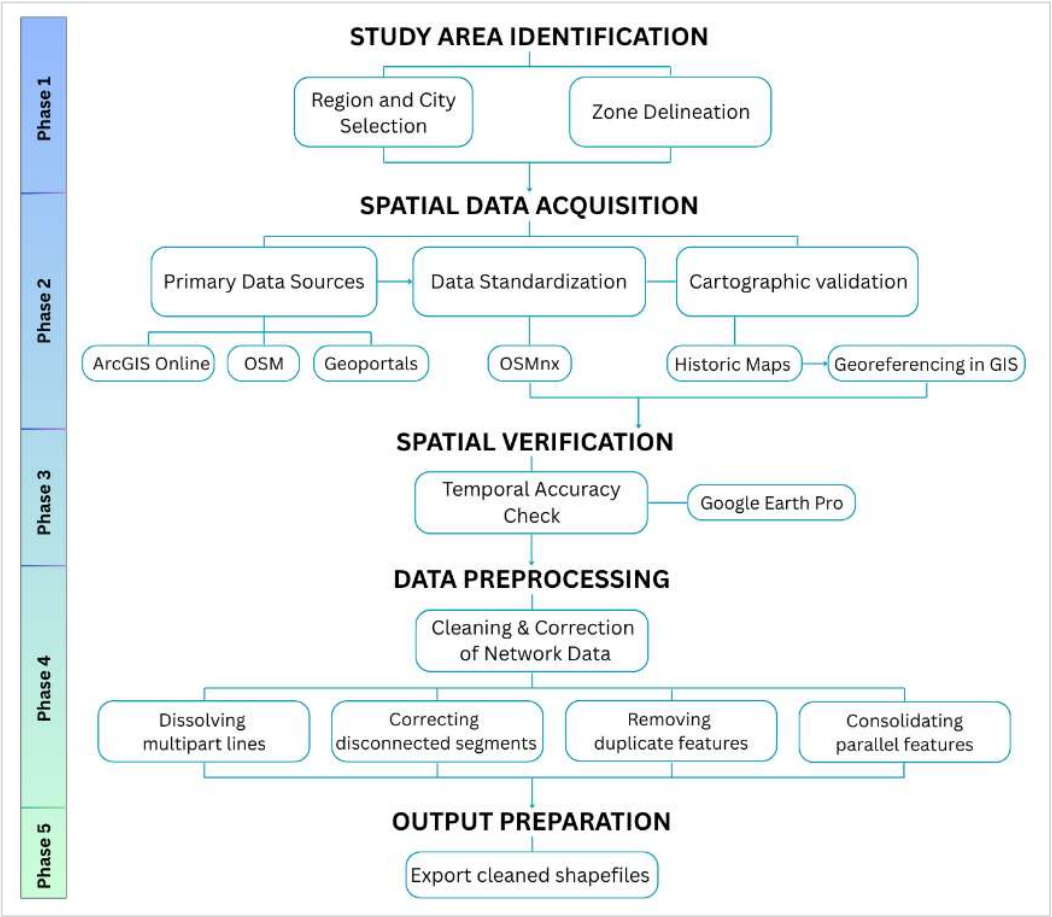

Figure 3.8. Geoprocessing workflow diagram

3.3. Fractal lens on urban street texture

Fractal analysis provides a robust framework for capturing geometric irregularity and hierarchical organization in road networks (Batty & Longley, 1994; Salingaros, 1998). This section details the methodological approach for estimating the fractal dimension (D) of each study area's street network, justifying the selected technique, and outlining the analytical workflow.

3.3.1. Method Selection and Software

Fractal dimension (D) can be estimated through several techniques, all grounded in logarithmic scaling relationships (Jevrić et al., 2016). These methods capture how an object's spatial detail varies across scales (Jahanshiri & Parker, 2022). Among the available options, the box-counting method was selected for its conceptual simplicity and adaptability to spatial network data (Frankhauser, 2004; Jevrić et al., 2016; Babič et al., 2022).

The D calculations were performed using Fractalyse 3.0 software, which implements the box-counting algorithm in a user-friendly environment designed for spatial analysis.

3.3.2. Computational Procedure

Data Preparation

Fractalyse supports both vector and raster formats, providing flexibility for urban form analysis. In this study, the road network data were maintained in vector format as line features extracted from ArcGIS (see Section 3.2). These shapefiles were loaded into Fractalyse, forming the basis for the fractal analysis while preserving geometric detail.

Counting Procedure

Once the data were imported, the box-counting procedure was automatically applied by the software. This involves overlaying a quadratic grid of varying cell sizes (ε) onto the vector network. At each iteration, the number of grid cells (N) intersected by the road segments was recorded, while systematically reducing the grid size. As the box size decreases, the level of geometric detail captured by the analysis increases, enabling analysis of multi-scale irregularity (Figure 3.9).

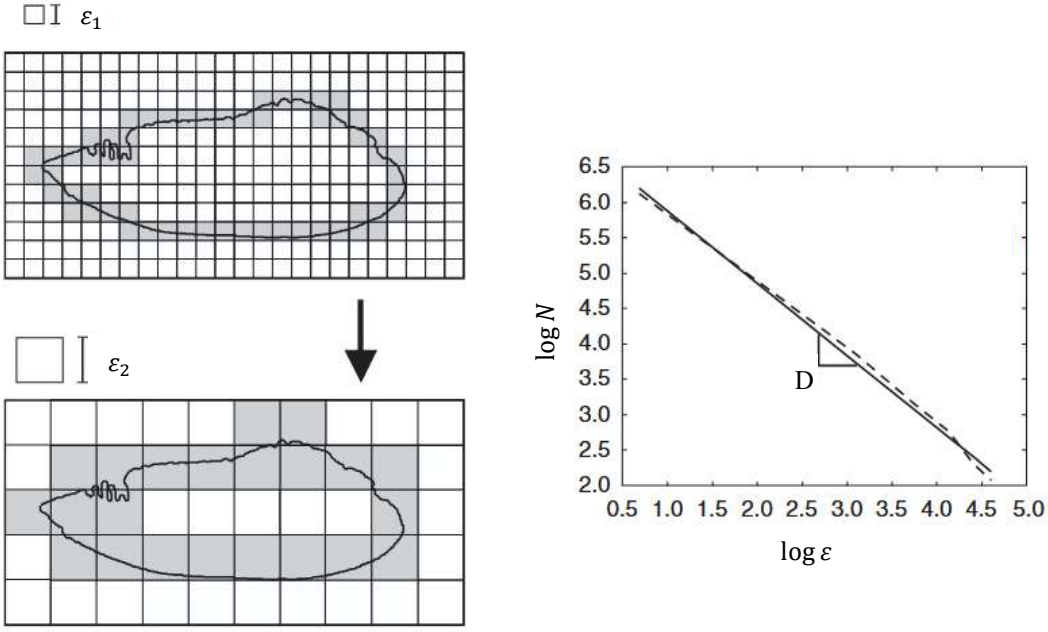

Figure 3.9. Schematic overview of the box-counting method for fractal analysis (Piera et al, 2005, p. 808)

The relationship between the number of occupied boxes (N) and the grid size (ε) follows a linear trend in logarithmic space, expressed as:

$$log\, N = -\, D * log\, \varepsilon + b \qquad (1)$$

where the slope of the fitted line represents the fractal dimension (D) and the intercept (b) is a constant. In this way, the D quantifies how the structural detail of the street network evolves across scales, acting as a geometric metric that expresses how thoroughly a pattern fills two-dimensional space.

Estimation

After the counting process, Fractalyse generates an empirical curve based on equation (1) and displays the results in the *Estimation* frame. The software also calculates the goodness-of-fit (R^2) to assess the goodness

of fit between the empirical data points and the fitted line. A higher R^2 indicates a stronger linear relationship, confirming the fractality of the urban pattern (Caglioni & Giovanni, 2004; Sreelekha et al, 2017). Conversely, a low correlation coefficient may suggest that the pattern does not exhibit fractal properties or that it is multifractal, in which case the data can be subdivided into separate scale ranges. In addition, Fractalyse reports the *p*-value for the regression, which should be below 0.001 to confirm statistical significance that the obtained relationship is unlikely to have occurred by chance.

Figure 3.10 illustrates the stages of this process, from data import to the estimation output.

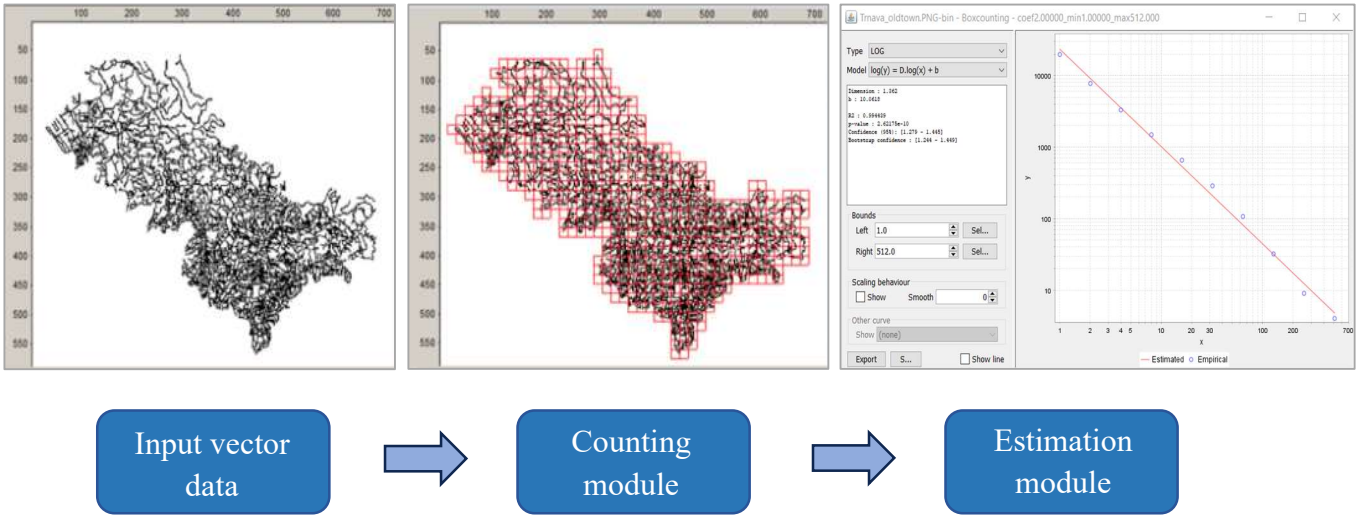

Figure 3.10. Calculation of fractal dimension using Fractalyse 3.0 software (Daniel et al, 2021)

This procedure was applied to 100 cities to analyze and compare their urban road network patterns. Any differences in the fractal dimension values (D) were interpreted as indicators of variations in road network space-filling density and multi-scale detail between the different urban zones.

3.3.3. Output and Interpretation

For every sampled district, the software generates a log–log plot of the number of occupied grid cells (N) against the box size (ε). As discussed earlier, the slope of the fitted line represents the estimated fractal dimension (D), which is displayed alongside the goodness-of-fit (R^2) of the log–log regression, p-value, and confidence intervals (Figure 3.10). The resulting D values typically fall within the expected range between 1 and 2, indicating varying degrees of branching or fragmentation present in street network (see Section 2.4). Values closer to 1 correspond to structures with more linear or directionally consistent configurations, while values approaching 2 reflect forms that spread more irregularly and occupy more of the two-dimensional space. Intermediate values indicate geometries that are more complex than a line but do not fully cover the plane. Thus, the recorded D serves as a central indicator for comparing the geometric character of historic and modern urban zones, forming the foundation for later analysis of their street network structure and potential for pedestrian accessibility.

3.4. Unpacking street network structure

Following the fractal analysis of spatial texture (Section 3.3), this section examines the structural dimension of urban street networks. Whereas fractal dimension captures the degree of geometric irregularity, the indicators introduced here quantify the morphological and topological organization of the network. Together, they reflect how street systems are organized to support pedestrian accessibility, connectivity, and travel efficiency.

To this end, the network is examined through two complementary lenses:

- **Morphological indicators**, which describe the physical arrangement of street pattern, focusing on urban grain and overall density. These measures reflect the tangible configuration of street networks – whether they form dense, walkable grids or more irregular, organic patterns.
- **Topological indicators,** which assess the relational properties of the street network by measuring how efficiently nodes are connected, how direct routes are, and how resilient the system is to disruption.

By bridging urban morphology with network science, this typology enables a multi-dimensional reading of street systems that goes beyond geometric description to include their structural logic. All indicators were computed using automated Python scripts (OSMnx, NetworkX, momepy), with consistent spatial preprocessing applied to each of the 200 urban samples (100 cities × 2 zones). All spatial data were projected to a local metric coordinate system to ensure valid computation of distances and areas.

The resulting indicators were then compiled into a unified database in the form of a master DataFrame, where each row corresponds to a specific urban sample and each column represents a quantified metric. This structure supports statistical comparison across cases and zones, and supports subsequent correlation and clustering analysis. The following subsections present the selected indicators grouped according to their conceptual focus – morphological (Section 3.4.1) and topological (Section 3.4.2) categories.

3.4.1. Morphological Indicators: Form-Focused Metrics

To examine the spatial grain of street networks, this study first considers a set of morphological indicators that describe the local geometric configuration of the street fabric. These include *average street (edge) length*, which measures the mean length of all street segments (edges) and acts as a proxy for block size and urban granularity; and *intersection density*, which reflects how tightly nodes are packed within the study area, indicating the overall intensity of the street network.

Each indicator is defined mathematically and linked to the Python libraries used for automated computation across the dataset of 100 cities (Table 3.1). Given the fixed spatial extent of each sample (1.2 × 1.2 km^2), the selected metrics emphasize local configuration rather than global connectivity.

Table 3.1. Morphological indicators used to characterize street network texture

Scale	Indicator	Formula	Units	Python's function
Local	Average Edge Length	$AEL = \frac{\Sigma\ Edge\ lengths}{Number\ of\ edges}$	meters	`momepy.Statistics`
Local	Intersection Density	$ID = \frac{Number\ of\ intersections}{Area\ in\ km^2}$	intersection/km^2	`osmnx.basic_stats()`

Note: All computations were performed on projected spatial networks to ensure metric accuracy.

Together, these measures provide a quantitative account of the physical configuration of street networks, allowing for the distinction between compact grid-like systems and more irregular organic structures without relying on categorical typologies. While morphological indicators emphasize surface-level geometric descriptors, they provide an essential baseline for the more structural analyses developed later in the chapter.

3.4.2. Topological Indicators: Structure-Focused Metrics

While geometric and fractal measures describe the visible spatial form of a street network, they do not reveal how street segments are arranged in relation to one another. To capture this internal organization, the analysis incorporates a set of graph-theoretic indicators that quantify structural properties such as reachability, compactness, route detour, and redundancy (Table 3.2). These measures do not describe movement or flow, but they provide a structural basis for comparing how different street layouts organize spatial connections.

Such differences become especially relevant when geometric indicators alone suggest similar spatial characteristics. Two street networks may share comparable intersection density or block size, yet differ substantially in how segments link, branch, or form loops. Topological measures therefore allow distinctions in connectivity and route options that may not be evident from geometric analysis alone, offering a deeper understanding of how street networks are configured.

Table 3.2. Topological indicators are used to assess street network connectivity and structure

Scale	Indicator	Formula	Units	Python's function
Local	Reachability index	For each node i, count nodes j such that $d(i,j) \leq 600\ m$; average across all i.	nodes	Custom Python function using NetworkX (Dijkstra algorithm)
Local	Meshedness Coefficient	$M = \frac{E - N + C}{2N - 5C}$ where E = № edges, N = № nodes, C = № components.	unitless [0,1]	`momepy.Meshedness()`

Global	Mean straightness	$S = \frac{2}{n(n-1)} \sum_{i \neq j} \frac{Euclid_{ij}}{d_{ij}}$ with Euclidean distances from node coordinates and d_{ij} shortest paths by metric length.	unitless [0,1]	Custom Python function using NetworkX (Dijkstra algorithm)
Global	Harmonic-mean shortest path	$L = \frac{N(N-1)}{\sum_{i \neq j} \frac{1}{d_{ij}}}$ where d_{ij} is the shortest path length between nodes i and j along the network.	meters	Custom Python function using NetworkX (Dijkstra algorithm)

Note: Calculations are based on undirected, simplified (near-planar) graphs constructed from OpenStreetMap data. All graphs were projected to a local metric CRS before computing distances; no planarization is applied.

The following interpretive summary clarifies the role of each metric in capturing structural properties of the street network:

- **Reachability index** quantifies local access potential by counting the number of nodes that can be reached within a 600-meter radius. The threshold is commonly associated with a 7–8-minute walking distance in urban studies, but here it functions strictly as a fixed spatial parameter for graph sampling, independent of any modelled behavior.
- **Harmonic-mean shortest path length** represents the average shortest distance between all pairs of nodes in the network. Lower values correspond to more compact and closely connected layout, whereas higher values suggest more sprawling or fragmented structures. For instance, if the harmonic mean is around *490 meters*, this can be interpreted as a typical navigation length within the street system.
- **Mean straightness** captures route directness, defined as the average ratio of Euclidean (straight-line) distance to actual path length. Values range from 0 to 1, with 0.75 meaning that routes are on average 33% longer (detour) than a direct line (i.e., 1/0.75=1.333). This offers a tangible way to assess legibility and alignment in the street structure: a higher value implies less detour, while lower values indicate more circuitous route.
- **Meshedness coefficient** measures how looped or redundant the street structure is – a proxy for choice (i.e., presence of alternative paths and redundancy) in the network. A tree-like (dendritic) system yields values near 0, while more interconnected planar graphs approach 1. Higher meshedness represents greater structural redundancy, which indicates the presence of alternative links and multiple ways to connect different parts of the network.

Together, these indicators complement the geometric and fractal measures introduced earlier by describing how connectivity is structured rather than merely how it is distributed in space. They provide the basis for assessing variation in network organization across different urban contexts.

3.5. Statistical analysis of Metric relationships

To examine how the fractal dimension (D) relates to the structural properties of street networks, two complementary statistical approaches were used. The first - the *paired within-city design* – assesses changes within individual cities by comparing historic and modern districts directly. The second, a *groupwise cross-sectional design*, analyzes the broader associations between D and other network measures separately within the full sets of historic and modern samples. These approaches provide both a city-level view on changes in street network structure and a group-level perspective on street patterns.

3.5.1. Paired within-city correlation analysis

This approach focuses on urban transformation at the city level by directly comparing each city's historic and modern districts. For each city and for each metric, the difference (Δ) is calculated as:

$$\Delta M = M_{old} - M_{new}$$

where M represents any network indicator, such as fractal dimension, intersection density, or reachability index.

The relationship between changes in fractal dimension (ΔD) and changes in other network indicators (ΔMetric) is then assessed across all cities using both:

- **Pearson's r** to detect linear relationships:

$$r = \frac{\sum(\Delta x_i - \Delta\bar{x})(\Delta y_i - \Delta\bar{y})}{\sqrt{\sum(\Delta x_i - \Delta\bar{x})^2} * \sqrt{\sum(\Delta y_i - \Delta\bar{y})^2}}$$

- **Spearman's ρ** to capture monotonic associations independent of distribution shape:

$$\rho = 1 - \frac{6\sum {d_i}^2}{n(n^2 - 1)}$$

  where d_i is the difference between the ranks of paired values.

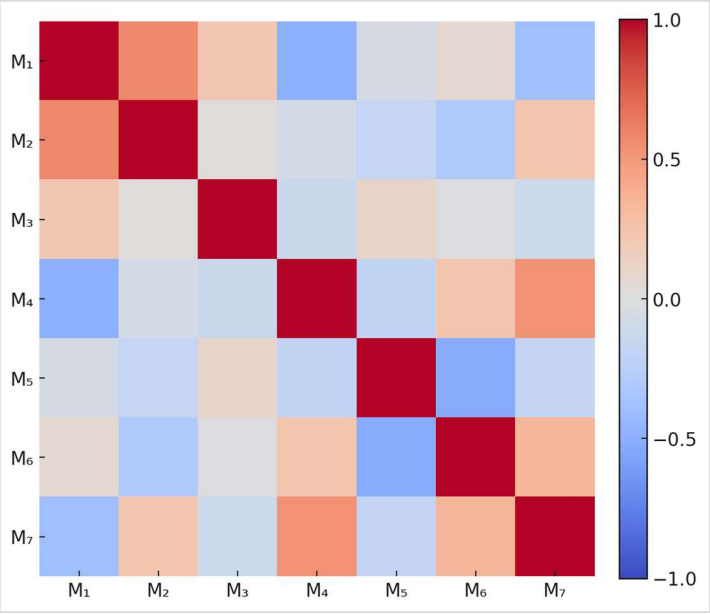

Figure 3.11. Heatmap of the correlation matrix

This method reveals whether increases or decreases in fractal dimension within cities are systematically associated with changes in other aspects of the street network. The results are presented as a correlation matrix (Figure 3.11), which visualizes the strength and direction of these paired relationships for all metrics.

Note: Cells represent pairwise correlations, colored from blue (−1) to red (+1); axes list indicators as placeholders (M_1– M_7). Actual coefficients and labels will appear in the Results chapter.

3.5.2. *Groupwise correlation analysis*

Groupwise analysis reveals the typical structural relationships that exist within historic and modern types of street system, independent of urban transformation processes. It shows whether, for example, higher fractal dimension is generally associated with finer network grain or greater meshedness within either group, regardless of city-specific change. In this analysis, all historic samples are combined into one group, and all modern samples into another.

For each group, both Pearson's and Spearman's correlation coefficients are calculated for D and the relevant network indicators. Results are summarized in correlation matrices (see Figure 3.11), and supported by scatterplots where relevant.

3.5.3. *Reconciling the two methods*

The two approaches can yield divergent outcomes, which is informative. For instance, a metric may correlate with fractal dimension in both samples, yet show weak Δ-correlation if historic and modern districts move in parallel within cities (i.e., there is little internal contrast). Conversely, Δ-correlations can be strong even when within-sample coefficients are modest, indicating systematic shifts in modern districts relative to their historic counterparts.

By comparing these results, the analysis clarifies whether relationships between fractal dimension and street network properties remain consistent across historic and modern settings, or if distinct patterns emerge in each context. Considering both views mitigates risks such as Simpson's paradox and scale effects: cross-sectional patterns may be driven by inter-city composition, whereas Δ highlights genuine within-city transformation.

Interpretation strategy. The Δ analysis is regarded as the main test of co-movement during urban transformation, while the within-sample analysis acts as a diagnostic that clarifies how *D* aligns with network structure across historic and modern landscapes. Convergent evidence across both designs is interpreted as robust; discrepancies are examined to determine whether associations are context-driven (between cities) or genuinely tied to intra-urban change.

Together, these statistical protocols complete the methodological framework. By linking fractal dimension with structural indicators through paired and cross-sectional correlations, the study establishes a rigorous analytical bridge between the measures of geometric texture (Section 3.3) and street network structure (Section 3.4). This integrated design provides the foundation for the **Results** chapter, where the empirical relationships will be evaluated and interpreted across Europe's historic and modern urban landscapes.

Chapter 4: Results and Analysis

4.1. Fractal dimensions analysis

Following the procedure detailed in Chapter 3, fractal dimension values (D) were computed for the street networks of 100 European metropolitan areas. Each city was analyzed in two distinct urban contexts: the historical urban core and a modern expansion zone. This comparative structure enables a consistent assessment of morphological differences associated with different phases of urban development.

To observe broader geographical patterns, the cities were grouped into four macro-regions: Northern, Southern, Western, and Eastern Europe. Within each region, the median fractal dimensions of historical (D_{old}) and modern (D_{new}) districts are reported, as well as the intra-city differences ($\Delta D = D_{old} - D_{new}$). Using medians, rather than averages, minimizes the influence of outliers that might otherwise distort the general tendencies. The following subsections present results for each region.

4.1.1. Northern Europe

The table below summarizes the fractal dimensions for 20 cities across Northern Europe.

Table 4.1. Numeric value of the fractal dimension of Northern European cities

Europe	Country	City	D_{old}	D_{new}	ΔD
North	Denmark	Odense	1.502	1.428	0.074
		Esbjerg	1.490	1.445	0.045
		Aalborg	1.498	1.395	0.103
		Aarhus	1.468	1.403	0.065
		Copenhagen	1.500	1.474	0.026
North	Finland	**Helsinki**	1.392	1.349	0.043
		Tampere	1.365	1.333	0.032
		Mikkeli	1.350	1.321	0.029
		Turku	1.390	1.362	0.028
		Pori	1.393	1.397	-0.004
North	Norway	Hamar	1.438	1.433	0.005
		Bergen	1.512	1.504	0.008
		Stavanger	1.457	1.452	0.005
		Tonsberg	1.437	1.388	0.049
		Oslo	1.479	1.439	0.040
North	Sweden	**Stockholm**	1.419	1.373	0.046
		Gothenburg	1.409	1.390	0.019
		Helsingborg	1.413	1.414	-0.001
		Malmo	1.390	1.354	0.036
		Vasteras	1.400	1.377	0.023
			$\widetilde{D}_{old} = 1.428$	$\widetilde{D}_{new} = 1.396$	$\Delta\widetilde{D} = 0.031$

As shown in Table 4.1, historical city cores in this region have a typical fractal dimension of $\widetilde{D}_{old} = 1.428$, slightly higher than their modern counterparts ($\overline{D}_{new} = 1.396$). While these values reflect the median fractal dimension per district type, the reported difference $\Delta\widetilde{D} = 0.031$, is not derived from subtracting the two medians. Instead, it represents the median of the city-level differences ($\Delta D = D_{old} - D_{new}$), offering a more robust indicator of the typical direction and magnitude of intra-city change across the region.

Among all cities, Bergen (Norway) displays the highest fractal dimensions for both historical and modern parts, with values of 1.512 and 1.504, respectively. This suggests a high degree of continuity in spatial structure across time. In contrast, Aalborg (Denmark) shows the largest intra-city contrast ($\Delta D = 0.103$), indicating a clear morphological shift between its old and new districts.

Notably, cities such as Pori (Finland) and Helsingborg (Sweden) show negligible or slightly negative ΔD values, implying that their modern areas are nearly as (or slightly more) geometrically complex in terms of street layout than their historical counterparts – an atypical pattern within the broader regional trend.

To better visualize these patterns, Figure 4.1 compares the historical and modern fractal dimension values for each city. This graphical representation reinforces the overall trend – older areas are generally more complex – but also makes local deviations more immediately visible.

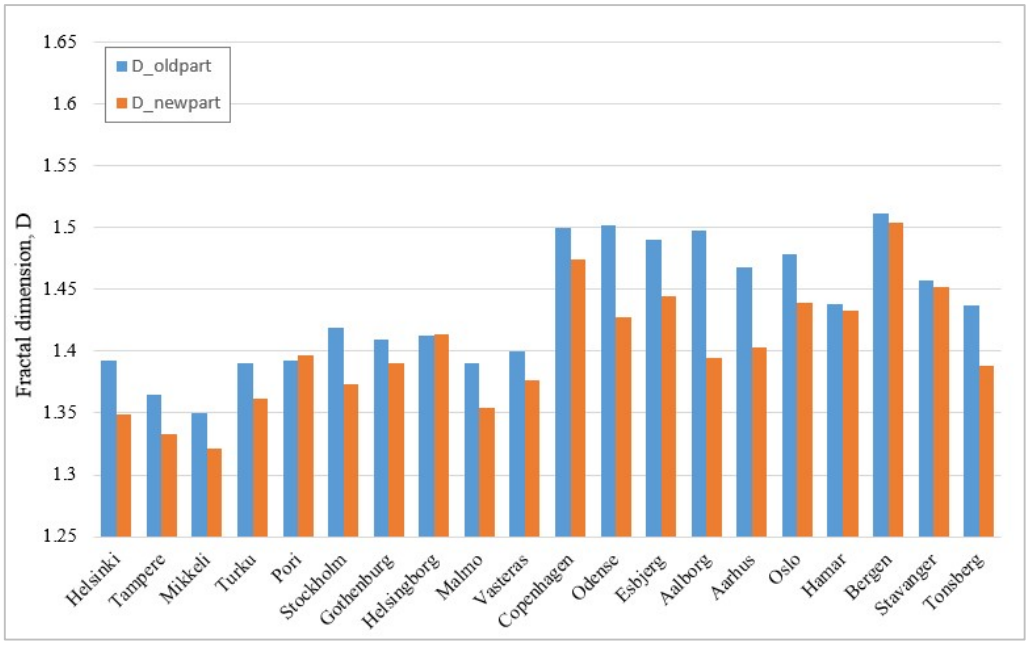

Figure 4.1. Fractal dimension by city: historic vs. modern districts (Northern Europe)

This shift from tabular to graphical representation enhances the interpretability of the results by making contrasts and continuities between historical and modern street forms more apparent. Presenting the data both numerically and visually enables precise comparisons, while also revealing broader pattern recognition, providing a stronger basis for deeper interpretation in later sections.

4.1.2. *Western Europe*

Western Europe presents a wider range of fractal dimension values than Northern Europe, reflecting greater diversity in urban histories and planning. Many cities with well-preserved medieval cores display relatively high fractal dimensions in their historical areas. For example, Béziers (D_{old} = 1.606) and Augsburg (D_{old} = 1.551) have the most fractal street layouts in the dataset – that is, their patterns are notably irregular.

At the same time, modern expansion areas generally show lower values, as seen in Ghent (D_{new} = 1.364) and Bruges (D_{new} = 1.382), though some variation persists across cities. This trend matches expectations for areas shaped by post-war planning, which often favored more regular and standardized block structures. Nevertheless, some cities, such as Toulouse (ΔD = 0.002) and Klagenfurt (ΔD = –0.001), exhibit near-parity between historical and modern districts, suggesting a continuity in street configuration across different historical periods.

To ground these patterns in the broader dataset, Table 4.2 reports the full set of values for cities in Western Europe, including both D_{old}, D_{new}, and intra-city difference (ΔD).

Table 4.2. Numeric value of the fractal dimension of Western European cities

Europe	Country	City	D_{old}	D_{new}	ΔD
Western	Austria	Graz	1.525	1.443	0.082
		Linz	1.463	1.458	0.005
		Innsbruck	1.471	1.462	0.009
		Klagenfurt	1.452	1.453	-0.001
		Vienna	1.527	1.498	0.029
Western	Belgium	Ghent	1.429	1.364	0.065
		Antwerp	1.417	1.392	0.025
		Bruges	1.440	1.382	0.058
		Brussels	1.429	1.418	0.011
		Ostend	1.408	1.399	0.009
Western	Germany	Hamburg	1.456	1.390	0.066
		Düsseldorf	1.453	1.425	0.028
		Nuremberg	1.503	1.475	0.028
		Augsburg	1.551	1.462	0.089
		Cologne (Koln)	1.482	1.449	0.033
Western	France	Bordeaux	1.502	1.461	0.041
		Toulouse	1.513	1.511	0.002
		Dijon	1.512	1.497	0.015
		Rouen	1.542	1.501	0.041
		Beziers	1.606	1.546	0.060
Western	Netherlands	Nijmegen	1.443	1.455	-0.012
		Eindhoven	1.445	1.438	0.007
		Tilburg	1.445	1.469	-0.024
		Zoetermeer	1.498	1.475	0.023
		Breda	1.429	1.476	-0.047
			$\widetilde{D}_{old}$ = 1.463	$\widetilde{D}_{new}$ = 1.458	$\Delta\widetilde{D}$ = 0.025

The regional medians ($\widetilde{D}_{old} = 1.463$, $\widetilde{D}_{new} = 1.458$) indicate a modest but consistent decrease in morphological richness from historical to modern districts. However, cities such as Tilburg, Breda, and Nijmegen display slightly negative ΔD values, where the modern sample is marginally more articulated than the historical cores. This may point to recent urban regeneration initiatives or design approaches that incorporate greater variability in block size and street alignment, as well as increased irregularity in the overall street pattern.

To better capture the distribution of values and highlight intra-city contrasts, Figure 4.2 visualizes the historical and modern fractal dimensions for each city.

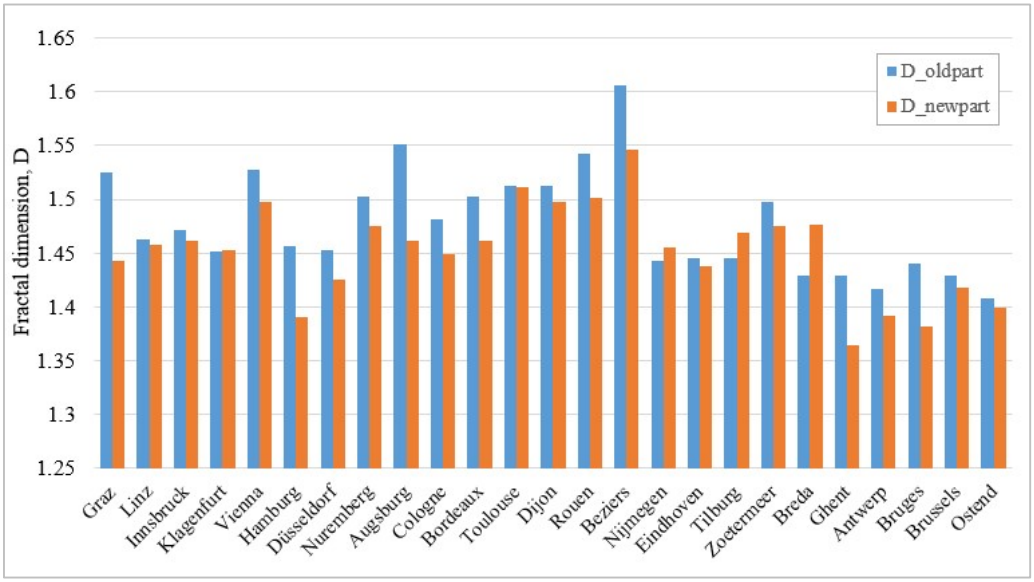

Figure 4.2. Fractal dimension by city: historic vs. modern districts (Western Europe)

This graphical representation enhances pattern recognition by making contrasts between cities more intuitive. It reveals cities with consistently high values of D (e.g., Béziers, Augsburg, Toulouse), as well as those with larger gaps between historical (old) and modern (new) areas, such as Graz or Augsburg. The relatively small spread in modern districts reinforces the impact of a more standardized urban planning approach in post-1950 development across much of Western Europe.

In summary, Western European cities reflect a mix of preserved historical intricacy and modern rationalization. While fractal dimension effectively captures morphological variation, further interpretation should be supported by complementary metrics (e.g., street length distribution or meshedness coefficient) to better understand the implications of these differences for street network configuration and urban form. This diversity in intra-city and regional patterns underscores the importance of historical context, planning ideologies, and socio-political factors in shaping urban form.

4.1.3. *Eastern Europe*

Preliminary analysis shows that Eastern Europe displays one of the most internally varied distributions of fractal dimension values. While a fuller comparison with all regions follows, the diversity – already apparent within this group – highlights how contrasting planning ideologies have shaped urban form over time (Table 4.3).

Table 4.3. Numeric value of the fractal dimension of Eastern European cities

Europe	Country	City	D_{old}	D_{new}	ΔD
East	Bulgaria	Haskovo	1.527	1.522	0.005
		Yambol	1.555	1.493	0.062
		Varna	1.578	1.571	0.007
		Plovdiv	1.555	1.523	0.032
		Ruse	1.540	1.531	0.009
East	Czech Republic	Brno	1.351	1.395	-0.044
		Prague	1.395	1.352	0.043
		Pilsen	1.414	1.387	0.027
		Liberec	1.389	1.385	0.004
		Ostrava	1.402	1.402	0
East	Hungary	Debrecen	1.492	1.477	0.015
		Gyongyos	1.532	1.522	0.010
		Nyiregyhaza	1.485	1.445	0.040
		Budapest	1.484	1.474	0.010
		Pecs	1.532	1.528	0.004
East	Poland	Poznan	1.391	1.322	0.069
		Częstochowa	1.331	1.365	-0.034
		Lodz	1.358	1.354	0.004
		Wroclaw	1.351	1.330	0.021
		Warsaw	1.368	1.363	0.005
East	Romania	**Bucharest**	1.575	1.530	0.045
		Craiova	1.551	1.474	0.077
		Oradea	1.435	1.420	0.015
		Satu Mare	1.416	1.387	0.029
		Timisoara	1.445	1.352	0.093
East	Slovakia	**Bratislava**	1.402	1.384	0.018
		Košice	1.363	1.318	0.045
		Nove Zamky	1.383	1.392	-0.009
		Trnava	1.362	1.398	-0.036
		Nitra	1.416	1.384	0.032
			$\widetilde{D}_{old} = 1.445$	$\widetilde{D}_{new} = 1.426$	$\Delta\widetilde{D} = 0.015$

While not reaching the highest extremes seen in Western Europe (e.g., Béziers or Augsburg), several cities in this region – such as Varna, Plovdiv, and Yambol – recorded D_{old} values exceeding 1.550, indicating considerable morphological richness. These figures reflect a patchwork of traditional urban structures shaped by a mix of Ottoman, Austro-Hungarian, and Soviet planning legacies (Stanilov, 2007; Hirt, 2012).

At the other end of the spectrum, cities like Brno, Częstochowa, and Wroclaw showed relatively low fractal dimensions in their historical cores (near or below 1.350), more aligned with the compact grid-like forms noted earlier in some Northern European cities (cf. Section 4.1.1). This range – from 1.331 to 1.578 –

highlights the intricate urban trajectories of post-socialist cities, where preservation, stagnation, and rapid redevelopment have coexisted (Tsenkova, 2006; Sýkora & Bouzarovski, 2012).

Interestingly, the variation between historical and modern areas is less predictable than in Western Europe. While a general trend of lower D_{new} values is apparent, the intra-city difference (ΔD) is not uniformly positive. Budapest and Nyíregyháza, for example, show moderate but expected drops ($\Delta D \approx 0.04$), while cities like Gyöngyös, Pécs, and Satu Mare exhibit almost no change – suggesting either an organic continuity in urban form or the integration of historical street patterns into more recent expansions.

In contrast, Brno, Częstochowa, and Trnava display negative ΔD values, with modern areas surpassing their historical cores in spatial intricacy. Whether due to post-war restructuring, socialist infill, or deliberate non-orthogonal planning, these reversals set Eastern Europe apart from the more consistent trends identified in both Sections 4.1.1 and 4.1.2.

Although the regional median values ($\widetilde{D}_{old} = 1.445, \widetilde{D}_{new} = 1.426$) suggest a mild overall decline in urban complexity, the small average gap masks significant internal heterogeneity. Romania, for instance, shows sustained high fractality in street configuration across both historical and modern districts. In contrast, the Czech Republic includes cities with low pattern differentiation (e.g., Brno), as well as tightly preserved ones (e.g., Pilsen). The presence of negative ΔD values, also seen occasionally in the Netherlands (see Section 4.1.2), reinforces the idea that morphological simplification is not a universal feature of modern development.

Rather than presenting a singular regional narrative, the Eastern European data reflects an ongoing tension between inherited street layouts and imposed spatial orders. This interplay is especially apparent in graphical form: Figure 4.3 traces the parallel trajectories of historical and modern D values, making visible the internal contrasts – some gradual, others abrupt.

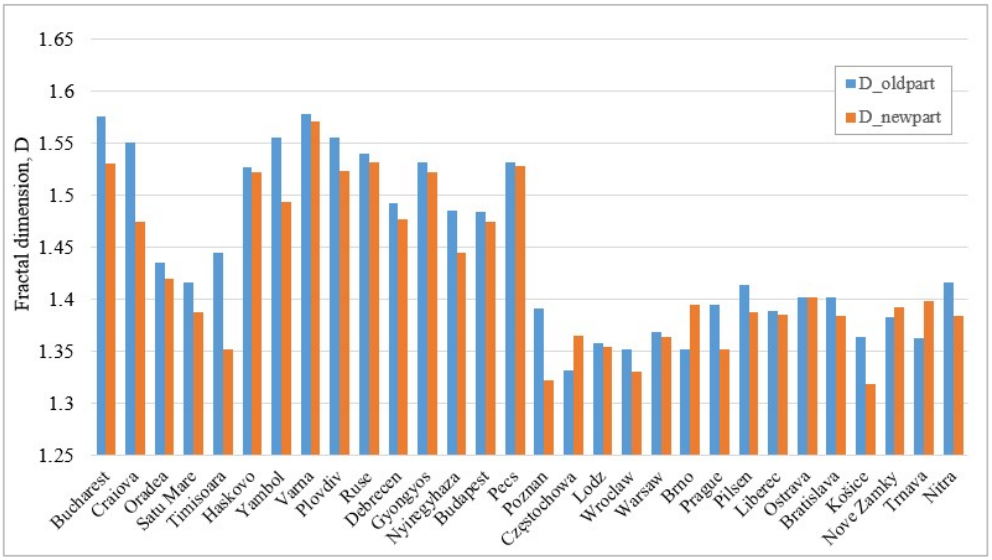

Figure 4.3. Fractal dimension by city: historic vs. modern districts (Eastern Europe)

Unlike the visual outputs for Northern and Western Europe, where the differences between bars followed a clearer pattern, the graph for Eastern Europe resists easy simplification. It draws attention to the region's varied local histories and differing interpretations of "modern" planning. In cities like Timișoara or Košice, the close alignment of values suggests planning that retained or mimicked traditional urban approaches. In others, like Trnava, the sharp drop may reflect post-war demolition or large-scale restructuring under centralized planning regimes.

In sum, the case of Eastern Europe reveals that fractal dimension – when viewed not as a singular indicator but as a distribution across cities – can expose both continuity and rupture. It invites closer attention to the political and cultural contexts shaping street morphology, and it cautions against assuming uniform patterns of spatial simplification in modernity.

4.1.4. Southern Europe

Among all macro-regions, Southern Europe exhibits the highest typical fractal dimension values in historical urban cores. Cities such as Palermo (D_{old} = 1.645) and Naples (D_{old} = 1.587) stand out for their intricate and organically evolved street networks – patterns commonly associated with older Mediterranean cities shaped by centuries of informal growth, constrained topography, and layers of cultural influence.

Similarly, cities such as Granada and Seville demonstrate relatively high fractal values in both their historical and modern districts, suggesting a continuity in morphological structure over time. This contrasts with the patterns observed in most Western and Eastern European cities (see Sections 4.1.2 and 4.1.3), where modern areas typically display a marked reduction in morphological richness, especially in terms of street network irregularity and density.

Frankhauser's work on the Bergamo region helps contextualize these findings, noting that Southern European towns often integrated surrounding rural settlements as they expanded, forming dendritic, interconnected patterns with moderate to high fractal dimensions. In that study, values ranged from 1.430 to 1.460, significantly higher than in more regulated urban forms like German Stuttgart with $D = 1.270$ or Lörrach with $D = 1.370$ (Frankhauser, 2004). Such contrasts reflect different spatial logics: gradual, layered urbanization in the south versus more centralized, planned growth in central and northern regions.

Another factor contributing to the distinctive street network patterns of Southern European cities is their coastal and leisure-oriented geography (Frankhauser, 2004). Cities along the Mediterranean – such as Naples, Setúbal, and Málaga – display highly articulated street layouts shaped by trade, climate, tourism, and cultural exchange. While modern developments tend to adopt more regular, planned street arrangements, the median of fractal dimension ($\widetilde{D}_{new} = 1.501$) remains higher than the corresponding

modern medians in the other three regions. This indicates a persistent tendency toward dense, finely subdivided, and irregular street networks even in newer districts.

Despite this, the shift from historical to modern street layouts remains evident. The typical intra-city difference in this region is $\Delta = 0.030$, slightly higher than in Western or Eastern Europe, indicating a gradual but consistent transition in street network structure over time. However, cities like Padua (D_{old} = 1.514; D_{new} = 1.513) deviate from this pattern, showing minimal change – likely due to limited urban expansion or design choices that preserved the historical street arrangement.

The diversity of these patterns is reflected in Table 4.4, which summarizes the historical and modern fractal dimensions for all Southern European cities in the study, along with intra-city differences.

Table 4.4. Numeric value of the fractal dimension of Southern European cities

Europe	Country	City	D_{old}	D_{new}	ΔD
South	Greece	Thessaloniki	1.543	1.538	0.005
		Katerini	1.480	1.461	0.019
		Larissa	1.518	1.506	0.012
		Ioannina	1.490	1.482	0.008
		Lamia	1.527	1.504	0.023
South	Italy	Florence	1.535	1.486	0.049
		Naples	1.587	1.540	0.047
		Palermo	1.645	1.548	0.097
		Bologna	1.534	1.466	0.068
		Padua	1.514	1.513	0.001
South	Portugal	Porto	1.450	1.433	0.017
		Lisbon	1.494	1.447	0.047
		Castelo Branco	1.471	1.416	0.055
		Setubal	1.512	1.481	0.031
		Evora	1.527	1.483	0.044
South	Republic of Cyprus	**Nicosia**	1.509	1.495	0.014
		Paphos	1.486	1.480	0.006
		Limassol	1.523	1.491	0.032
		Larnaca	1.494	1.477	0.017
		Famagusta	1.500	1.464	0.036
South	Spain	Granada	1.643	1.577	0.066
		Seville	1.600	1.565	0.035
		Cordoba	1.588	1.578	0.010
		Zaragoza	1.572	1.566	0.006
		Malaga	1.526	1.496	0.030
			$\widetilde{D}_{old} = 1.531$	$\widetilde{D}_{new} = 1.501$	$\Delta\widetilde{D} = 0.030$

The data confirm that a high degree of fractality remains a defining characteristic of street form in Southern Europe, even as planning becomes more structured. However, this continuity is not evenly distributed across the region. For example, while cities such as Bologna and Florence exhibit notable drops in D, others – like Seville, Zaragoza, and Cordoba – maintain very high values in both historical and modern samples.

Figure 4.4 presents this data visually, making the consistency of elevated fractal dimension values across Southern European cities more apparent. Unlike Eastern Europe, where bar pairs fluctuate dramatically, or Northern Europe, where modern areas are consistently lower, the Southern pattern is more balanced – yet still subtly declining.

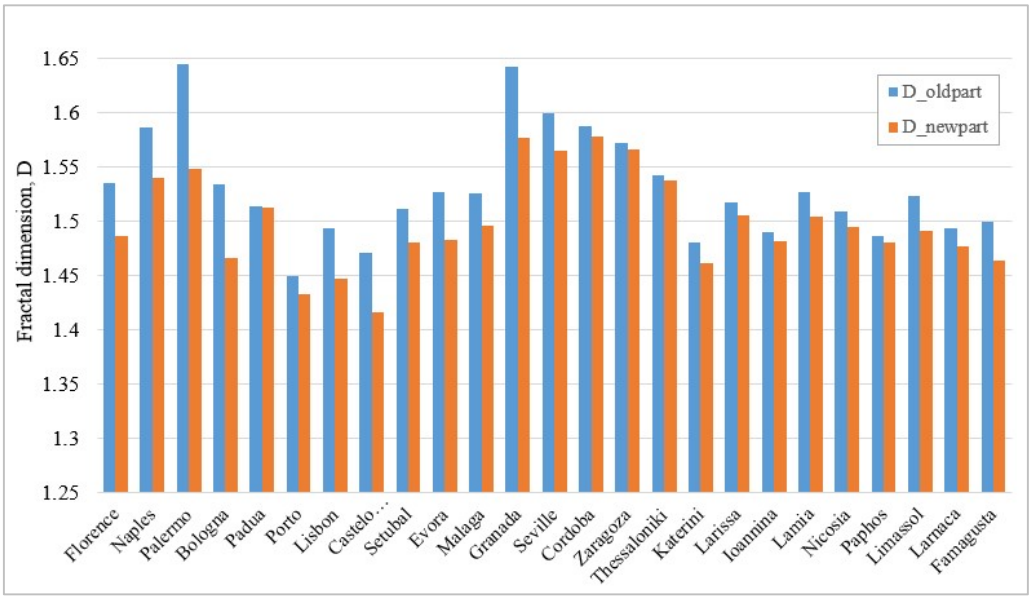

Figure 4.4. Fractal dimension by city: historic vs. modern districts (Southern Europe)

The overall picture is one of gradual transformation rather than abrupt change. While Southern Europe shares with other regions the general pattern of lower fractal dimension values in newer developments, it also demonstrates a stronger resistance to morphological simplification. This may reflect a planning culture that values historical continuity, or the geographic and cultural constraints that limit standardization. Either way, the region's fractal signature remains among the most consistently high in the entire dataset.

4.1.5. Observations in unraveling Europe's Street DNA

Having explored regional patterns in detail, it becomes crucial to step back and examine how these local dynamics translate into broader continental trends. This synthesis moves beyond individual case studies to draw out cross-regional regularities and divergences in the morphological evolution of European cities. This broader perspective is underscored by the spatial distribution of fractal dimension values across European historic cores (Figure 4.5), which illustrates regional clustering and inter-city variation at a continental scale.

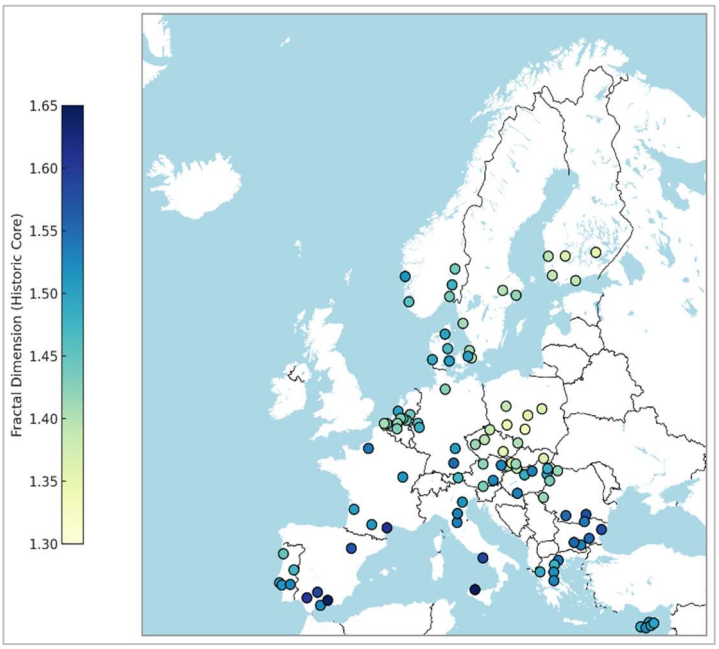

Figure 4.5. Fractal dimension city-level values across Europe

To this end, Table 4.5 presents a comparative summary of typical values of fractal dimensions for historical and modern samples across the four macro-regions.

Table 4.5. Regional summary of median fractal dimensions

Region	$\widetilde{D}_{old}$	$\widetilde{D}_{new}$	$\Delta\widetilde{D}$
Northern Europe	1.428	1.396	0.031
Western Europe	1.463	1.458	0.025
Eastern Europe	1.445	1.426	0.015
Southern Europe	1.531	1.501	0.030
	$\widetilde{D}_{old} = 1.488$	$\widetilde{D}_{old} = 1.445$	

Note: Values reflect the median fractal dimension across all sampled cities per region. The reported difference ($\Delta\widetilde{D}$) is not the difference between the two medians but rather the median of city-level differences ($\Delta D = D_{old} - D_{new}$). This approach provides a robust estimate of the typical intra-city change in spatial complexity.

These results provide a regional overview of changes in street network geometry over time. For example, Southern Europe maintains high levels of fractality in both historical and modern areas, suggesting continuity in morphological richness. Meanwhile, Eastern Europe appears as the most heterogeneous, with smaller differences but variable trajectories across cities.

To visualize these dynamics, Figure 4.6 presents a line plot of regional medians for D_{old} and D_{new}. This format was selected to compress data from over 100 city samples into eight summary values (4 regions × 2 urban types), thereby making directional trends and regional differences more immediately apparent in a compact visual format.

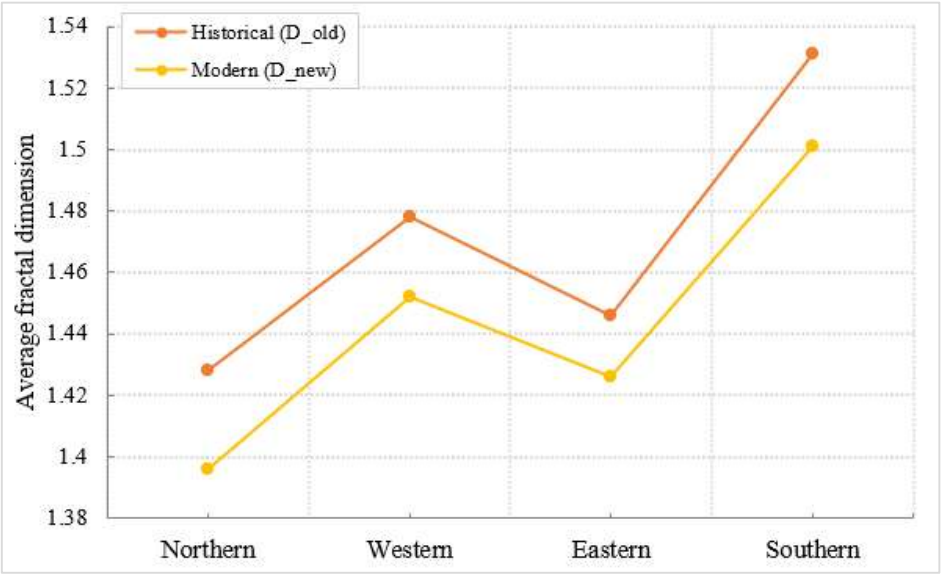

Figure 4.6. Line plot of the average $\widetilde{D}$ per region (historical vs. modern)

As shown in the figure, the two lines remain nearly parallel, indicating that across all four regions, historical urban cores are consistently more fractal than their modern counterparts. However, the magnitude of this gap varies:

- Northern Europe exhibits the steepest drop in fractal dimension, reinforcing earlier observations of distinct shifts in planning ideologies between periods (see Section 4.1.1).

- Eastern Europe, while internally diverse (Section 4.1.3), shows the smallest average ΔD, possibly indicating continuity or the persistence of inherited street network features in modern extensions.
- Southern Europe stands out not for the difference between values, but for the overall elevation of both historical and modern levels. This suggests that modern growth often inherited or reproduced richness of historical street patterns (see 4.1.4).
- Western Europe falls in between, reflecting a moderate degree of change, yet still retaining a clear distinction between organic and planned urban typologies (as discussed in 4.1.2).

Thus, the line plot not only confirms key findings from the previous sections but also provides a comparative lens for framing the subsequent, more detailed analyses – those which will consider not just typical values for each region, but also city-level variability, distribution overlap, and underlying spatial regimes.

To complement this regional overview, Figure 4.7 introduces a *violin plot*. Unlike standard boxplots, violin plots display both the full range and the underlying *distribution shape* of the data, enabling the observation of differences in medians as well as variation in spread (interquartile range) and skewness between historical and modern cores.

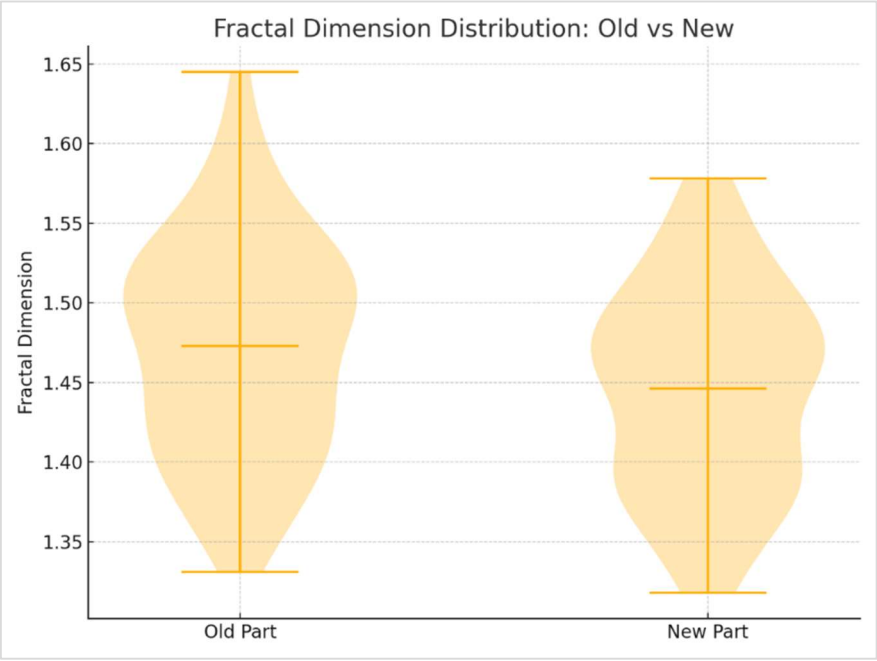

Figure 4.7. Violin plot comparing FD distributions for historical vs. modern core samples

As the plot demonstrates, historical areas exhibit both a higher median and greater dispersion of fractal dimension values (Figure 4.7). This reflects the diversity of older urban cores – ranging from highly intricate medieval fabrics to more regularized but still organic pre-modern forms. In contrast, modern areas cluster more tightly within a narrower band of D values, a pattern consistent with the more regularized street layouts commonly observed in planned developments. This reinforces the idea that, although cities

differ in their absolute level of fractality, modernization often brings a reduction in morphological diversity, likely due to functionalist or grid-oriented expansion models.

To move beyond regional medians, a more nuanced understanding of urban morphological shifts emerges by examining the variation within each group, both in terms of magnitude and direction of change. The full distribution of ΔD values for all 100 cities is included in Appendix A-3. This allows for:

- **ranking cities** from greatest to smallest change, visually separating those that retain spatial richness from those that undergo significant simplification;
- **highlighting outliers** – both positive and negative – enabling identification of atypical cases where modern areas exceed or nearly match the fractality of their historical cores;
- and mapping the **broader landscape** of morphological transitions across Europe, providing insight into how local planning ideologies may have shifted at the local scale;

While this ranked chart provides the full picture, Figure 4.8 narrows the focus to the **extremes** of the spectrum. It highlights the ten cities with the largest positive and negative ΔD values, offering a sharper analytical lens into cases where urban growth either substantially diverged from historical structure or remained remarkably consistent.

In the chart, green bars represent cities where modern areas are significantly less fractal than historical cores (large positive ΔD), whereas red bars indicate cities where modern areas closely match or even surpass the fractality of older districts (negative ΔD). This visual contrast helps identify planning cultures that actively reshaped street form.

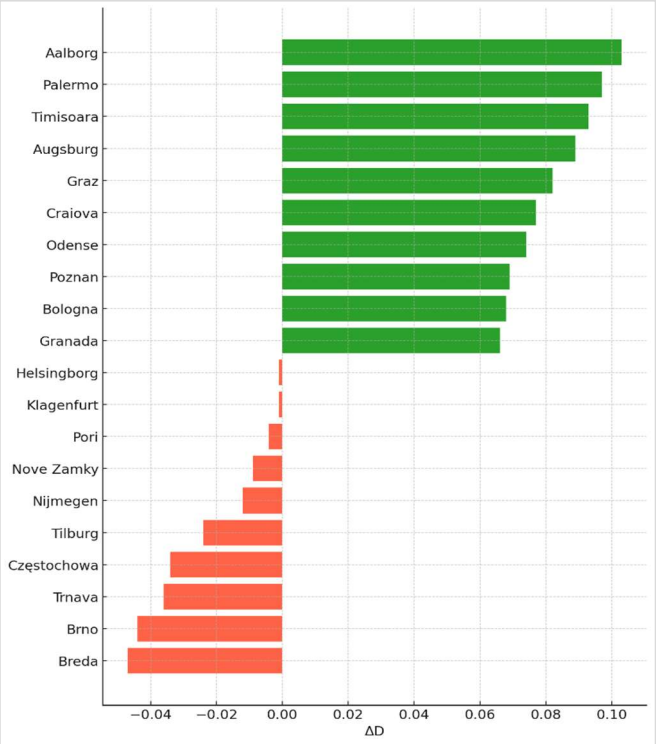

Figure 4.8. 10 Highest and 10 Lowest ΔD shifts in cityscapes

To assess whether deeper structural tendencies underlie the observed differences in fractal dimension, Figure 4.9 plots each city's historical versus modern D values in a two-dimensional scatterplot. Cities are grouped using **K-means clustering** to detect latent structural similarities among cities without imposing predefined regional boundaries.

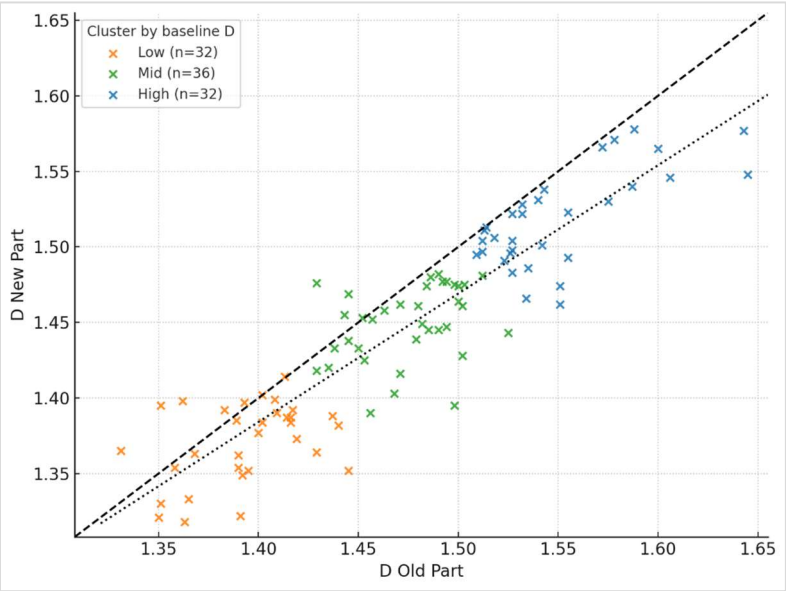

Figure 4.9. Scatter plot of D_{old} vs. D_{new}, grouped via K-means

The resulting visual classification yields several key insights. First, most cities fall below the 1:1 diagonal line ($y = x$), indicating that, in most cases, the fractal richness of street networks tends to diminish in modern extensions. It is defined that $\Delta D = D_{old} - D_{new}$, and positive values of ΔD denote a reduction in fractality over time – that is, a decline in the degree of space-filling structure.

Second, cities cluster into three broad morphological groups:

- **High–High** (blue) – cities whose historic cores exhibit the highest D values remain fractally rich in their modern areas. However, nearly all observations in this group lie beneath the 1:1 line, suggesting a systematic reduction in fractal properties in the transition from old to new districts.
- **Mid–Mid** (green) – the modal cluster, comprising cities with intermediate D values in both historical and modern areas. Here, the reduction in fractality is more moderate and variable, with most cities showing slight declines and a smaller subset exhibiting stability or mild gains.
- **Mixed/Inverted** (orange) – a distinct minority of cases where the modern extension equals or exceeds the complexity of the historical core ($\Delta D \leq 0$). These cases, previously highlighted in Figure 4.8, challenge the presumption of inevitable simplification and instead suggest conditions under which newer districts may evolve or be planned with comparable or even greater multi-scale richness.

Taken together, historic cores exhibit slightly higher average fractal dimension than modern expansions, though the difference is modest. Yet, the presence of inverted or stable cases implies that this trend is neither universal nor structurally deterministic. Instead, it calls for closer examination of the spatial, regulatory, and cultural mechanisms that can preserve or even foster fractal richness in contemporary urban extensions.

In sum, the observed variation in fractal dimension (D) between historical and modern areas highlights meaningful shifts in how street form is organized. These shifts raise practical questions about the spatial

implications of different planning paradigms – for instance, whether the pursuit of geometric clarity in modern layouts has reduced walkable complexity, or whether grid patterns can achieve legibility without diminishing the spatial diversity of the street network.

While the present analysis focuses on form, even small shifts in geometric order can coincide with wider changes in planning logic. To explore these possibilities, the next section turns to network-based indicators, examining how variations in street configuration relate to properties such as connectivity, route directness, and spatial integration.

4.2. Network Metrics Analysis

Building on the fractal-based assessment in §4.1, this section shifts focus to structural and connective attributes of street network using graph-theoretical measures. Here, each street layout is reinterpreted as a graph, allowing exploration of internal configuration – how connections enable or constrain movement, and where alternative routes arise. The dataset remains unchanged; only the analytic framework is modified.

To operationalize this approach, each polyline trace is converted into a primal graph (Figure 4.10), where intersections correspond to nodes and street segments to edges. This graph-based model underpins all subsequent metrics and ensures consistency when comparing historical and modern districts. The figure below is provided to concretize the analytic representation.

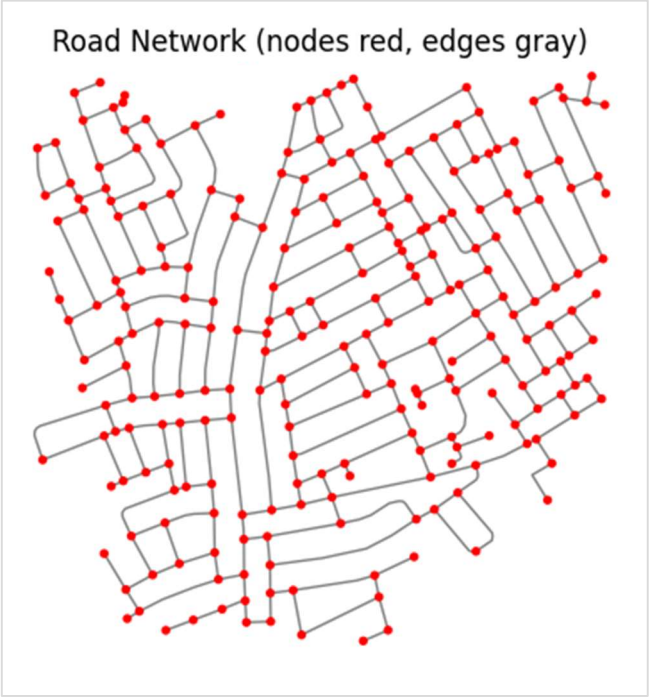

Figure 4.10. Graph model of the street network: intersections = nodes (red); segments = edges (gray)

Building on this common framework, six indicators serve as complementary perspectives on street network structure:

- Urban grain: intersection density and average edge length;

- Pedestrian-scale access potential: reachability index within 600 meters;
- Distance efficiency: harmonic mean of shortest path lengths
- Route directness: mean straightness of routes
- Redundancy: meshedness coefficient (cycle-based connectivity)

These metrics are derived through a common processing pipeline using OSMnx and NetworkX, ensuring methodological consistency for both the historic and modern areas. The same graph objects are used for both visual and quantitative analysis to ensure alignment between representations. The following analysis interprets these metrics across the entire dataset as well as in within-city comparisons.

4.2.1. Corpus Overview: distributions by district type

Before exploring regional and city-level differences, it is useful to establish how key street network indicators vary across the entire sample of 200 urbanized samples. This section focuses on broad distinctions between historic cores and modern districts, without yet considering differences between countries or urban regions.

Table 4.6 summarizes each indicator's descriptive statistics: mean, median, minimum, maximum, and standard deviation. This overview serves two main purposes. First, it gives a sense of the *central tendency and variability* across the entire dataset, without privileging any specific city or region. Second, by organizing the results by district type – historic versus modern – it enables a preliminary contrast between inherited and planned urban forms.

Table 4.6. Summary statistics for six street-network indicators by district type

EUROPE	**Historic district (Old part of the city)**					**Modern district (new part of the city)**				
	Mean	Max	Min	Median	σ	Mean	Max	Min	Median	σ
Intersection Density, km^{-2}	113.9	302.8	52.1	102.8	45.63	96.3	243.1	31.4	86.8	39.22
Avg. Edge Length, m	79.35	125.6	44.1	78.01	16.18	90.6	162.8	52.8	87.5	21.41
HM shortest path, m	479.1	605.7	371.1	478.9	45.41	477.1	659.1	333.7	477.2	54.20
Reachability Index, nodes	68.62	193.4	24.4	63.09	32.64	59.83	209.6	16.31	53.11	31.94
Mean straightness	0.753	0.841	0.60	0.756	0.043	0.749	0.835	0.56	0.756	0.053
Meshedness Coefficient	0.197	0.285	0.06	0.200	0.038	0.191	0.287	0.03	0.189	0.051

A close look at Table 4.6 yields several interpretive insights:

1. Intersection density declines in modern districts (median≈86.8 per km^2), reflecting a shift toward larger blocks and fewer junctions compared to historic cores (≈103 per km^2).

2. Edge lengths increase, indicating longer street segments and wider spacing between intersections in modern layouts.
3. Local reachability declines by ~15–20% in most cases, suggesting that contemporary layouts tend to limit the number of destinations reachable within one walkable radius (600 m).

These observations suggest a general movement away from compact, fine-grained street structures toward more spacious, less connected arrangements.

Complementing this, Figure 4.11 visualizes the same data using boxplots. Each plot displays the interquartile range (IQR), median (horizontal line), and mean (triangle) for each indicator, along with outliers shown as individual points. Taken together, these visualizations enable rapid, side-by-side assessment of not only the *typical values* (i.e., medians) but also the *distributional shapes and variability* associated with each type of urban district.

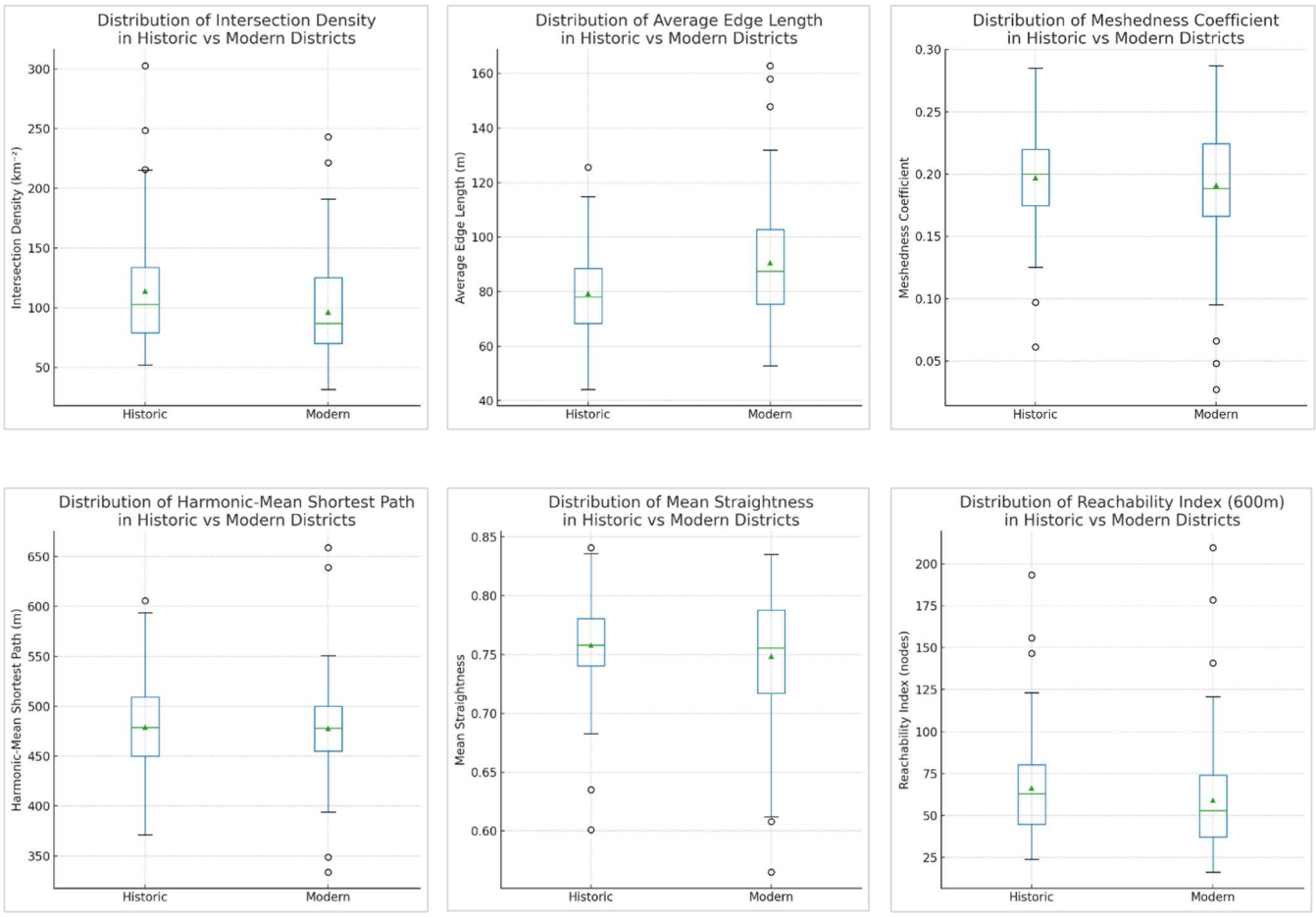

Figure 4.11. Distributions of six street network indicators across historic and modern districts (n = 200)

Note. **Top row** – Morphology (network grain & cyclicity): intersection density, average edge length, and meshedness (redundancy via cycles).
Bottom row – Topology (local accessibility & routing efficiency): harmonic-mean shortest paths (aggregate efficiency), mean straightness (route directness), and reachability within 600 m.
Boxplots show the interquartile range (IQR); green lines indicate medians; dots represent statistical outliers.

Meanwhile, some indicators show little distinction between district types:

- Harmonic-Mean Shortest Path and Mean Straightness vary only modestly. While both district types share similar central values, historic areas tend to support shorter and slightly more direct routes – reflecting greater compactness and integrated street layout.
- Meshedness coefficient reveals a small but consistent advantage in route redundancy for historic areas, implying greater resilience to traffic disruption and better support for route choice.

This comparative, corpus-wide analysis serves as a benchmark before disaggregating results by region. By framing broad differences between historic and modern districts, it becomes easier to interpret whether specific regional trends reinforce or diverge from these general patterns. For example, does Southern Europe consistently reflect the historic model? Do modern districts in Eastern Europe resemble their Western counterparts, or not?

The regional breakdowns that follow – Northern, Western, Eastern, and Southern Europe – build directly on this foundation, tracing which morphological and connectivity traits recur, and which diverge across the European urban landscape.

4.2.2. Street Network Signatures: Northern European cities

To introduce the regional dynamics of street network structure, Northern Europe provides a natural starting point. Drawing on cities from Denmark, Sweden, Norway, and Finland, the analysis below synthesizes six key network indicators to examine variations in spatial configuration, connectivity, and block structure between historical and modern districts (Table 4.7). Full city-level metrics are included in Appendix A-4.

Table 4.7. Six Street Network Metrics: Northern Europe Summary

NORTHERN EUROPE	**Historic district (Old part of the city)**					**Modern district (new part of the city)**				
	Mean	Max	Min	Median	σ	Mean	Max	Min	Median	σ
Intersection Density, km^{-2}	89.29	129.9	59.17	93.44	18.67	76.21	125.0	31.4	77.09	22.25
Avg. Edge Length, m	84.65	109.1	65.13	81.6	11.00	96.41	157.9	71.7	91.69	20.83
HM shortest path, m	477.3	546.4	402.6	473.7	41.39	481.2	639.2	348.9	477.4	63.47
Reachability Index, nodes	53.11	100.1	24.04	55.87	17.28	46.78	77.52	16.31	43.80	16.66
Mean straightness	0.754	0.809	0.661	0.766	0.039	0.718	0.814	0.565	0.717	0.069
Meshedness Coefficient	0.203	0.276	0.137	0.204	0.032	0.162	0.265	0.027	0.156	0.057

Across Northern Europe, historic districts typically feature 93 intersections per square kilometer, with street segments averaging 81.6 meters in length. Within a 600-meter walking distance, the average resident can

access approximately 56 junctions – a useful proxy for pedestrian-scale connectivity. In contrast, modern districts exhibit reduced intersection density (77 nodes/km²) and longer average segment lengths (91.7 m), reflecting planning trends favoring larger blocks and more streamlined layouts.

Despite these geometric shifts, the harmonic mean shortest path remains essentially stable between historical and modern districts (473.7 m vs. 477.4 m). This suggests that while routes may lengthen and nodes become sparser, overall accessibility does not substantially decline. This impression is reinforced by mean straightness values: modern areas exhibit around 71.7% route directness (straightness = 0.717), compared to 76.6% in historic cores. In practical terms, this indicates that routes in modern districts deviate more from the Euclidean distance between two points. This reflects reduced permeability, whereas historic networks enable more direct routing despite their irregular geometries.

The reachability index is perhaps more revealing, showing a noticeable decline in modern areas: from a median of 56 reachable nodes to just 43, capturing the cumulative effect of fewer junctions and longer segments. Meanwhile, meshedness coefficients drop modestly, from 0.204 in historical districts to 0.156 in modern ones. This indicates a slightly less looped and potentially less resilient street network, though the change is less dramatic than in other regions.

Taken together, these findings point to a moderately pronounced spatial divergence in street network structure between older and newer districts in Northern Europe. While modern zones feature fewer intersections and slightly longer routes, overall performance in terms of path efficiency and route directness remains relatively high. This continuity suggests that recent expansions, despite a greater emphasis on vehicular access and zoning, preserve elements of human-scaled coherence – especially in comparison to more fragmented patterns observed elsewhere.

A few cities exemplify these dynamics. Stockholm, for instance, maintains high connectivity in both historic and modern sectors, with minimal differences in reachability and path length, reinforcing its polycentric, transit-integrated street form (Figure 4.12). Helsinki, on the other hand, exhibits one of the sharpest contrasts in meshedness between old and new sectors (0.25 vs. 0.14), suggesting a transition toward more tree-like road systems (see Appendix A-3). These exceptions highlight the value of maintaining disaggregated analyses even within otherwise coherent regional trends.

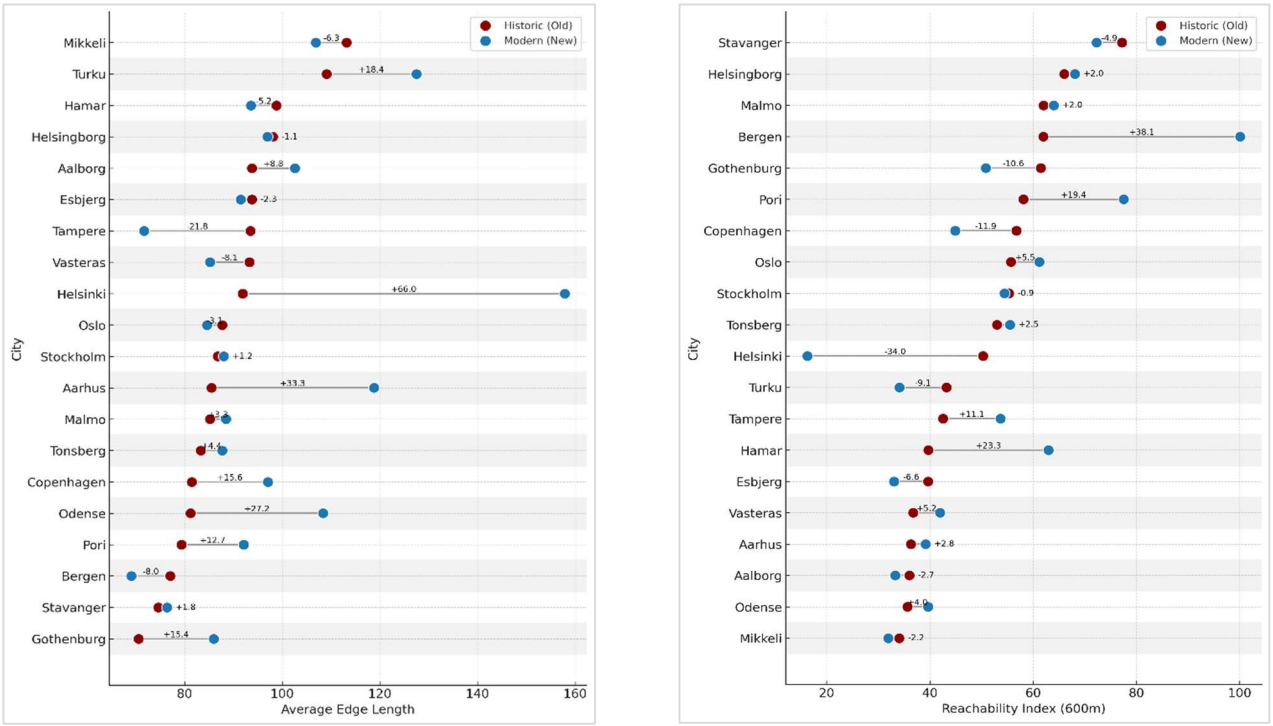

Figure 4.12. City-level variation in street network characteristics across Northern Europe

4.2.3. Street Network Signatures: Western European cities

To capture the structural tendencies of street networks in Western Europe, this analysis examines 25 cities across five countries – Austria, Belgium, Germany, France, and the Netherlands. As detailed in Section 3.4, six key indicators were computed using OSMnx, providing a consistent framework for comparing street network configuration and topology between historic and modern districts. Summary statistics for each indicator are presented in Table 4.8, while full city-by-city data can be found in Appendix A-4.

Table 4.8. Six Street Network Metrics: Western Europe Summary

WESTERN EUROPE	Historic district (Old part of the city)					Modern district (new part of the city)				
	Mean	Max	Min	Median	σ	Mean	Max	Min	Median	σ
Intersection Density, km^{-2}	117.9	248.6	71.50	115.9	37.83	92.4	164.6	39.62	88.93	26.42
Avg. Edge Length, m	76.6	111.3	50.51	74.5	13.37	88.9	128.2	63.54	85.41	14.68
HM shortest path, m	480.3	605.7	371.1	478.5	51.74	479.6	570.7	393.9	477.9	34.20
Reachability Index, nodes	70.24	155.8	30.54	65.1	25.26	54.52	93.6	22.83	50.03	19.08
Mean straightness	0.758	0.841	0.643	0.759	0.05	0.753	0.835	0.608	0.752	0.050
Meshedness Coefficient	0.200	0.285	0.097	0.203	0.04	0.189	0.287	0.104	0.184	0.041

The resulting patterns reflect a region shaped by centuries of gradual transformation, moving from irregular, often organic medieval cores to the more rational geometries of post-industrial expansion. The selected

indicators enable a comparative understanding of how morphology and topology shift over time – facilitating analysis without relying on typological assumptions.

Based on regional medians, a typical historic district in Western Europe contains approximately 116 intersections per square kilometer, with an average segment length of 74.5 meters, and supports access to 65 nodes within a 600-meter walk. This combination indicates a fine-grained, compact street network with high local accessibility. In contrast, modern districts exhibit a coarser structure: 89 intersections/km^2, 85.4 meters average segment length, and a reachability index of 50 nodes – all suggesting larger blocks and less favorable conditions for walkability.

Notably, although modern districts contain longer street segments and fewer intersections, mean straightness remains relatively high (0.752). This indicates that many streets follow continuous, geometrically aligned paths, allowing relatively direct movement despite a sparser network structure. Meanwhile, the meshedness coefficient – a measure of street network redundancy – declines slightly from 0.203 to 0.184, indicating fewer alternative paths in newer developments.

Overall, these results are in line with expectations: historical districts are characterized by a finer street network structure and stronger support for pedestrian movement, whereas modern layouts are sparser and more oriented toward efficient vehicular flows. Nonetheless, the relatively modest differences across most indicators suggest a smoother morphological transition between historic cores and the outer districts shaped by modern planning principles in this region.

4.2.4. Street Network Signatures: Eastern European cities

Eastern European cities provide an important dimension to the regional comparison, due in large part to the diversity of urban trajectories observed across the subcontinent. From compact centers rooted in pre-industrial layouts to peripheral zones shaped by planned expansion and infrastructure-led growth, this region reflects a spectrum of spatial development patterns formed over time. The dataset covers 30 cities across Bulgaria, the Czech Republic, Hungary, Poland, Romania, and Slovakia, capturing representative contrasts between central and peripheral districts. Table 4.9 summarizes the distribution of six core street network indicators for both district types, with more detailed results are available in Appendix A-4.

Historic districts in this group tend to balance moderate intersection density (~79/km²) with relatively long segments (88.5 m), reflecting compact layouts that were nonetheless shaped by grand axes or planning traditions. Interestingly, this spatial structure does not diverge dramatically in modern districts: intersection density drops only slightly (to ~73/km²), and segment length increases modestly (~99 m). At first glance, this suggests a conservative evolution in block structure – more a recalibration than a rupture.

Table 4.9. Six Street Network Metrics: Eastern Europe Summary

EASTERN EUROPE	Historic district (Old part of the city)					Modern district (new part of the city)				
	Mean	Max	Min	Median	σ	Mean	Max	Min	Median	σ
Intersection Density, km^{-2}	85.21	155.6	52.08	79.17	24.50	79.37	190.9	41.67	72.92	30.85
Avg. Edge Length, m	91.70	125.6	69.09	88.53	13.77	102.1	162.8	65.30	98.86	23.14
HM shortest path, m	472.36	590.9	380.1	470.6	45.69	470.7	629.6	333.7	480.9	61.26
Reachability Index, nodes	50.38	93.57	24.15	45.49	18.43	48.29	115.9	19.90	40.47	23.02
Mean straightness	0.755	0.831	0.635	0.755	0.037	0.753	0.816	0.620	0.767	0.041
Meshedness Coefficient	0.196	0.264	0.061	0.198	0.041	0.195	0.286	0.048	0.192	0.047

Yet, a more nuanced reading emerges when geometric characteristics are considered alongside topological measures. The harmonic mean shortest path reveals near-parity between historical and modern districts (470.6 m vs 480.9 m), and straightness index improves marginally in modern districts – from 0.755 to 0.767, or roughly 76.7% of a straight-line route. In essence, newer districts attain similar levels of perceived legibility while simplifying street alignment. This combination – longer blocks paired with straighter routes – suggests an optimization logic: fewer intersections, but more continuous movement paths.

However, this geometric streamlining comes with trade-offs. Reachability drops from 45 to 40 nodes, indicating that spatial legibility does not guarantee proximity. This subtle decoupling between local walkability and junction density reflects a shift in planning intent – less emphasis on closely-knit accessibility, more on streamlined circulation. The meshedness coefficient, serving as a proxy for redundancy and fallback options, also declines slightly (from 0.198 to 0.192), reinforcing the idea that while detour routes remain, their overall density may be diminishing.

A closer look at individual cases anchors these trends. Warsaw's modern district, for example, combines extremely low intersection density (49.3/km²) and long edge lengths (131.9 m) with a reachability value of just 27.7, exemplifying a landscape of large superblocks and limited connectivity. Meanwhile, Timisoara's modern sector stands out for its high straightness (0.826), suggesting fewer detours and more direct routing between points, even though looping alternatives are limited.

Altogether, the Eastern European sample reflects a quiet but perceptible reconfiguration of urban street form. While changes in geometry are clear – especially in block size and junction frequency – the continuity in accessibility and route directness tempers their overall impact. The region offers a case where structural evolution does not entirely sever ties with inherited street patterns, but rather, reinterprets them within new

socio-political and planning frameworks. This restrained transition stands out, particularly when viewed against sharper divergences observed in other regions.

4.2.5. Street Network Signatures: Southern European cities

Among the regions examined, Southern Europe displays the strongest morphological continuity between historic cores and modern expansions, while also revealing some of the most distinctive patterns in street network grain and redundancy. Spanning cities across Greece, Italy, Portugal, Spain, and Cyprus, this sample presents a nuanced interplay of organic legacies and geometric interventions – shaped by centuries of incremental growth and post-war transformations.

As summarized in Table 4.10, Southern European cities stand out for their fine-grained historical layouts. Historic districts here show high central tendency in intersection density (median = 164.6 nodes/km^2) – by far the densest among all four regions – paired with the shortest mean edge lengths (64.3 m). Together, these values reinforce the presence of a compact, pedestrian-oriented street network. Even in their modern counterparts, intersection density remains comparatively elevated (131.3/km²), indicating that subsequent urban development did not fully abandon the dense, permeable structure of earlier periods.

Table 4.10. Six Street Network Metrics: Southern Europe Summary

SOUTHERN EUROPE	**Historic district (Old part of the city)**					**Modern district (new part of the city)**				
	Mean	Max	Min	Median	σ	Mean	Max	Min	Median	σ
Intersection Density, km^{-2}	164.2	302.8	88.89	164.6	44.34	134.9	243.1	54.17	131.3	41.54
Avg. Edge Length, m	62.96	76.45	44.11	64.31	8.539	73.73	120.3	52.82	72.89	13.87
HM shortest path, m	487.2	593.6	415.0	485.2	43.68	478.8	659.1	380.7	473.4	56.12
Reachability Index, nodes	101.4	193.4	44.78	94.94	37.66	89.45	209.6	21.07	81.17	42.11
Mean straightness	0.747	0.819	0.601	0.753	0.048	0.763	0.824	0.616	0.779	0.048
Meshedness Coefficient	0.191	0.271	0.125	0.200	0.036	0.212	0.286	0.095	0.215	0.049

This relative consistency in granularity helps explain the minimal difference in harmonic mean shortest path values across the two periods (485.2 m in historic cores vs. 473.4 m in newer districts). In fact, modern areas slightly outperform older ones on this indicator – an inversion of the usual trend seen in other regions. At first glance, this appears counterintuitive, since longer blocks and lower intersection densities typically lengthen travel distances. However, when considered alongside a 2.6% increase in mean straightness (from 0.753 to 0.779), a clearer picture emerges: modern districts offset lower permeability through linear, well-aligned street geometries. In practical terms, this means that movement remains relatively direct even in sparser networks, with routes deviating from the straight-line distance by ~22% in modern districts

compared with ~26% in historic cores. Together, these findings suggest that routing efficiency in modern layouts is achieved through continuity of alignment that limit angular deviation.

these results suggest that modern districts compensate for fewer junctions through more linear and continuous street alignments. In practical terms, routing in modern areas remains close to the geometric shortest path – where approximately 22% detour is required on average – compared with about 26% in historic areas. This indicates that directness in modern networks is achieved through long, aligned corridors rather than through dense local permeability.

This subtle shift suggests a strategic reconfiguration rather than outright simplification. Longer street segments, if arranged in well-aligned routes, may help preserve or even enhance route efficiency. The city of Florence offers a notable example: its modern district improves both straightness and meshedness compared to the historic center, despite a drop in intersection density – pointing to a coherent, if more top-down, spatial approach (see Appendix A-4).

Meshedness coefficients, often reflective of redundancy and alternative routing options, show one of the rare increases in modern districts across all regions (from 0.200 to 0.215). This outcome, observed in several Portuguese cities such as Lisbon and Setúbal, hints at deliberate planning for looped or hierarchical grid structures – potentially blending historic permeability with newer, traffic-calming layouts. Nonetheless, regional variability is substantial. In some cases (e.g., Larissa or Ioannina), modern districts maintain or even surpass the meshedness of historic cores; in others (e.g., Larnaca), simplification is more evident (see Appendix A-4).

If reachability serves as a final lens on navigability, the street pattern in Southern Europe is more muted than elsewhere. From a median of 95 reachable nodes in older areas, modern zones decline to about 81, still high relative to other regions, and reflective of the enduring compactness of Southern European urbanism. This soft decline contrasts with the more abrupt reachability drops seen in Northern and Eastern Europe, further reinforcing the impression that, in this region, modern expansion often retained core aspects accessibility rooted in earlier morphologies.

Taken together, these indicators point to a planning tradition in Southern Europe that, while accommodating modern demands, remains structurally tied to a deep culture of walkability and connectivity. Unlike the sharp contrasts seen in other contexts, the distinction between old and new districts here is more porous – shaped by both inherited street forms and selective adaptation, rather than by radical restructuring.

4.2.6. Within-city contrasts: Δ Values of street network metrics

While earlier sections examined differences between historic and modern districts both at the European scale (Section 4.2.1) and across macro-regions (Sections 4.2.2–4.2.5), this section presents a more focused and formalized comparison by computing within-city differences across all six network indicators.

For each city in the corpus, delta values ($\Delta = M_{old} - M_{new}$) were calculated to capture both the magnitude and direction of change in street network structure. This approach allows for consistent interpretation: positive Δ values indicate a decline in the given metric in modern areas (e.g., lower intersection density), while negative values suggest an increase (e.g., longer average street segments). In this way, the analysis systematically assesses how internal spatial configurations have evolved over time.

The values in Table 4.11 represent the median intra-city differences for each indicator, aggregated by macro-region. That is, for every city, a pairwise metric difference was computed, and regional medians were then derived to summarize the most typical internal shifts per region. While the resulting table displays regional tendencies (see Table 4.11), the analysis remains grounded in city-level contrasts, ensuring that the interpretation reflects micro-scale structural changes rather than broad generalizations.

Table 4.11. Overview of regional median Δ in structural indicators

Region	Δ Intersection Density	Δ Avg. Edge Length	Δ Reachability index	Δ HM Shortest Path	Δ Straightness index	Δ Meshedness coefficient
Northern Europe	12.15	-8.77	6.18	-8.49	0.046	0.034
Western Europe	19.45	-10.64	14.48	-2.83	0.006	0.021
Eastern Europe	4.86	-6.44	0.025	-1.74	0.007	0.007
Southern Europe	28.47	-6.77	12.27	7.60	-0.019	-0.005

Note: *City-level Δ values are detailed in Appendix A-5.*

Building on these results, Figure 4.13 illustrates the indicators showing the most pronounced intra-city variation: Intersection Density, Average Edge Length, Reachability, and Harmonic Mean Shortest Path.

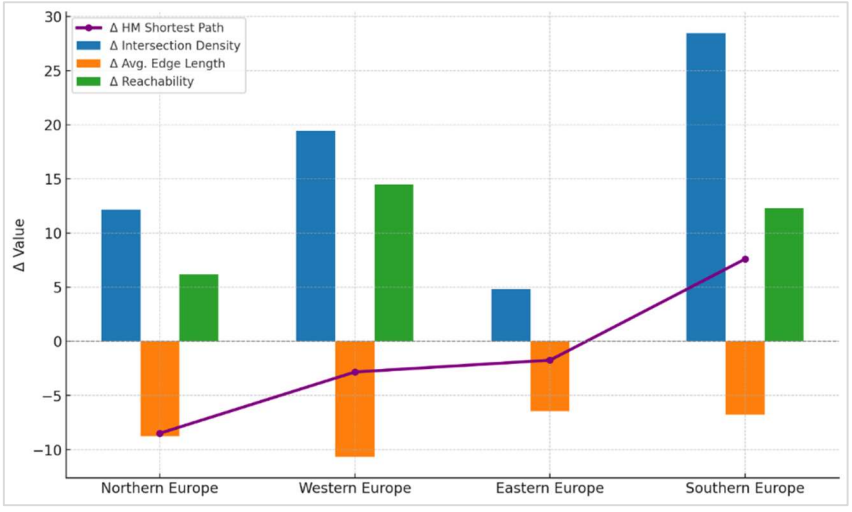

Figure 4.13. Regional median Δ values in network indicators with the strongest historic–modern contrasts

These metrics were selected not only for their statistical variability but also for their conceptual relevance: together, they describe key aspects of street network grain, continuity, and accessibility – all of which are essential for understanding spatial organization. The chart illustrates a set of contrasting dynamics between historical and modern districts:

- **Intersection Density** consistently declines (positive Δ), most strongly in Southern and Western Europe, pointing to coarser street grids in newer areas.
- **Average Edge Length** increases (negative Δ), reinforcing the pattern of longer street segments and larger block structures.
- **Reachability index** generally drops, suggesting reduced access to the broader street network in many modern districts.
- **Harmonic Mean Shortest Path** displays a more mixed pattern: positive Δ in the North and West indicates shorter path values in modern areas (suggesting more direct routing, typical of planned grids), while negative Δ in the South reflects longer paths, possibly associated with fragmented growth or suburban sprawl.

These shifts reveal common morphological tendencies and region-specific trajectories. They also illustrate how cities have moved away from the fine-grained, irregular street patterns of historic cores toward modern layouts defined by longer blocks, straighter streets, and more predictable geometry — yet offering fewer junctions and less spatial variety at the local scale.

Two other indicators, Straightness Index and Meshedness Coefficient, were excluded from the visual summary due to low intra-city variation and minimal regional contrast. While conceptually important, these metrics did not demonstrate sufficient divergence to justify comparative visualization, and are instead referenced descriptively in other sections. Their exclusion sharpens the focus of the chart, allowing clearer visual emphasis on structurally dynamic variables.

Overall, these results underscore the significance of intra-city contrasts, showing that modern districts tend to lose street density, reduce accessibility horizons, and lengthen routes structures relative to their historic counterparts. By highlighting the four indicators with the most dynamic shifts, the analysis isolates the variables most likely to explain regional differences in urban street structure. This, in turn, sets the stage for the correlation analysis in Section 4.3, where these metrics are analyzed in relation to fractal dimension to reveal potential interdependencies.

4.3. Fractal Dimension and Network Indicators: Correlation Analysis

This section investigates whether the fractal dimension (D) of street networks is aligned with, or adds explanatory value beyond key indicators from graph theory. The analysis follows the two-step design

introduced in Section 3.5. First, a paired within-city comparison tests whether changes in fractal dimension (ΔD) co-move with changes in street network metrics when shifting from historic to modern districts. Second, groupwise cross-sectional analyses are conducted separately for historic cores and modern areas, revealing how these relationships manifest without differencing. Together, these complementary views distinguish internal transformations within cities from broader cross-sectional patterns across the European sample.

4.3.1. From Paired Differences to Correlation

To understand how changes in street morphology relate to changes in structural properties across time, the analysis begins by examining the paired differences (Δ) between historic and modern districts. Here, Δ refers to the difference between historic and modern values ($\Delta M = \Delta M_{old} - \Delta M_{new}$), such that positive values indicate a higher value in the historic district.

Figure 4.14 visualizes these pairwise correlations as a Δ-matrix heatmap, where positive or negative associations between the metrics are expressed in both sign and magnitude. The matrix offers an initial overview of the relative direction and strength of each association across the 100 city pairs, with darker shades denoting stronger linear relationships.

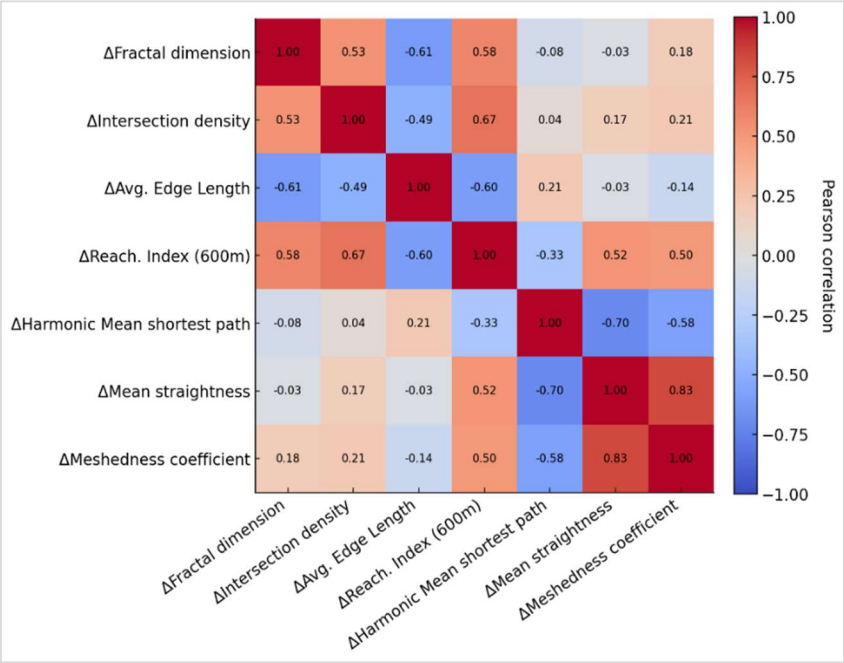

Figure 4.14. Heatmap correlation matrix (ΔFD vs. ΔMetrics)

Table 4.12 reports the same correlations numerically and confirms which of these associations are statistically significant under both Pearson's *r* and Spearman's ρ. This dual reporting addresses potential non-linearity in the bivariate relationships while also revealing which findings are robust to rank-based comparison.

Table 4.12. Paired Comparative Analysis (ΔD vs. ΔMetric)

	Pearson's *r*	***p*-value**	**Spearman's *ρ***	***p*-value**
Δ Intersection Density	0.53	$4.23*10^{-8}$	0.64	$6.27*10^{-5}$
Δ Average Edge Length	-0.61	$8.71*10^{-15}$	-0.52	$3.04*10^{-17}$
Δ Reachability Index (600m)	0.58	$2.14*10^{-11}$	0.65	$1.88*10^{-12}$
Δ Harmonic Mean Shortest Path	-0.08	0.074	-0.16	0.128
Δ Mean Straightness	-0.03	0.002	-0.02	0.057
Δ Meshedness Coefficient	0.18	0.038	0.27	0.094

The clearest relationships appear in the first column, where ΔD shows strong, significant alignment with three other differences: average edge length, intersection density, and the reachability index. Higher ΔD values (where historic districts have higher fractal dimension than their modern counterparts) tend to coincide with shorter street segments, more intersections per hectare, and denser local connectivity. Taken together, these trends suggest that shifts toward more articulated, fine-grained geometries are strongly associated with increased local-scale structural connectivity within the 600 m network radius.

By contrast, changes in harmonic mean shortest path length (HMSP), straightness, and meshedness coefficient do not exhibit consistently strong associations with ΔD or with one another. In several cases, their relationships are weak, statistically insignificant, or context-dependent, indicating that these indicators capture more localized aspects of connectivity that are less tightly coupled to geometric scaling.

As an interim reading, these findings suggest that transitions toward longer segments and sparser junctions are generally linked to declines in fractal dimension, whereas densification and improved local access accompany its increases. In this sense, D functions here as a geometric signal of how finely the network is subdivided and how densely it embeds local connections, especially when these patterns shift over time.

The next step is to test whether these alignments persist when historic and modern districts are analyzed separately, without differencing.

4.3.2. Groupwise correlation analysis

While the paired-difference analysis in Section 4.3.1 highlights how fractal dimension (ΔD) co-varies with shifts in street-network structure, this section examines whether the same relationships hold when historic and modern districts are analyzed separately. This perspective clarifies whether geometric scaling is systematically aligned with other structural properties across districts of the same type, and whether planning regimes shape these alignments in distinct ways.

Historic districts

In the historic sample (Table 4.13), fractal dimension is strongly associated with several indicators of morphological articulation and local-scale connectivity. Higher D values correspond to shorter average street segment lengths and higher intersection density, indicating that finer-grained networks exhibit greater

geometric subdivision. This alignment also extends to the reachability index, where denser local connections within 600 meters co-occur with more articulated street geometries. These relationships are statistically strong across the sample, indicating that historic street networks tend to link finer geometric grain with higher local reachability.

Table 4.13. Statistical representation for historic cores (D vs. Metric)

	Pearson's *r*	***p*-value**	**Spearman's *ρ***	***p*-value**
Intersection Density	0.56	$1.95*10^{-9}$	0.59	$5.86*10^{-9}$
Average Edge Length	-0.63	$2.87*10^{-12}$	-0.58	$1.72*10^{-11}$
Reachability Index	0.51	$4.77*10^{-8}$	0.53	$9.53*10^{-8}$
Harmonic Mean Shortest Path	0.26	0.009	0.20	0.011
Mean Straightness	-0.27	0.007	-0.14	0.011
Meshedness Coefficient	-0.18	0.067	-0.11	0.067

By contrast, measures such as straightness, meshedness coefficient, and harmonic mean shortest path length (HMSP) show weak or inconsistent correlations with D among historic districts. These indicators are more sensitive to path continuity across larger portions of the street network, and their weak alignment here suggests that fractal dimension is more closely linked to local geometric intensity than to properties related to global route continuity or looped structure.

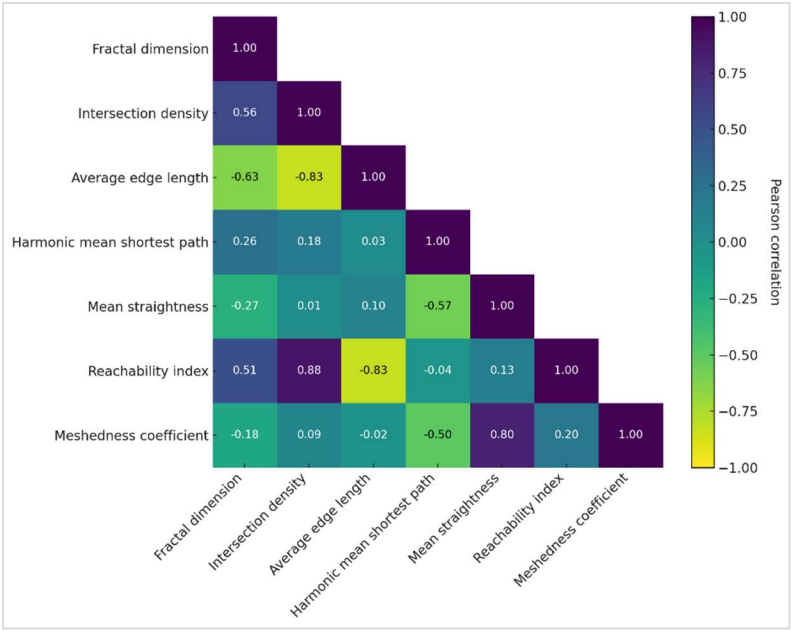

Figure 4.15. Heatmap of correlation matrix for historic cores

Modern Districts

Turning to the modern sample (Table 4.14), the structural relationships involving fractal dimension follow a similar general pattern but are notably more compact. Higher D values are again associated with shorter segment lengths and higher intersection densities, reflecting the same structural principle as in historic districts. However, these relationships fall within a narrower statistical range, consistent with the more standardized design norms and block layouts characteristic of contemporary planning.

Table 4.14. Statistical representation for modern districts (D vs. Metric)

	Pearson's *r*	***p*-value**	**Spearman's *ρ***	***p*-value**
Intersection Density	0.748	$3.87*10^{-19}$	0.771	$6.06*10^{-21}$
Average Edge Length	-0.714	$7.35*10^{-17}$	-0.709	$1.52*10^{-16}$
Reachability Index	0.691	$1.71*10^{-15}$	0.755	$1.07*10^{-19}$
Harmonic Mean Shortest Path	0.072	0.475	0.037	0.717
Mean Straightness	0.251	0.012	0.260	0.009
Meshedness Coefficient	0.354	$2.99*10^{-4}$	0.337	$6.13*10^{-4}$

Notably, the relationship between D and reachability remains significant, though slightly weaker than in historic districts. This suggests that while geometric and connective detail co-vary in newer areas, the strength of this alignment may be moderated by regularized spatial templates, zoning constraints, or other factors. As in the historic sample, indicators such as straightness, HMSP, and meshedness show weak or inconsistent alignment with fractal dimension, pointing to their more independent or context-dependent behavior.

Figure 4.16 visually reinforces this pattern: the matrix cells linking fractal dimension to indicators of grain and local accessibility intensify, while those tied to network-scale path efficiency remain subdued. Read side by side, the two matrices show continuity in direction and greater magnitude in the modern pattern – consistent with a wider dispersion of block sizes and junction densities, to which fractal dimension responds accordingly.

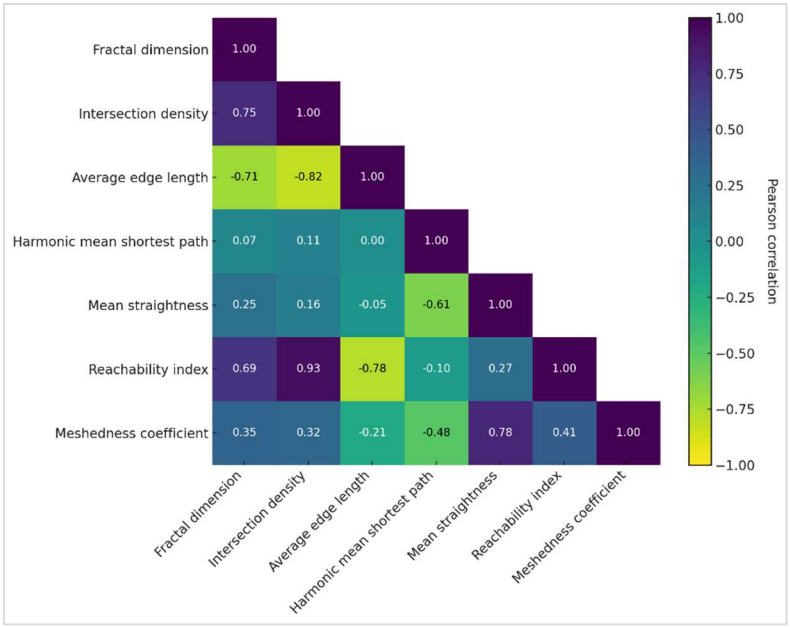

Figure 4.16. Heatmap of correlation matrix for modern districts

Taken together, these patterns indicate that fractal dimension consistently tracks variations in geometric granularity and local-scale access across both historic and modern street networks, but with stronger expression and greater variability in central districts. Modern networks cluster within a tighter band of morphometric and topological values, pointing to a reduction in diversity driven by regulations. Yet the

underlying structural principle holds: where streets are more finely subdivided and intersections denser, fractal dimension increases, and so does the potential for short-range movement.

Because correlation matrices compress information into compact form, two scatterplots are included as visual interpretation. Panel (a) shows the relationship between fractal dimension and average segment length, while panel (b) displays fractal dimension versus the reachability index. These illustrate the consistent inverse and positive associations, respectively, in both district groups, reinforcing the tendency for finer-grained geometries to coincide with higher fractal dimensions.

The full list of scatterplots – fractal dimension plotted against each of the six-network metrics – is provided in Appendix A-6 for reference.

Taken together with the paired-difference analysis in Section 4.3.1, these findings provide a second line of evidence for the interpretive role of fractal dimension as an integrative geometric indicator. It consistently captures how planar subdivision and local-scale connectivity co-vary within distinct typological groups.

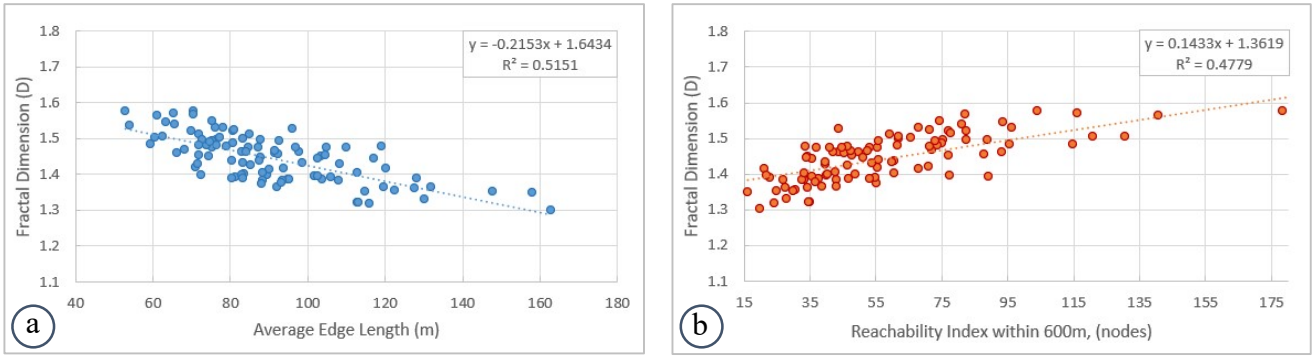

Figure 4.17. Scatter plots of Fractal dimension vs. Metric (modern districts)

Chapter 5: Discussion

This chapter interprets the results presented in Chapter 4 in relation to the thesis aim: to clarify the extent to which fractal dimension (D) provides a quantitative basis for differentiating street-network structures through its relationship with selected topological indicators. Rather than restating numerical outcomes, the focus is on examining how the observed relationships between fractal dimension and selected network metrics refine current understandings of street-network morphology.

Accordingly, this chapter is structured around four main aspects.

- First, it considers how fractal dimension relates to measurable features of street form;
- Second, it discusses the relationships between fractal dimension and local-scale connectivity indicators
- Third, it identifies the limits of what fractal dimension can capture – in particular, in relation to alignment and directional structure;
- Fourth, it synthesizes these results in relation to the research questions and hypotheses, highlighting the scope and limits of fractal dimension as an indicator of street-network structure.

5.1. Fractal Dimension as a descriptor of street-network structure

The results demonstrate that fractal dimension is systematically associated with certain geometric characteristics of street layouts in both historic and modern districts, though the strength and direction of these relationships vary between the two urban contexts. Across the sample, higher values of fractal dimension generally coincide with denser intersections, shorter street segments, and more articulated block structures, indicating that D reflects variation in the spatial grain of street-network structure.

This pattern becomes particularly evident when comparing historic cores with modern extensions. On average, historic districts exhibit higher fractal dimensions and a broader distribution of values, whereas modern districts cluster within a narrower band (Sections 4.1 and 4.2). Median differences in fractal dimension ($\Delta\tilde{D}$) between historic and modern areas range from approximately 0.015 to 0.031 across the four macro-regions (Figure 4.5; Table 4.5), indicating a consistent tendency for older districts to display more finely articulated street structures. These observations align with the first objective of the study (O1) and provide overall support for Hypothesis H1, which anticipated higher geometric complexity in historic street networks.

However, the results also reveal that this pattern is not uniform across all cities. While most cases follow the expected direction, several cities display negligible differences in fractal dimension between historic and modern areas, and in a small number of cases modern districts exhibit marginally higher values (e.g. Pori, Brno, Tilburg, Breda; see Figure 4.7). These exceptions indicate that geometric complexity is not determined solely by urban age. Instead, it also reflects specific development strategies and subdivision practices, particularly where modern planning has retained or reintroduced fine-grain configurations.

Regional analysis further clarifies these differences. In Northern Europe, historic districts consistently display higher fractal dimensions than their modern counterparts, reflecting a slight shift from intricate historic fabrics to relatively regularized modern extensions (Figure 4.1; Table 4.1). Western Europe exhibits a similar tendency but with greater internal variation, including cities where modern districts approach the fractal values of historic cores (Figure 4.2; Table 4.2). Eastern Europe is characterized by a wider dispersion and less consistent directional change, suggesting divergent trajectories of urban development (Table 4.3). In Southern Europe, both historic and modern districts maintain relatively high fractal dimensions, indicating a continuity in subdivision patterns rather than a sharp structural transition (Section 4.1.4).

These regional patterns refine the response to RQ1 by demonstrating that historic and modern districts differ systematically in street-network morphology, while also showing that the magnitude and expression of this difference are shaped by local development histories and planning traditions. The results therefore support the general tendency toward higher geometric complexity in historic cores, while confirming that modern development does not follow a singular spatial model.

Additional insight is provided by the paired-difference analysis presented in Section 4.3.1. The correlations between changes in fractal dimension and changes in intersection density and average edge length (Table 4.12; Figure 4.13) demonstrate that increases in D within cities are closely associated with shorter segments and denser junction patterns. Where historic districts exhibit higher fractal dimension than their modern counterparts, corresponding difference in street grain are more pronounced; where ΔD is small or negative, variation in these geometric measures is reduced.

Taken together, these findings address RQ2 by showing that fractal dimension captures a substantial portion of the geometric contrast between historic and modern street layouts. While D does not impose a rigid dichotomy between “historic” and “modern” forms, it identifies systematic variations in subdivision density and spatial irregularity across urban contexts, providing a credible basis for comparison at the mapped scale.

At the same time, these results also suggest that geometric complexity alone does not fully define structural differentiation. The extent to which fractal dimension relates to broader aspects of street-network

configuration – particularly connectivity and detour structure – requires further examination. This forms the focus of the following sections.

5.2. Fractal dimension and local-scale connectivity patterns

Where Section 5.1 examined fractal dimension primarily as an indicator of geometric complexity, this section turns to its relationship with selected topological indicators associated with local-scale connectivity, addressing Objectives O2 & O3 and Research Question RQ3. The focus here is on meshedness coefficient, reachability index, and their correspondence with variations in fractal dimension within and between historic and modern districts.

These indicators were selected because fractal dimension describes how finely space is subdivided, and meshedness and reachability reflect how that subdivision affects movement and local connectivity. If fractality meaningfully captures the structural grain of the street network, then higher values should relate to more route options and improved short-range accessibility.

At the scale of individual districts, higher values of fractal dimension generally coincide with increased levels of local-scale connectivity. This tendency is visible in the paired-difference analysis, where positive changes in fractal dimension (ΔD) are accompanied by increases in both meshedness coefficient and reachability index within a 600 m radius (Table 4.12; Figure 4.13). Districts exhibiting higher geometric subdivision therefore tend to show denser and more interlinked local networks, characterized by a greater number of alternative connections and shorter access distances between nodes. In this respect, the results lend support to Hypothesis H2, which anticipated higher pedestrian-scale reachability and structural redundancy in districts with finer urban grain.

This alignment also corresponds with the theoretical expectation that finer fractal subdivision should relate positively to local permeability and redundancy: if fractal dimension reflects the degree of spatial granularity, then higher values would reasonably be associated with more cross-linkages, alternative route choices, and shorter access distances at the pedestrian scale.

This relationship is further clarified by the groupwise correlation matrices presented in Tables 4.13 and 4.14. In historic districts, fractal dimension shows a weak negative association with meshedness ($r = -0.18$) while maintaining a positive association with reachability index, indicating that higher levels of geometric subdivision are not necessarily accompanied by increased network redundancy in organic street patterns. In modern districts, by contrast, fractal dimension displays a positive association with both reachability and meshedness, suggesting that in these contexts finer subdivision more frequently coincides with denser local interconnections. These contrasting patterns indicate that the relationship between geometric subdivision

and local street-network structure differs between historic and modern contexts, and that increases in D do not translate into the same configuration of connectivity across periods.

At the same time, the results indicate that the association between fractal dimension and local-scale connectivity is not perfectly linear or universal. Several districts display moderate to high fractal dimension values without a corresponding increase in meshedness, reflecting configurations in which dense subdivision coexists with limited cross-connections. This pattern is particularly apparent in certain modern districts where fine-grain subdivision is combined with selective permeability rather than a fully interconnected grid.

Taken together, these findings refine the interpretation of H2 and the local-scale component of H3. Fractal dimension does not merely reflect visual intricacy or block density in abstract terms; it corresponds in many cases to tangible differences in how densely local street segments are interconnected and how readily short-distance movement can occur. However, the variability observed across cities and between historic and modern contexts indicates that fractal dimension alone cannot fully account for the diversity of local connectivity structures.

Importantly, the results also reveal that the strongest correspondence between fractal dimension and connectivity measures occurs at the local scale. This supports the third hypothesis that structural differences between historic and modern districts are more strongly expressed through local indicators than through global network measures. The next section therefore turns to the alignment-related indicators, examining where and why these relationships weaken when broader-scale network characteristics are considered.

5.3. Fractal dimension and global-scale network characteristics

While the preceding section demonstrated a patterned association between fractal dimension and local-scale connectivity, the relationship becomes markedly weaker when examined in relation to alignment-related and global-scale indicators. Because fractal dimension reflects the degree of geometric irregularity and fine-grain subdivision, a negative association with alignment-oriented measures was initially expected: higher fractality was presumed to correspond with more winding geometries, lower directional coherence, and therefore reduced route directness. This section examines whether such a relationship materializes by evaluating the correspondence between fractal dimension and mean straightness, as well as harmonic mean shortest-path length, thereby addressing the alignment-oriented component of RQ3 and the broader implications of H3.

The paired-difference analysis presented in Table 4.12 and Figure 4.13 indicates that changes in fractal dimension across historic and modern districts are only weakly associated with changes in straightness index and harmonic mean shortest path length. In several cases, districts displaying higher fractal dimension

show little change, or even an opposite trend, in these alignment-related measures. This contrasts with the clearer pattern observed for reachability index and confirms that increases in geometric subdivision do not systematically coincide with more direct or cohesive route structures.

This divergence is further evident in the groupwise correlation matrices (Tables 4.13 and 4.14). In historic districts, the relationship between fractal dimension and mean straightness is weak and inconsistent, while its association with harmonic mean shortest path length remains negligible. In modern districts, these relationships become only marginally stronger, yet still highly variable, indicating that finer geometric subdivision is not a reliable marker of improved route directness or reduced detour. In other words, fractality may increase spatial texture without meaningfully influencing directional alignment.

These findings provide partial confirmation of H3, which anticipated a weaker association between fractal dimension and global network measures than with local connectivity indicators. While D aligns in many cases with short-range accessibility and local interconnectedness, it does not track the structural properties that shape longer-range route geometry and directional coherence. In practical terms, this suggests that districts with intricate, fine-grain layouts may still exhibit circuitous movement patterns or segmented route progression, particularly where street orientation, continuity, and overall network layout structure limit direct travel paths.

The contrast between Sections 5.2 and 5.3 therefore clarifies an important boundary in the interpretive scope of fractal dimension. While D reflects variations in geometric subdivision and, in many instances, local-scale interconnection, it does not sufficiently describe how clearly street networks guide movement across wider spatial extents. Accordingly, fractal dimension should be understood as an indicator of spatial texture rather than of directional structure within the network.

This distinction plays a central role in evaluating the overarching aim of the thesis. The following section synthesizes these findings by revisiting the research questions and hypotheses, clarifying where fractal dimension provides a meaningful basis for differentiating street-network structures and where its explanatory relevance remains limited.

5.4. Synthesis and Implications

This section integrates the findings discussed in Sections 5.1–5.3 and considers their broader implications for interpreting fractal dimension as a basis for describing street-network structures. Rather than repeating the detailed analyses, it consolidates the central patterns and clarifies their significance within the framework of the study's aims and hypotheses.

Across the sample, finer street grain – expressed through higher intersection densities and shorter average street segments – is systematically associated with higher fractal dimension and expanded short-range accessibility. This relationship affirms the theoretical expectation that organically evolved fabrics tend to produce denser local structures than planned modern grids. At the same time, the results demonstrate that higher fractal dimension alone does not ensure more direct or coherent route structures. The weak and inconsistent relationships observed with straightness and harmonic mean shortest path length indicate that additional subdivision yields diminishing returns for route geometry unless it is accompanied by clearer continuity across the street network.

The paired design further clarifies that 'modernization' is not synonymous with simplification. While many modern districts exhibit reduced subdivision and extended block structures, others retain or reintroduce finer-grain characteristics that approach those of historic cores. Regional narratives further confirm that context – from planning ideology to topography and land assembly – shapes how structural change unfolds. Not all modern development reduces complexity, and not all visual order translates into stronger local accessibility.

Importantly, the relatively narrow dispersion of fractal dimension values within each group ($\widetilde{D}_{old} \approx 1.50 \pm 0.07$; $\widetilde{D}_{new} \approx 1.40 \pm 0.07$) indicates that these differences are systematic rather than incidental. Although the absolute numerical difference may appear modest, fractal dimension operates within a constrained theoretical range for planar networks, meaning such shifts reflect meaningful variation in subdivision density and spatial organization. In this sense, D does not merely restate visual distinctions but formalises them into a quantifiable structure capable of cross-city comparison.

Overall, the findings demonstrate that the longstanding assumption in the literature – that organically evolved, fractal-like street networks enhance local accessibility relative to more regular grids – is partially supported. Higher D aligns clearly with local-scale accessibility and street network grain, yet it does not consistently predict global-scale topological measures. Fractal dimension therefore differentiates street-network structures most effectively in terms of geometric texture and local articulation, while its explanatory reach remains bounded with respect to broader network geometry.

In relation to the research design, this synthesis confirms that the selected contrast between organic historic cores and planned modern districts provides a valid theoretical testing ground. The results affirm the value of fractal dimension as a meaningful analytical tool, while also clarifying the limits within which such interpretation remains defensible.

Conclusion

This thesis set out to examine whether fractal dimension (D) provides a reliable quantitative basis for differentiating street-network structures through its relationship with selected geometric and topological indicators across contrasting urban contexts. By applying a consistent paired design to historic and modern districts in 100 European cities, the study has demonstrated that fractal dimension captures systematic variation in the spatial subdivision of street layouts, particularly in relation to intersection density and average segment length.

The results show that historic districts generally exhibit higher fractal dimensions than their modern counterparts, confirming a persistent tendency toward finer-grain subdivision in organically evolved urban fabrics. These differences, while numerically modest, are consistent across the majority of cases and operate within a constrained theoretical range, indicating that even small shifts in D reflect meaningful variation in spatial structure. At the same time, the analysis reveals that this pattern is not universal. In several contexts, modern districts display levels of geometric complexity comparable to, or exceeding, those of historic cores, illustrating that subdivision intensity is shaped not only by age but also by planning strategies and development regimes.

The study further demonstrates that fractal dimension aligns most clearly with local-scale characteristics of street networks. Higher values of D correspond in many cases with increased reachability and, in certain contexts, with meshedness, indicating an association with denser short-range interconnections. By contrast, its relationship with alignment-related indicators such as straightness and harmonic mean shortest path length is weak and inconsistent. This confirms that fractal dimension does not represent broader route geometry or directional structure and should not be interpreted as a comprehensive descriptor of overall network configuration.

Taken together, these findings indicate that fractal dimension provides a meaningful, but bounded, analytical lens for comparing urban street networks. Its primary value lies in representing geometric subdivision and aspects of local articulation, allowing the systematic comparison of spatial texture across cities and urban periods. At the same time, its interpretive scope remains limited with respect to alignment-related characteristics, reinforcing the necessity of combining fractal measures with complementary topological indicators when examining street-network structure.

Overall, the thesis contributes to the literature by offering an empirically grounded evaluation of fractal dimension in relation to widely cited claims about the structural advantages of organically developed street networks. It demonstrates that such claims are partially supported, particularly at the local scale, while also clarifying the limits of fractal metrics in capturing broader network organization. These conclusions establish a clear foundation for the subsequent discussion of methodological constraints and potential directions for further research.

Research limitations

This chapter outlines the principal constraints that shape the scope and interpretation of the findings presented in this thesis. These limitations do not undermine the validity of the analysis; rather, they clarify the precise conditions under which the results should be understood and the boundaries beyond which direct generalization is not warranted.

Methodological and scale-related constraints

Fractal dimension is conceptually grounded in scale-dependent analysis, as its theoretical formulation concerns how spatial patterns change across varying levels of observation. In this study, however, fractal dimension was estimated from street-network representations at a fixed cartographic scale (1:10,000). As a result, the reported values reflect geometric subdivision at this resolution rather than explicitly tested multi-scale behavior. The analysis therefore does not examine how fractal properties might vary under different levels of spatial aggregation. Consequently, the findings should not be interpreted as characterizing true scale invariance, but rather as relative differences under a consistent mapping scale.

Additionally, the fixed spatial sampling window of 1.2 km × 1.2 km ensured comparability but introduces constraints. While suitable for neighborhood-level analysis, this frame does not capture wider urban infrastructure patterns, regional connectivity, or peripheral network structures. Large-scale structural dynamics beyond the selected grid therefore fall outside the analytical scope of the study.

A further methodological limitation concerns the absence of road-type differentiation within the analysis. Streets were not categorized according to functional hierarchy (e.g. arterial, collector, local), primarily due to inconsistent tagging across cities, particularly in newer urban areas. As a result, the analysis does not distinguish between different functional roles within the network and therefore cannot address how hierarchical street organization may influence the structural indicators examined.

In addition, the analytical framework is based entirely on structural indicators derived from graph representations of street networks. Measures such as reachability index, meshedness coefficient, mean straightness, and harmonic mean shortest path length describe potential accessibility and network configuration, not observed mobility or pedestrian behavior. No empirical data on movement patterns, travel frequencies, or user experience were incorporated. Therefore, the results pertain to the structural conditions that shape possible movement rather than to actual patterns of use or perceived walkability.

Data, selection, and scope-related constraints

The study adopts a paired design based on the comparison of historic cores and modern planned extensions within the same city. This selection strategy strengthens internal comparability by isolating structural differences attributable to development period and planning logic while holding broader contextual factors constant. However, it also limits the scope of generalization to urban forms that clearly display this dual morphology. The results therefore apply most directly to cities characterized by a discernible contrast between organically evolved historic areas and formally planned modern districts. Other configurations, such as suburban sprawl or hybrid transitional fabrics, are not directly represented and may exhibit different structural relationships between fractal dimension and network configuration.

The study relies on spatial data derived from publicly available cartographic sources and standardized preprocessing procedures. Although care was taken to ensure consistency in data preparation, minor variations in mapping detail or digitization practices may persist, particularly in older or fragmented urban fabrics. These factors may introduce small deviations in the calculation of certain indicators, although the overall comparative patterns observed across the sample remain robust.

Analytical and interpretive constraints

The analysis is based on a defined set of geometric and topological indicators, including intersection density, average edge length, meshedness coefficient, reachability index, mean straightness, and harmonic mean shortest path length. While these measures capture key aspects of street-network structure, they do not exhaust the range of possible analytical perspectives. Alternative metrics such as betweenness centrality, closeness, or angular integration may reveal additional structural dimensions not addressed in this study. The interpretive conclusions therefore reflect the adopted analytical frame rather than a comprehensive representation of all possible network properties.

The statistical approach adopted in this study identifies associations between fractal dimension and selected street-network indicators through correlation-based analysis. While these relationships provide insight into structural co-variation, they do not establish causal mechanisms. Observed correlations should therefore not be interpreted as evidence that changes in fractal dimension directly produce specific connectivity outcomes or vice versa. The findings describe patterned relationships within the sampled networks, not deterministic or predictive rules governing street form.

Taken together, these limitations define the analytical boundaries of the thesis. The results provide a consistent and empirically grounded assessment of how fractal dimension relates to particular aspects of street-network structure within a controlled methodological framework. At the same time, they highlight the importance of maintaining conceptual precision and avoiding the overextension of fractal interpretation beyond the scale, data, and indicator set employed in the present analysis.

Recommendations and Future research

This thesis examined street-network form and configuration by situating fractal dimension as a central descriptor of geometric subdivision and structural organization. A focused direction for future research is to extend this line of inquiry toward movement-based and perceptual dimensions interpreted through fractal variation.

Future studies should therefore examine whether districts exhibiting higher or lower fractal dimension display systematic differences in pedestrian flow, vehicle circulation, congestion patterns, and travel time distributions. The use of traffic counts, GPS traces, mobile positioning data, or pedestrian sensors would enable direct comparison between fractal-based structural characteristics and movement patterns, clarifying the extent to which fractal-like street configurations align with modes or intensities of use under real-world conditions.

Beyond movement volume, future work should incorporate temporal dynamics into the analysis. Evaluating how street networks accommodate under varying conditions – such as peak versus off-peak periods, weekday versus weekend patterns, or seasonal fluctuations – would further clarify how fractal street structure interacts with time-dependent operational pressures. This would shift analysis from static representation toward process-oriented understanding of street network behavior.

A parallel line of research should address perceptual and cognitive aspects of navigability in relation to fractal geometry. Future research could explore whether higher levels of geometric subdivision, as expressed through fractal dimension, influence perceived legibility, orientation, and wayfinding ease. Methods such as cognitive mapping, controlled navigation experiments, or survey-based assessments would allow evaluation of whether fractal complexity supports or hinders intuitive spatial comprehension.

Together, these approaches would enable a more comprehensive framework for interpreting street networks, situating fractal dimension within a broader set of structural, operational, and experiential indicators that describe how urban form shapes movement and navigation.

Reference List

Alexander, C. (1965). *A city is not a tree*. Architectural Forum, 122, 58–62.

Alexander, C. (2001). *The Nature of Order: An Essay on the Art of Building and the Nature of the Universe*. Oxford University Press.

Arcaute, E., Molinero, C., Hatna, E., Murcio, R., Vargas-Ruiz, C., Masucci, P. & Batty, M. (2016). Cities and regions in Britain through hierarchical percolation. *Royal Society Open Science, 3*(4). https://doi.org/10.1098/rsos.150691

Babič, M., Marinkovic, D., Kovacic, M., Šter, B. & Calì, M. (2022). A New Method of Quantifying the Complexity of Fractal Networks. *Fractal and Fractional, 6*(282), 1-11. https://doi.org/10.3390/fractalfract6060282

Badhrudeen, M., Derrible, S., Verma, T., Kermanshah, A., & Furno, A. (2022). A geometric classification of world urban road networks. *Urban Science, 6*(1), 1–15. https://doi.org/10.3390/urbansci6010011

Batty, M. (1991). Generating Urban Forms from Diffusive Growth. *Environment and Planning A: Economy and Space*, *23*(4), 511-544. https://doi.org/10.1068/a230511

Batty, M., & Longley, P. (1994). *Fractal Cities: A Geometry of Form and Function.* Academic Press.

Batty, M., & Xie, Y. (1996). Preliminary Evidence for a Theory of the Fractal City. *Environment and Planning A: Economy and Space*, *28*(10), 1745-1762. https://doi.org/10.1068/a281745 (Original work published 1996)

Batty, M. (1997). Cellular automata and urban form: A primer. *Journal of the American Planning Association, 63*(2), 266–274. https://doi.org/10.1080/01944369708975918

Batty, M. (2005). *Cities and Complexity: Understanding Cities with Cellular Automata, Agent-Based Models, and Fractals*. MIT Press.

Batty, M. (2008). The size, scale, and shape of cities. *Science, 319*(5864), 769–771.

Batty, M., & Milton, R. (2021). A new framework for very large-scale urban modelling. *Urban Studies, 58*(15), 3071–3094. https://doi.org/10.1177/0042098020982252

Ben-Hamouche, M. (2009). Complexity of urban fabric in traditional Muslim cities: Importing old wisdom to present cities. *Urban Design International*, *14*(1), 22-35. https://doi.org/10.1057/udi.2009.7

Boeing, G. (2017). OSMnx: New methods for acquiring, constructing, analyzing, and visualizing complex street networks. *Computers, Environment and Urban Systems, 65*, 126–139. https://doi:10.1016/j.compenvurbsys.2017.05.004

Boeing, G. 2018. Measuring the Complexity of Urban Form and Design. *Urban Design International, 23*, 281–292. https://doi.org/10.1057/s41289-018-0072-1

Boeing, G. (2020). Off the Grid … and Back Again? *Journal of the American Planning Association, 1-15.* http://doi:10.1080/01944363.2020.1819382

Boeing, G. (2021). Street Network Models and Indicators for Every Urban Area in the World. *Geographical Analysis*, 1–19. http://dx.doi.org/10.2139/ssrn.3695331

Boccaletti, S., Latora, V., Moreno, Y., Chavez, M., & Hwang, D. U. (2006). Complex networks: Structure and dynamics. *Physics Reports*, *424*(4), 175–308. https://doi.org/10.1016/j.physrep.2005.10.009

Bunimovich, L. & Skums, P. (2024). Fractal networks: Topology, dimension, and complexity. *Chaos: An Interdisciplinary Journal of Nonlinear Science, 34*(4). https://doi.org/10.1063/5.0200632.

Caglioni, M., & Giovanni, R. (2004). Contribution to the fractal analysis of cities: A study of the metropolitan area of Milan. *Cybergeo*. https://doi.org/10.4000/cybergeo.3634

Chen, Y. & Luo, J. (1998). The fractal features of the transport network of Henan Province. *Journal of Xinyang Teachers College, 11*(2), 172-177.

Chen, Y. (2013). Fractal analytical approach of urban form based on spatial correlation function. *Chaos, Solitons & Fractals*, *49*, 47-60. https://doi.org/10.1016/j.chaos.2013.02.006

Chen, Y. & Huang, L. (2019). Modeling the growth curve of the fractal dimension of the urban form of Beijing. *Physica A: Statistical Mechanics and its Applications*, *523*, 1038-1056. https://doi.org/10.1016/j.physa.2019.04.165

Clifton, K., Ewing, R., Knaap, G., & Song, Y. (2008). Quantitative analysis of urban form: a multidisciplinary review. *Journal of Urbanism: International Research on Placemaking and Urban Sustainability*, *1*(1), 17–45. https://doi.org/10.1080/17549170801903496

Coates, G. J. (2013). The sustainable urban district of Vauban In Freiburg, Germany. *International Journal of Design & Nature and Ecodynamics*, *8*(4), 265–286. https://doi.org/10.2495/DNE-V8-N4-265-286

Daniel, C. B., Mathew, S., & Saravanan, S. (2021). Spatial interdependence of fractal dimension and topological parameters of road network: a geographically weighted regression approach. *Spatial Information Research, 29*, 737-747. doi:10.1007/s41324-021-00390-w

Duany, A., Plater-Zyberk, E., & Speck, J. (2000). *Suburban Nation: The Rise of Sprawl and the Decline of the American Dream*. New York: North Point Press.

Fleischmann, M., Samardzhiev, K., Brazdova, A. Dancejova, D. & Winkler, L. (2025). The Hierarchical Morphotope Classification: A Theory-Driven Framework for Large-Scale Analysis of Built Form. *Computers and Society*. https://doi.org/10.48550/arXiv.2509.10083

Frankhauser, P. (1998). The fractal approach: A new tool for the spatial analysis of urban agglomerations. *Population: An English Selection, 10*(1), 205–240.

Frankhauser, P. (2004). Comparing the morphology of urban patterns in Europe – a fractal approach. In A. Borsdorf & P. Zembri (Eds.), *European cities—Insights on outskirts* (Vol. 2, pp. 79–105). Université de Bourgogne Franche-Comté.

Goodchild, M. F., & Mark, D. M. (1987). The Fractal Nature of Geographic Phenomena. *Annals of the Association of American Geographers*, *77*(2), 265-278. https://doi.org/10.1111/j.1467-8306.1987.tb00158.x

Hakim, B. S. (1986). *Arabic-Islamic Cities: Building and Planning Principles*. London: Routledge.

Hillier, B., & Hanson, J. (1984). *The Social Logic of Space*. Cambridge University Press.

Hillier, B. (1996). *Space is the machine: A configurational theory of architecture*. Cambridge Univ. Press.

Holston, J. (1989). *The Modernist City: An Anthropological Critique of Brasília*. Univ. of Chicago Press.

Howard, E. (1902). *Garden Cities of To-morrow*. London: Swan Sonnenschein & Co.

Hyseni, R., Nepravishta, F. & Asanbejlli, K. (2021). Measuring the complexity of urban form. *International Journal of Ecosystems and Ecology Science, 11*(3), 557-568. https://doi.org/10.31407/ijees11.327

Encarnacao, S., Gaudiano, M., Santos, F.C., Tenedório, J.A., & Pacheco, J.M. (2012). Fractal cartography of urban areas. *Scientific Report, 2*. https://doi.org/10.1038/srep00527

Ewing, R., & Handy, S. (2009). Measuring the Unmeasurable: Urban Design Qualities Related to Walkability. *Journal of Urban Design*, *14*(1), 65–84. https://doi.org/10.1080/13574800802451155

Essex Planning Officers Association. (2018, January 31). *Urban Grain*. Retrieved from https://www.essexdesignguide.co.uk/design-details/layout-details/urban-grain/

Jacobs, J. (1961). *The death and life of great American cities*. Random House.

Jahanmiri, F., & Parker, D. C. (2022). An overview of fractal geometry applied to urban planning. *Land, 11*(4). https://doi.org/10.3390/land11040475

Jevric, M., Kneževic, M., Kalezic, J., Kopitovic-Vukovic, N., & Cipranic, I. (2014). Application of fractal geometry in urban pattern design. *Technical Gazette, 4*, 873-879.

Jevric, M., & Romanovich, M. (2016). Fractal dimensions of urban border as a criterion for space management. *Procedia Engineering, 165*, 1478-1482. https://doi.org/10.1016/j.proeng.2016.11.882

Jiang, B., & Claramunt, C. (2004). Topological analysis of urban street networks. *Environment and Planning B: Planning and Design, 31*(1), 151–162. https://doi.org/10.1068/b306

Jiang, B. (2007). A topological pattern of urban street networks: Universality and peculiarity. *Physica A: Statistical Mechanics and its Applications, 384*(2), 647–655. https://doi.org/10.1016/j.physa.2007.05.064

Jiang, B. (2009). Street hierarchies: a minority of streets account for a majority of traffic flow. *International Journal of Geographical Information Science*, *23*(8), 1033–1048. https://doi.org/10.1080/13658810802004648

Jiang, B. (2021). Geography as a science of the Earth's surface founded on the third view of space. *Annals of the American Association of Geographers, 112*(6), 1576–1592. https://doi.org/10.1080/19475683.2021.1966502

Jin, Y., Wu, Y., Li, H., Zhao, M., & Pan, J. (2017). Definition of fractal topography to essential understanding of scale-invariance. *Scientific Report, 7*, 46672. https://doi.org/10.1038/srep46672

Kartal S., & Inceoglu, M. (2023). Evaluating Street Character Using the 3D Fractal Analysis Method: Lefkosa. *Journal of Design Studio, 5*(2), 207-222. https://doi.org/10.46474/jds.1368023

King, A. D. (2004). *Spaces of Global Cultures: Architecture, Urbanism, Identity*. London: Routledge.

Knowles, R.D. (2006). Transport shaping space: Differential collapse in time-space. *Journal of Transport Geography*, *14*, 407-425. https://doi.org/10.1016/j.jtrangeo.2006.07.001

Kostof, S. (1991). *The city shaped: Urban patterns and meanings through history*. Thames & Hudson.

Labatut, V. (2018). Continuous average Straightness in spatial graphs. *Journal of Complex Networks*, *6*(2), 269–296. https://doi.org/10.1093/comnet/cnx033

Lagarias, A. & Prastacos, P. (2021). Fractal dimension of European Cities: A comparison of the patterns of built-up areas in the urban core and the peri-urban ring. *Cybergo: European Journal of Geography*. https://doi.org/10.4000/cybergeo.37243

Le Corbusier. (1935). *La Ville Radieuse*. Boulogne: Editions de l'Architecture d'Aujourd'hui.

Louf, R. & Barthelemy, M. (2014). A typology of street patterns. *Journal of the Royal Society: Interface, 11*. http://dx.doi.org/10.1098/rsif.2014.0924

Lu, Y., & Tang, J. (2004). Fractal Dimension of a Transportation Network and its Relationship with Urban Growth: A Study of the Dallas-Fort Worth Area. *Environment and Planning B: Planning and Design*, *31*(6), 895-911. https://doi.org/10.1068/b3163

Lu, Z., Zhang, H., Southworth, F., & Crittenden, J. (2016). Fractal dimensions of metropolitan area road networks and the impacts on the urban built environment. *Ecological Indicators, 70*, 285–296. https://doi.org/10.1016/j.ecolind.2016.06.016

Lynch, K. A. (1960). *The Image of the City*. MIT Press.

Mandelbrot, B. B. (1983). *The fractal geometry of nature*. W. H. Freeman and Company.

Marshall, S. (2004). *Streets and patterns*. Routledge.

Marshall, S. (2009). *Cities, Design and Evolution*. Routledge.

Masucci, A. P., Smith, D., Crooks, A. & Batty, M. (2009). Random planar graphs and the London street network. *European Physical Journal B, 71*. 259-271. https://doi.org/10.1140/epjb/e2009-00290-4

Mehaffy, M. W., Porta, S., Rofè, Y., & Salingaros, N. A. (2010). Urban nuclei and the geometry of streets: The 'emergent neighborhoods' model. *Urban Design International*, 15(1), 22–46. https://doi.org/10.1057/udi.2009.26

Merlo, A., & Lavoratti, G. (2024). Documenting Urban Morphology: From 2D Representations to Metaverse. *Land*, *13*(2), 136. https://doi.org/10.3390/land13020136

Monclús, F. J. (2003). The Barcelona model: An original formula? From 'reconstruction' to strategic urban projects (1979–2004). *Planning Perspectives*, 18(4), 399–421. https://doi.org/10.1080/0266543032000117514

Moreira, S. (2020, October 10). *Orthogonal Grids and Their Variations in 17 Cities Viewed from Above. ArchDaily.* https://www.archdaily.com/949094/orthogonal-grids-and-their-variations-in-17-cities-viewed-from-above

Mulligan, G. F. (1997). [Review of the book *Fractal Cities: A geometry of form and function*, by M. Batty & P. Longley]. *Cities, 14*(1). 54-55. https://doi.org/10.1016/S0264-2751(97)89331-6

Mumford, L. (1961). *The City in History: Its Origins, Its Transformations, and Its Prospects*. New York: Harcourt Brace Jovanovich.

Pafka, E., & Dovey, K. (2016). Permeability and interface catchment: measuring and mapping walkable access. *Journal of Urbanism: International Research on Placemaking and Urban Sustainability*, *10*(2), 150–162. https://doi.org/10.1080/17549175.2016.1220413

Pagliardini, P., Porta, S., & Salingaros, N. A. (2010). Geospatial analysis and living urban geometry. *Geospatial Analysis and Modelling of Urban Structure and Dynamics*, *99*, 331-353. https://doi.org/10.1007/978-90-481-8572-6_17

Piera, J., Parisi-Baradad, V., García-Ladona, E., Lombarte, A., Recasens, L. & Cabestany, J. (2005). Otolith shape feature extraction oriented to automatic classification with open distributed data. *Marine and Freshwater Research, 56*(5), *805–814.* https://doi:10.1071/mf04163

Porta, S., Crucitti, P., & Latora, V. (2006). The network analysis of urban streets: A dual approach. *Physica A: Statistical Mechanics and its Applications, 369*(2), 853–866. https://doi.org/10.1016/j.physa.2005.12.063

Portugali, J. (2011). *Complexity, Cognition and the City*. Springer.

Reza, S., Ferreira, M.C., Machado, J. & Tavares. J. (2024). Road network structure analysis: A preliminary network science-based approach. *Annals of Mathematics and Artificial Intelligence, 92*, 215–234. https://doi.org/10.1007/s10472-022-09818-x

Salingaros, N. A. (1998). Theory of the urban web. *Journal of Urban Design, 3*(1), 53-71. https://doi.org/10.1080/13574809808724416

Salingaros, N. A. (2000). Complexity and Urban Coherence. *Journal of Urban Design, 5*(3), 291–316. https://doi.org/10.1080/713683969

Salingaros, N. A. (2003, April). *Connecting to the fractal city* [Keynote speech]. 5th Biennial of Town Planners in Europe, Barcelona, Spain.

Salingaros, N. A., & Pagliardini, P. (2016). Geometry and life of urban space. In *Back to the sense of the city* (pp. 13–31). Centre of Land Policy and Valuations (Centre de Política de Sòl i Valoracions).

Scott, J. C. (1998). *Seeing Like a State: How Certain Schemes to Improve the Human Condition Have Failed*. New Haven, CT: Yale University Press.

Sennett, R. (2018). *Building and Dwelling: Ethics for the City*. New York: Farrar, Straus and Giroux.

Shen, G. (2002). Fractal dimension and fractal growth of urbanized areas. *International Journal of Geographical Information Science, 16*, 419-437.

Sevtsuk, A., Kalvo, R. & Ekmekci, O. (2016). Pedestrian accessibility in grid layouts: the role of block, plot, and street dimensions. *Urban Morphology, 20*(2), 89–106. https://doi.org/10.51347/jum.v20i2.4056

Southworth, M., & Ben-Joseph, E. (2003). *Streets and the Shaping of Towns and Cities*. Washington, DC: Island Press.

Sreelekha, M. G., Krishnamurthy, K. & Anjaneyulu, M.V. (2017). Fractal Assessment of Road Transport System. *European Transport, 65*(5), 1-13.

Sreelekha, M. G., Krishnamurthy, K. & Anjaneyulu, M.V. (2020). Urban Road Network and its Topology: Case Study of Calicut, India. *European Transport, 78*(6), 1-15 https://doi.org/10.48295/ET.2020.78.6

Strano, E., Nicosia, V., Latora, V., Porta, S., & Barthélemy, M. (2012). Elementary processes governing the evolution of road networks. *Scientific Reports, 2*, 296. https://doi.org/10.1038/srep00296

Strano, E., Viana, M., da Fontoura Costa, L., Cardillo, A., Porta, S., & Latora, V. (2014). Urban Street Networks, a Comparative Analysis of Ten European Cities. *Environment and Planning B: Planning and Design*, *40*(6), 1071-1086. https://doi.org/10.1068/b38216

Sýkora, L., & Bouzarovski, S. (2012). Multiple transformations: Conceptualising the post-communist urban transition. *Urban Studies, 49*(1), 43–60. https://doi.org/10.1177/0042098010397402.

Talen, E. (2003). Measuring urbanism: issues in smart growth research. *Journal of Urban Design, 8*(3), 195–215. https://doi.org/10.1080/1357480032000155141

Tannier, C., & Pumain, D. (2005). Fractals in urban geography: A theoretical outline and an empirical example. *Cybergeo: European Journal of Geography*. https://doi.org/10.4000/cybergeo.3275

Terzidis, K. (2006). *Algorithmic Architecture.* Oxford, Elsevier Architectural Press.

Thomas, I., Frankhauser, P., & De Keersmaecker, M. L. (2007). Fractal dimension versus density of built-up surfaces in the periphery of Brussels. *Papers in Regional Science, 86*, 287–308. https://doi.org/10.1111/j.1435-5957.2007.00122.x

Thomas, I., Frankhauser, P., & Badariotti, D. (2012). Comparing the fractality of European urban neighborhoods: Do national contexts matter?. *Journal of Geographical Systems, 14*(2), pp. 189-208. https://doi.org/10.1007/s10109-010-0142-4

Tiefenbacher, J. P. (2020). *Environmental Management - Pollution, Habitat, Ecology, and Sustainability.* InTechOpen. https://doi.org/10.5772/intechopen.94788

Tsenkova, S. (2006). Beyond transitions: Understanding urban change in post-socialist cities. *Contributions to Economics*, 21–50. https://doi.org/10.1007/3-7908-1727-9_2

van Vliet, J., Hurkens, J., White, R., & van Delden, H. (2012). An activity-based cellular automaton model to simulate land-use dynamics. *Environment and Planning B: Planning and Design, 39*(2), 198–212. https://doi.org/10.1068/b36015

Verkade, Thalia. (2020). *De oplossing voor het fileprobleem: nu hebben we hem echt!* De correspondent. Retrieved from https://decorrespondent.nl/11363/de-oplossing-voor-het-fileprobleem-nu-hebben-we-hem-echt/c33eed4c-a7ad-0826-0e54-35ae5bd10cb8

Vragović, I., Louis, E. & Díaz-Guilera, A. (2005). Efficiency of informational transfer in regular and complex networks. *Physical review E: Statistical, nonlinear, and soft matter physics*, *71*(3). https://doi: 10.1103/PhysRevE.71.036122.

Wagner & Debes. (1899). *Sevilla city map* [Map]. Leipzig, Germany.

Wang, H., Luo, S., & Luo, T. (2017). Fractal characteristics of urban surface transit and road networks: Case study of Strasbourg, France. *Advances in Mechanical Engineering, 9*(2). https://doi.org/10.1177/1687814017692289

Wang, J., Huang, W., & Biljecki, F. (2024). Learning visual features from figure-ground maps for urban morphology discovery. *Computers, Environment and Urban Systems*, *109*. https://doi.org/10.1016/j.compenvurbsys.2024.102076

Wasserman, S. & Faust, K. (1994). *Social Network Analysis*. Cambridge University Press

White, R., & Engelen, G. (1993). Cellular automata and fractal urban form: A cellular modelling approach to the evolution of urban land-use patterns. *Environment and Planning A: Economy and Space, 25(8)*, 1175–1199. https://doi.org/10.1068/a251175

Wu, C. Y., Hu, M. B., Jiang, R. & Hao, Q. Y. (2021). Effects of road network structure on the performance of urban traffic systems. *Physica A: Statistical Mechanics and its Applications, 563.* https://doi:10.1016/j.physa.2020.125361

Yoo, C., & Lee, S. (2017). When organic urban forms and grid systems collide: Application of space syntax for analyzing the spatial configuration of Barcelona, Spain. *Journal of Asian Architecture and Building Engineering*, *16*(3), 597-604. https://doi.org/10.3130/jaabe.16.597

Yu, X., & Zhao, Z. (2021). Fractal characteristic evolution of coastal settlement land use: A case of Xiamen, China. *Land, 11*, 50. https://doi.org/10.3390/land11010050

Yuan, M., Song, Y., & Guo, L. (2018). Exploring Determinants of Urban Form in China through an Empirical Study among 115 Cities. *Sustainability*, *10*(10), 3648. https://doi.org/10.3390/su10103648

Zhang, H., & Li, Z. L. (2012). Fractality and self-similarity in the structure of road networks. *Annals of the Association of American Geographers, 102(2)*, 350–365. https://doi.org/10.1080/00045608.2011.620505

Zhao, J., Hao, X. & Yang, Y. (2023). Research on Urban Sustainability Indicators Based on Urban Grain: A Case Study in Jinan, China. *Sustainability, 15*. https://doi.org/10.3390/su151813320

Appendix

A-1. The list of cities by region and country

Europe	Country	City
North	Denmark	Odense
		Esbjerg
		Aalborg
		Aarhus
		Copenhagen
North	Finland	**Helsinki**
		Tampere
		Mikkeli
		Turku
		Pori
North	Norway	Hamar
		Bergen
		Stavanger
		Tonsberg
		Oslo
North	Sweden	**Stockholm**
		Gothenburg
		Helsingborg
		Malmo
		Vasteras
Europe	**Country**	**City**
East	Bulgaria	Haskovo
		Yambol
		Varna
		Plovdiv
		Ruse
East	Czech Republic	Brno
		Prague
		Pilsen
		Liberec
		Ostrava
East	Hungary	Debrecen
		Gyongyos
		Nyiregyhaza
		Budapest
		Pecs
East	Poland	Poznan
		Częstochowa
		Lodz
		Wroclaw
		Warsaw

Europe	Country	City
Western	Austria	Graz
		Linz
		Innsbruck
		Klagenfurt
		Vienna
Western	Belgium	Ghent
		Antwerp
		Bruges
		Brussels
		Ostend
Western	Germany	Hamburg
		Düsseldorf
		Nuremberg
		Augsburg
		Cologne (Koln)
Western	France	Bordeaux
		Toulouse
		Dijon
		Rouen
		Beziers
Western	Netherlands	Nijmegen
		Eindhoven
		Tilburg
		Zoetermeer
		Breda
Europe	**Country**	**City**
South	Greece	Thessaloniki
		Katerini
		Larissa
		Ioannina
		Lamia
South	Italy	Florence
		Naples
		Palermo
		Bologna
		Padua
South	Portugal	Porto
		Lisbon
		Castelo Branco
		Setubal
		Evora

East	Romania	**Bucharest**		South	Republic of Cyprus	**Nicosia**
		Craiova				Paphos
		Oradea				Limassol
		Satu Mare				Larnaca
		Timisoara				Famagusta
East	Slovakia	**Bratislava**		South	Spain	Granada
		Košice				Seville
		Nove Zamky				Cordoba
		Trnava				Zaragoza
		Nitra				Malaga

A-2. Python scripts for downloading and projecting street network data

The following Python script reads a road network shapefile from a local directory, reprojects it to the appropriate city-specific projected coordinate system (CRS), and plots the result. To adapt the script for different cities, it is necessary to change the values of `shapefile_path` (the file location) and `local_crs` (EPSG code).

```
import geopandas as gpd
import matplotlib.pyplot as plt
import neatnet

# User-defined variables
shapefile_path = r"PATH/TO/FILE.shp"  # <-- Change to shapefile path for desired city
local_crs = EPSG_CODE                 # <-- Change to appropriate CRS (EPSG code)

# Loading streets from a shapefile
roads = gpd.read_file(shapefile_path)

# Ensuring it is in a local projected CRS
if roads.crs.is_geographic:
    roads = roads.to_crs(epsg=local_crs)

# Plot streets
ax = roads.plot(figsize=(15, 15), linewidth=0.5, color='black')
ax.set_axis_off()
plt.title(f"{place} Road Network")
plt.show()

# Neatify
simplified = neatnet.neatify(roads)
```

A-3. Differences in fractal dimension between Historic and Modern samples across 100 Cities

Note: Positive ΔD values indicate that historic areas are more complex; negative values, vice versa.

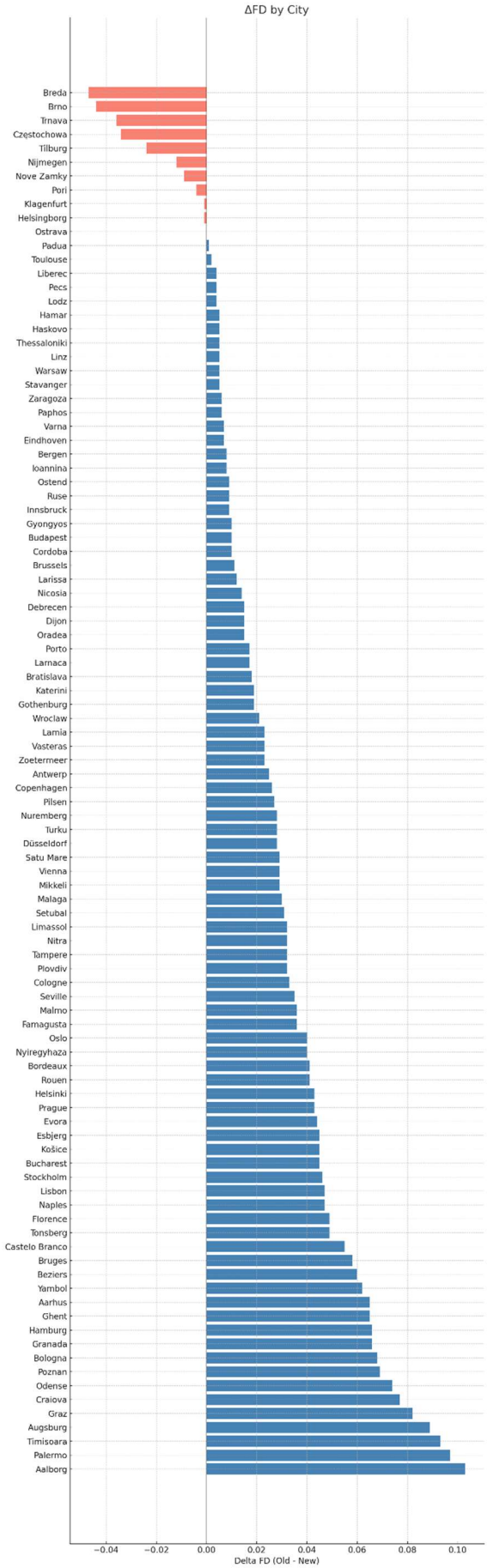

A-4. Descriptive statistics of network indicators for historic and modern districts by regions.

Northern Europe

Country	City	District	Intersection Density	Avg. Edge Length	Reach. Index (600m)	Harmonic Mean shortest path	Mean straightness	Meshedness coefficient
Denmark	Odense	Old	70.1	81.2	35.66	452.5	0.785	0.208
		New	86.8	108.4	39.69	639.2	0.565	0.027
	Esbjerg	Old	68.1	93.8	39.65	493.9	0.766	0.234
		New	65.9	102.6	33.95	489.9	0.758	0.148
	Aalborg	Old	75.0	93.8	36.94	513.5	0.746	0.157
		New	59.7	102.6	22.03	594.2	0.653	0.066
	Aarhus	Old	74.3	85.5	36.33	504.6	0.685	0.137
		New	61.8	112.8	33.17	478.4	0.802	0.154
	Copenhagen	Old	90.9	81.47	56.75	451.1	0.774	0.186
		New	83.3	97.1	44.90	464.0	0.801	0.216
Finland	Helsinki	Old	84.7	91.9	50.30	464.8	0.804	0.251
		New	31.4	157.9	16.31	546.1	0.679	0.146
	Tampere	Old	69.2	93.5	42.58	515.5	0.733	0.210
		New	70.3	71.7	53.70	543.2	0.641	0.193
	Mikkeli	Old	59.2	106.9	31.19	533.3	0.738	0.198
		New	46.2	113.2	34.68	462.1	0.712	0.122
	Turku	Old	61.5	109.1	24.04	515.0	0.765	0.183
		New	44.4	127.5	34.23	348.9	0.814	0.175
	Pori	Old	97.2	79.1	58.13	422.5	0.799	0.276
		New	106.9	72.4	77.52	420.5	0.745	0.265
Norway	Hamar	Old	99.3	79.8	63.08	479.8	0.770	0.199
		New	66.7	98.8	39.72	496.5	0.722	0.155
	Bergen	Old	113.2	65.1	54.99	533.4	0.661	0.154
		New	79.2	77.2	62.00	431.7	0.612	0.122
	Stavanger	Old	129.8	69.1	100.09	402.6	0.767	0.206
		New	125.0	74.6	77.22	478.9	0.695	0.177
	Tonsberg	Old	95.8	76.4	72.28	425.0	0.750	0.217
		New	84.7	83.3	53.07	456.6	0.726	0.157
	Oslo	Old	103.5	81.7	65.21	442.0	0.809	0.223
		New	81.9	87.7	55.73	434.0	0.805	0.224
Sweden	Stockholm	Old	100.7	84.9	48.84	546.4	0.709	0.186
		New	88.9	88.0	55.34	455.9	0.752	0.260
	Gothenburg	Old	88.2	76.6	61.49	459.8	0.754	0.208
		New	102.1	80.6	54.84	480.8	0.712	0.172
	Helsingborg	Old	95.8	78.1	56.93	435.2	0.779	0.199
		New	93.8	90.1	68.04	431.8	0.788	0.194
	Malmo	Old	106.3	85.2	64.96	467.5	0.778	0.225
		New	70.1	88.5	42.70	476.4	0.710	0.127
	Vasteras	Old	102.8	78.9	62.76	486.6	0.710	0.201
		New	75.0	93.3	36.80	494.8	0.660	0.145

Country	City	District	Intersection Density	Avg. Edge Length	Reach. Index (600m)	Harmonic Mean shortest path	Mean straightness	Meshedness coefficient
Austria	Graz	Old	81.3	80.2	51.54	446.2	0.746	0.175
		New	63.2	117.2	35.79	481.4	0.784	0.217
	Linz	Old	72.2	100.5	32.42	518.6	0.756	0.200
		New	91.7	92.3	45.59	508.7	0.745	0.179
	Innsbruck	Old	81.9	74.0	53.17	447.8	0.772	0.219
		New	72.2	83.2	49.96	427.9	0.812	0.258
	Klagenfurt	Old	71.5	111.3	30.53	525.8	0.737	0.158
		New	77.8	104.6	47.86	459.1	0.789	0.218
	Vienna	Old	121.5	70.5	57.17	568.9	0.662	0.152
		New	102.8	87.8	62.06	483.7	0.795	0.287
Belgium	Ghent	Old	163.2	62.3	108.72	462.4	0.780	0.203
		New	86.1	92.0	43.1	500.3	0.726	0.135
	Antwerp	Old	125.0	68.3	72.55	371.1	0.771	0.193
		New	92.4	81.2	89.19	488.6	0.822	0.235
	Bruges	Old	152.8	69.7	90.88	491.4	0.746	0.179
		New	75.0	88.3	26.86	570.7	0.608	0.104
	Brussels	Old	118.1	83.2	77.86	449.0	0.841	0.285
		New	98.6	93.9	55.69	459.7	0.835	0.263
	Ostend	Old	113.9	77.8	83.51	429.5	0.826	0.251
		New	86.8	83.0	40.49	497.4	0.651	0.116
Germany	Hamburg	Old	74.3	102.5	41.21	476.6	0.739	0.212
		New	39.6	128.2	22.83	455.0	0.752	0.152
	Düsseldorf	Old	78.5	79.3	62.46	380.6	0.836	0.272
		New	75.0	85.4	46.54	467.0	0.748	0.172
	Nuremberg	Old	99.3	90.1	51.44	530.5	0.766	0.208
		New	68.8	104.9	36.96	509.9	0.756	0.158
	Augsburg	Old	123.6	69.0	75.71	480.3	0.701	0.166
		New	81.3	97.8	42.21	483.6	0.772	0.189
	Cologne	Old	102.8	77.9	63.01	433.8	0.797	0.242
		New	66.7	103.5	34.25	471.5	0.747	0.137
France	Bordeaux	Old	143.1	72.0	83.31	478.5	0.805	0.241
		New	78.50	91.7	43.91	490.2	0.750	0.176
	Toulouse	Old	121.5	74.9	72.31	450.4	0.784	0.215
		New	102.1	85.0	59.32	454.9	0.766	0.184
	Dijon	Old	113.2	66.2	65.06	503.2	0.695	0.207
		New	127.8	76.6	75.41	471.1	0.790	0.220
	Rouen	Old	116.0	77.0	68.32	472.9	0.788	0.226
		New	111.1	83.3	65.75	472.4	0.770	0.186
	Beziers	Old	248.6	50.5	155.82	500.9	0.749	0.235
		New	164.6	63.5	93.62	533.0	0.750	0.164
Netherlands	Nijmegen	Old	109.7	74.5	63.22	468.8	0.769	0.176
		New	137.5	71.8	87.76	470.0	0.781	0.200
	Eindhoven	Old	117.4	74.1	63.10	519.9	0.739	0.168
		New	95.1	80.5	60.74	393.9	0.745	0.199
	Tilburg	Old	131.3	71.8	80.73	506.8	0.759	0.150
		New	125.7	68.2	71.88	509.7	0.702	0.175
	Zoetermeer	Old	161.8	58.8	85.43	605.7	0.643	0.097
		New	88.9	84.7	53.16	477.9	0.735	0.180
	Breda	Old	106.3	79.5	64.37	486.7	0.744	0.178
		New	100.0	75.4	71.23	451.6	0.701	0.214

Country	City	District	Intersection Density	Avg. Edge Length	Reach. Index (600m)	Harmonic Mean shortest path	Mean straightness	Meshedness coefficient
Bulgaria	Haskovo	Old	155.6	70.7	93.57	509.7	0.747	0.202
		New	147.2	80.9	76.94	539.7	0.715	0.193
	Yambol	Old	96.5	87.6	78.3	422.4	0.831	0.254
		New	97.9	92.8	55.85	511.7	0.773	0.225
	Varna	Old	120.1	69.1	77.95	499.5	0.705	0.196
		New	191.0	65.3	115.96	479.5	0.816	0.286
	Plovdiv	Old	121.5	81.6	70.40	528.8	0.748	0.195
		New	113.9	81.2	71.21	489.5	0.761	0.213
	Ruse	Old	121.5	84.9	68.52	517.3	0.797	0.228
		New	97.2	76.3	67.84	430.0	0.774	0.231
Czech Republic	Brno	Old	61.8	98.0	31.93	467.5	0.733	0.171
		New	73.6	101.6	40.03	468.6	0.788	0.255
	Prague	Old	93.8	93.5	42.9	514.4	0.767	0.264
		New	56.3	114.8	29.98	484.9	0.713	0.179
	Pilsen	Old	77.8	91.8	54.68	452.0	0.782	0.198
		New	72.2	95.1	37.57	537.8	0.706	0.155
	Liberec	Old	79.2	100.6	40.01	493.4	0.740	0.163
		New	77.8	95.2	43.20	499.9	0.716	0.186
	Ostrava	Old	89.6	88.5	50.51	492.4	0.755	0.208
		New	93.8	83.5	60.73	453.0	0.769	0.167
Hungary	Pecs	Old	98.6	83.9	56.01	481.1	0.706	0.155
		New	75.0	96.1	43.76	500.2	0.755	0.173
	Budapest	Old	88.2	95.8	44.84	505.5	0.782	0.198
		New	73.6	109.9	40.90	482.4	0.805	0.286
	Debrecen	Old	55.6	114.8	24.15	533.1	0.719	0.158
		New	57.7	119.1	33.62	525.0	0.782	0.232
	Gyongyos	Old	88.2	82.3	67.59	399.0	0.809	0.219
		New	113.9	69.9	82.40	423.8	0.786	0.215
	Nyiregyhaza	Old	72.2	98.7	39.44	461.0	0.734	0.165
		New	47.2	162.8	19.90	488.8	0.718	0.191
Poland	Poznan	Old	61.8	102.3	33.90	449.0	0.757	0.204
		New	62.5	112.8	34.97	437.6	0.754	0.201
	Częstochowa	Old	55.6	112.5	29.20	469.6	0.763	0.201
		New	55.6	119.6	38.68	464.4	0.717	0.116
	Lodz	Old	52.1	125.6	29.87	471.5	0.743	0.155
		New	62.5	122.6	30.5	513.0	0.734	0.185
	Wroclaw	Old	70.1	97.7	45.17	428.0	0.796	0.237
		New	48.6	130.1	28.08	435.5	0.773	0.228
	Warsaw	Old	53.5	113.0	32.00	461.3	0.775	0.174
		New	49.3	131.9	27.67	472.4	0.765	0.188
Romania	Bucharest	Old	127.8	69.1	90.59	461.2	0.773	0.223
		New	134.7	78.2	96.37	469.3	0.769	0.178
	Craiova	Old	84.0	86.5	45.81	484.8	0.749	0.187
		New	92.4	87.2	55.43	487.2	0.776	0.185
	Oradea	Old	99.3	86.5	63.85	450.7	0.783	0.233
		New	92.4	71.2	70.90	333.7	0.799	0.214
	Satu Mare	Old	73.6	94.6	38.54	479.3	0.740	0.176
		New	66.7	103.9	46.67	356.6	0.784	0.220
	Timisoara	Old	73.6	107.4	36.95	500.9	0.776	0.260
		New	47.9	147.9	24.97	462.8	0.808	0.238

Slovakia	Bratislava	Old	83.3	84.7	54.79	464.0	0.755	0.225
		New	74.3	108.0	33.16	511.3	0.711	0.195
	Košice	Old	78.5	76.2	46.95	389.6	0.767	0.224
		New	41.7	115.9	24.15	350.3	0.717	0.140
	Nove Zamky	Old	68.8	79.0	47.96	380.1	0.727	0.168
		New	66.0	106.1	35.83	506.3	0.725	0.155
	Trnava	Old	75.0	88.5	40.49	412.9	0.748	0.187
		New	72.2	89.7	48.73	375.8	0.774	0.174
	Nitra	Old	79.2	87.6	34.67	590.9	0.635	0.061
		New	70.1	93.5	32.80	629.6	0.620	0.048

Southern Europe

Country	City	District	Intersection Density	Avg. Edge Length	Reach. Index (600m)	Harmonic Mean shortest path	Mean straightness	Meshedness coefficient
Greece	Thessaloniki	Old	302.8	47.8	146.65	523.1	0.760	0.207
		New	243.1	54.1	209.55	493.3	0.792	0.247
	Katerini	Old	170.1	65.4	103.7	512.1	0.783	0.210
		New	150.0	66.2	93.34	488.1	0.791	0.206
	Larissa	Old	216.0	59.4	105.66	474.2	0.819	0.271
		New	179.9	62.5	120.87	518.2	0.708	0.221
	Ioannina	Old	167.4	66.4	123.05	444.3	0.781	0.202
		New	153.5	72.0	95.55	488.1	0.807	0.286
	Lamia	Old	204.2	59.2	116.47	518.9	0.747	0.198
		New	171.5	60.5	130.62	473.4	0.773	0.195
Italy	Florence	Old	116.7	65.7	84.87	424.7	0.795	0.236
		New	102.1	80.9	74.96	429.0	0.808	0.226
	Naples	Old	146.5	64.3	94.49	465.7	0.750	0.200
		New	131.3	65.7	81.17	491.1	0.743	0.177
	Palermo	Old	164.6	56.5	86.58	593.6	0.601	0.129
		New	138.2	75.3	74.31	501.6	0.782	0.277
	Bologna	Old	88.9	76.5	44.78	498.2	0.673	0.140
		New	81.3	91.4	47.43	450.0	0.789	0.236
	Padua	Old	99.3	69.9	59.71	491.0	0.674	0.125
		New	131.3	72.0	77.84	551.1	0.693	0.114
Portugal	Porto	Old	129.9	68.1	73.08	485.2	0.753	0.179
		New	84.0	83.3	60.02	399.0	0.824	0.255
	Lisbon	Old	169.4	64.0	103.35	484.6	0.759	0.208
		New	86.1	87.9	51.10	473.6	0.724	0.168
	Castelo Branco	Old	141.0	56.6	110.15	441.4	0.772	0.200
		New	54.2	120.3	21.07	380.7	0.813	0.235
	Setubal	Old	169.4	62.7	115.38	517.6	0.733	0.162
		New	106.3	74.0	61.71	460.7	0.732	0.167
	Evora	Old	215.3	44.1	191.62	429.6	0.756	0.222
		New	147.2	59.4	114.73	440.7	0.723	0.205
Republic of Cyprus	Nicosia	Old	161.1	75.5	72.81	572.8	0.740	0.151
		New	129.9	75.5	88.72	453.7	0.817	0.215
	Paphos	Old	129.9	73.7	78.61	497.7	0.744	0.153
		New	132.6	76.6	73.78	515.1	0.747	0.172
	Limassol	Old	187.5	70.2	93.08	536.5	0.758	0.203
		New	159.0	74.7	73	544.1	0.713	0.176
	Larnaca	Old	173.6	68.3	95.57	509.0	0.780	0.202
		New	126.4	79.0	46.48	659.1	0.616	0.095

	Famagusta	Old	157.6	68.2	84.05	474.4	0.809	0.192
		New	104.2	84.2	52.40	523.6	0.759	0.193
Spain	Malaga	Old	204.2	57.7	154.63	447.1	0.791	0.252
		New	129.9	72.9	82.62	465.5	0.748	0.188
	Granada	Old	175.7	44.3	193.37	499.0	0.741	0.191
		New	221.5	52.8	178.28	447.6	0.788	0.230
	Seville	Old	158.6	60.5	73.57	415.0	0.683	0.144
		New	146.8	61.1	140.84	429.8	0.805	0.278
	Cordoba	Old	111.1	63.7	69.13	459.2	0.753	0.185
		New	134.7	70.5	103.9	434.9	0.779	0.273
	Zaragoza	Old	144.9	65.4	59.97	466.0	0.709	0.206
		New	129.0	70.4	82.03	458.4	0.794	0.272

A-5. City-level differences ($\Delta = old - new$) between historic and modern districts for six street-network indicators.

Northern Europe

Country	City	Δ Intersection Density	Δ Average Edge Length	Δ Harmonic Mean shortest path	Δ Mean straightness	Δ Reach. Index (600m)	Δ Meshedness coefficient
Denmark	Odense	-16.67	-27.20	-186.70	0.220	-4.03	0.182
	Esbjerg	2.09	-8.80	4.01	0.008	5.700	0.086
	Aalborg	15.28	-8.74	-80.65	0.093	14.91	0.091
	Aarhus	12.50	-27.34	26.11	-0.117	3.16	-0.017
	Copenhagen	7.64	-15.66	-12.86	-0.027	11.85	-0.030
Finland	Helsinki	53.36	-66.04	-81.29	0.125	33.99	0.105
	Tampere	-1.02	21.81	-27.69	0.092	-11.12	0.016
	Mikkeli	13.02	-6.27	71.14	0.026	-3.49	0.076
	Turku	17.16	-18.41	166.11	-0.049	-10.19	0.008
	Pori	-9.72	6.66	2.00	0.054	-19.39	0.011
Norway	Hamar	32.64	-18.94	-16.71	0.048	23.36	0.044
	Bergen	34.02	-12.09	101.63	0.049	-7.01	0.033
	Stavanger	4.86	-5.54	-76.27	0.072	22.87	0.029
	Tonsberg	11.11	-6.87	-31.56	0.024	19.21	0.060
	Oslo	21.53	-6.00	8.00	0.004	9.48	-0.001
Sweden	Stockholm	11.80	-3.09	90.49	-0.044	-6.50	-0.074
	Gothenburg	-13.89	-4.04	-20.94	0.043	6.65	0.035
	Helsingborg	2.08	-12.02	3.42	-0.009	-11.11	0.005
	Malmo	36.11	-3.33	-8.82	0.068	22.26	0.098
	Vasteras	27.78	-14.44	-8.17	0.050	25.96	0.056
		$\tilde{x} = 12.15$	$\tilde{x} = -8.77$	$\tilde{x} = -8.49$	$\tilde{x} = 0.046$	$\tilde{x} = 6.18$	$\tilde{x} = 0.034$

Western Europe

Country	City	Δ Intersection Density	Δ Average Edge Length	Δ Harmonic Mean shortest path	Δ Mean straightness	Δ Reach. Index (600m)	Δ Meshedness coefficient
Austria	Graz	18.06	-37.01	-35.20	-0.037	15.75	-0.042
	Linz	-19.45	8.21	9.91	0.012	-13.17	0.021
	Innsbruck	9.72	-9.20	19.89	-0.040	3.21	-0.039
	Klagenfurt	-6.25	6.64	66.65	-0.052	-17.33	-0.060
	Vienna	18.75	-17.31	85.23	-0.133	-4.89	-0.134
Belgium	Ghent	77.08	-29.77	-37.85	0.055	65.62	0.068
	Antwerp	32.64	-12.91	-117.50	-0.052	-16.64	-0.043
	Bruges	77.78	-18.68	-79.27	0.138	64.02	0.075
	Brussels	19.45	-10.64	-10.67	0.006	22.17	0.022
	Ostend	27.08	-5.19	-67.93	0.175	43.02	0.135
Germany	Hamburg	34.73	-25.71	21.61	-0.013	18.38	0.061
	Düsseldorf	3.47	-6.15	-86.46	0.088	15.92	0.100
	Nuremberg	30.56	-14.74	20.63	0.010	14.48	0.050
	Augsburg	42.36	-28.82	-3.32	-0.071	33.50	-0.023
	Cologne	36.11	-25.58	-37.72	0.050	28.76	0.104
France	Bordeaux	64.59	-19.64	-11.71	0.055	39.40	0.065
	Toulouse	19.45	-10.09	-4.58	0.018	12.99	0.032
	Dijon	-14.59	-10.34	32.14	-0.095	-10.35	-0.013
	Rouen	4.86	-6.33	0.55	0.018	2.570	0.040
	Beziers	84.03	-12.94	-32.13	-0.001	62.20	0.071
Netherlands	Nijmegen	-27.78	2.71	-1.15	-0.012	-24.54	-0.024
	Eindhoven	22.22	-6.45	126.04	-0.006	2.36	-0.031
	Tilburg	5.56	3.62	-2.83	0.057	8.85	-0.026
	Zoetermeer	72.92	-25.94	127.87	-0.092	32.27	-0.084
	Breda	6.25	4.16	35.09	0.043	-6.86	-0.036
		$\tilde{x} = 19.45$	$\tilde{x} = -10.6$	$\tilde{x} = -2.83$	$\tilde{x} = 0.006$	$\tilde{x} = 14.48$	$\tilde{x} = 0.021$

Eastern Europe

Country	City	Δ Intersection Density	Δ Average Edge Length	Δ Harmonic Mean shortest path	Δ Mean straightness	Δ Reach. Index (600m)	Δ Meshedness coefficient
Bulgaria	Haskovo	8.34	-10.15	-30.00	0.033	16.63	0.009
	Yambol	-1.39	-5.13	-89.30	0.057	22.45	0.029
	Varna	-70.83	3.80	20.06	-0.111	-38.01	-0.089
	Plovdiv	7.64	0.48	39.32	-0.013	-0.81	-0.018
	Ruse	24.31	8.61	87.30	0.023	0.68	-0.003
Czech Republic	Brno	-11.80	-3.69	-1.09	-0.055	-8.10	-0.085
	Prague	37.50	-21.30	29.52	0.054	12.92	0.085
	Pilsen	5.56	-3.23	-85.79	0.076	17.11	0.043
	Liberec	1.39	5.39	-6.48	0.024	-3.19	-0.023
	Ostrava	-4.17	4.97	39.43	-0.014	-10.22	0.041
Hungary	Pecs	23.61	-12.16	-19.12	-0.050	12.25	-0.018
	Budapest	14.58	-14.19	23.12	-0.023	3.94	-0.088
	Debrecen	-2.09	-4.36	8.05	-0.062	-9.47	-0.074
	Gyongyos	-25.70	12.38	-24.81	0.023	-14.81	0.004
	Nyiregyhaza	25.00	-64.06	-27.78	0.016	19.54	-0.026
Poland	Poznan	-0.69	-10.45	11.38	0.003	-1.07	0.003
	Częstochowa	0	-7.06	5.14	0.046	-9.48	0.085
	Lodz	-10.42	2.96	-41.44	0.009	-0.63	-0.031
	Wroclaw	21.53	-32.43	-7.54	0.023	17.09	0.009
	Warsaw	4.16	-18.88	-11.06	0.010	4.33	-0.014
Romania	Bucharest	-6.94	-9.09	-8.10	0.005	-5.78	0.045
	Craiova	-8.34	-0.69	-2.38	-0.028	-9.62	0.002
	Oradea	6.95	15.32	117.04	-0.016	-7.05	0.019
	Satu Mare	6.94	-9.27	122.71	-0.044	-8.13	-0.044
	Timisoara	25.69	-40.53	38.07	-0.032	11.98	0.022
Slovakia	Bratislava	9.02	-23.27	-47.33	0.044	21.63	0.030
	Košice	36.80	-39.73	39.28	0.050	22.80	0.084
	Nove Zamky	2.78	-27.05	-126.18	0.002	12.13	0.014
	Trnava	2.78	-1.14	37.09	-0.026	-8.24	0.013
	Nitra	9.03	-5.81	-38.66	0.015	1.87	0.014
		$\tilde{x} = 4.86$	$\tilde{x} = -6.44$	$\tilde{x} = -1.74$	$\tilde{x} = 0.007$	$\tilde{x} = 0.025$	$\tilde{x} = 0.007$

Southern Europe

Country	City	Δ Intersection Density	Δ Average Edge Length	Δ Harmonic Mean shortest path	Δ Mean straightness	Δ Reach. Index (600m)	Δ Meshedness coefficient
Greece	Thessaloniki	59.72	-6.31	29.71	-0.031	-62.90	-0.041
	Katerini	20.14	-0.83	24.02	-0.008	10.36	0.004
	Larissa	36.11	-3.10	-43.98	0.111	-15.21	0.050
	Ioannina	13.89	-5.66	-43.79	-0.026	27.50	-0.085
	Lamia	32.64	-1.25	45.53	-0.027	-14.15	0.002
Italy	Florence	14.59	-15.17	-4.31	-0.013	9.91	0.011
	Naples	15.28	-1.39	-25.40	0.007	13.32	0.023
	Palermo	26.39	-18.79	92.01	-0.182	12.27	-0.148
	Bologna	7.64	-14.97	48.14	-0.115	-2.65	-0.096
	Padua	-31.94	-2.09	-60.14	-0.019	-18.13	0.011
Portugal	Porto	45.83	-15.22	86.23	-0.071	13.06	-0.076
	Lisbon	83.33	-23.88	11.05	0.034	52.25	0.040
	Castelo Branco	86.80	-63.71	60.72	-0.041	89.08	-0.035
	Setubal	63.19	-11.23	56.89	0.001	53.67	-0.005
	Evora	68.06	-15.27	-11.13	0.033	76.89	0.017
Republic of Cyprus	Nicosia	31.25	-0.01	119.10	-0.077	-15.91	-0.065
	Paphos	-2.78	-2.97	-17.40	-0.003	4.83	-0.019
	Limassol	28.47	-4.50	-7.55	0.045	20.08	0.027
	Larnaca	47.22	-10.67	-150.13	0.164	49.09	0.107
	Famagusta	53.47	-16.04	-49.24	0.050	31.65	-0.001
Spain	Malaga	74.31	-15.20	-18.37	0.043	72.01	0.065
	Granada	-45.84	-8.48	51.38	-0.047	15.09	-0.039
	Seville	11.77	-0.64	-14.82	-0.121	-67.27	-0.133
	Cordoba	-23.61	-6.77	24.30	-0.026	-34.77	-0.088
	Zaragoza	15.89	-5.07	7.60	-0.085	-22.06	-0.066
		$\tilde{x} = 28.47$	$\tilde{x} = -6.77$	$\tilde{x} = 7.6$	$\tilde{x} = -0.02$	$\tilde{x} = 12.27$	$\tilde{x} = -0.005$

A-6. Extended Correlation Results for Fractal Dimension and Network Indicators

A-6.1. Fractal dimension vs 6 network indicators in the historic part of the city (across 100 European cities)

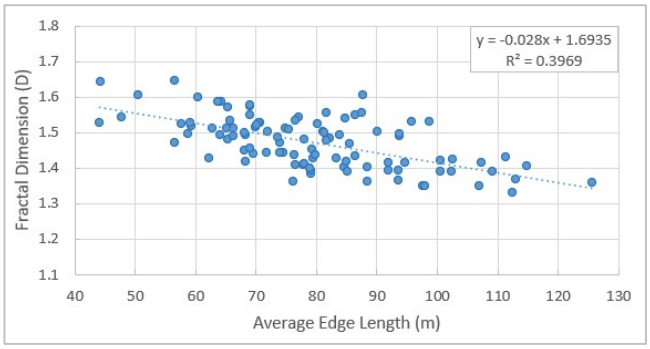

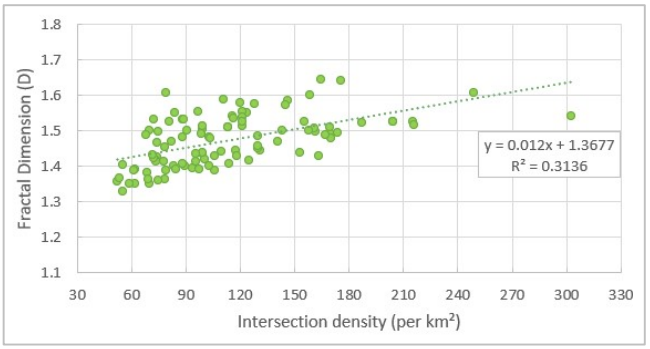

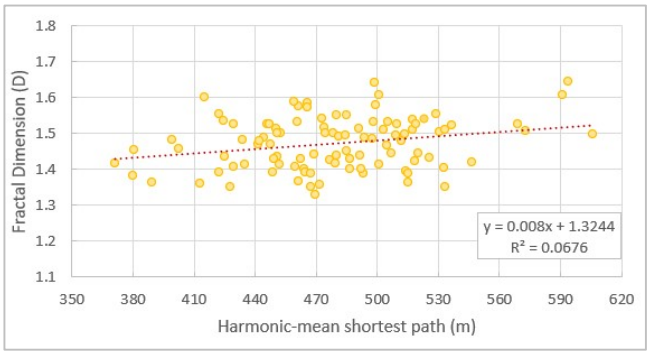

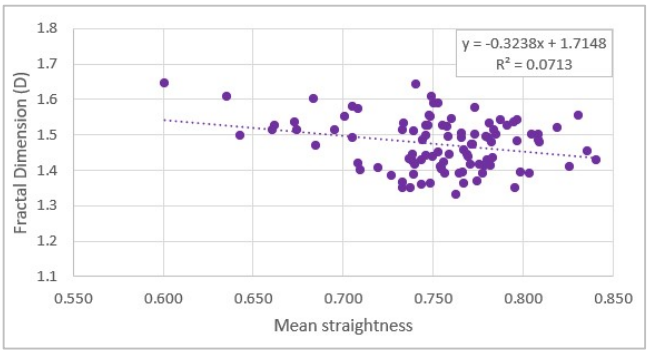

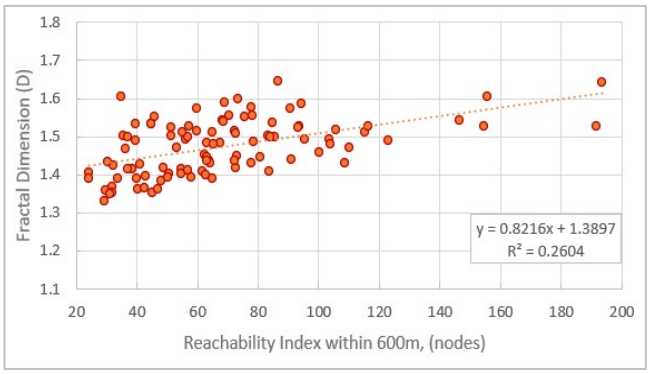

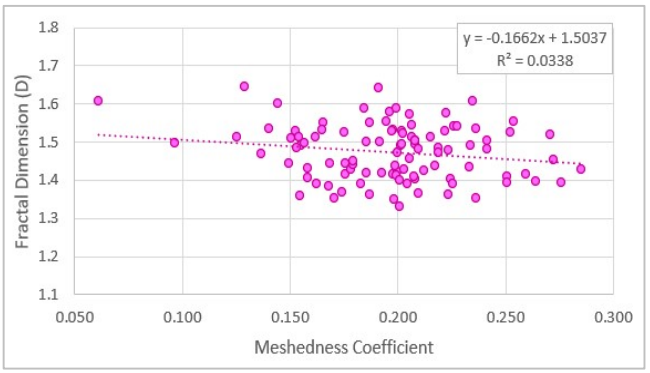

A-6.2. Fractal dimension vs 6 network indicators in the modern part of the city (across 100 European cities)